INTERDEPENDENT INFRASTRUCTURES AND MULTI-MODE ATTACKS AND FAILURES: IMPROVING THE SECURITY OF URBAN WATER SYSTEMS AND FIRE RESPONSE

A Dissertation

by

ELIZABETH CATHERINE BRISTOW

Submitted to the Office of Graduate Studies of
Texas A&M University
in partial fulfillment of the requirements for the degree of

DOCTOR OF PHILOSOPHY

December 2006

Major Subject: Civil Engineering

INTERDEPENDENT INFRASTRUCTURES AND MULTI-MODE ATTACKS AND FAILURES: IMPROVING THE SECURITY OF URBAN WATER SYSTEMS AND FIRE RESPONSE

A Dissertation

by

ELIZABETH CATHERINE BRISTOW

Submitted to the Office of Graduate Studies of
Texas A&M University
in partial fulfillment of the requirements for the degree of

DOCTOR OF PHILOSOPHY

Approved by:

Chair of Committee,	Kelly Brumbelow
Committee Members,	David H. McIntyre
	Carla S. Prater
	Ralph A. Wurbs
Head of Department,	David V. Rosowsky

December 2006

Major Subject: Civil Engineering

ABSTRACT

Interdependent Infrastructures and Multi-Mode Attacks and Failures: Improving the Security of Urban Water Systems and Fire Response. (December 2006)

Elizabeth Catherine Bristow, B.S., Texas A&M University;

M. Eng., Texas A&M University

Chair of Advisory Committee: Dr. Kelly Brumbelow

This dissertation examines the interdependence between urban water distribution systems and urban fire response. The focus on interdependent critical infrastructures is driven by concern for security of water systems and the effects on related infrastructures if water distribution systems are damaged by terrorist attack or natural disaster.

A model of interdependent infrastructures (principally water distribution systems and fire response) is developed called the Model of Urban Fire Spread (MUFS). The model includes the capacity to simulate firefighting water demands in a community water system hydraulic model, building-to-building urban fire spread, and suppression activities. MUFS is an improvement over previous similar models because it allows simulation of urban fires at the level of individual buildings and it permits simulation of interdependent infrastructures working in concert.

MUFS is used to simulate a series of multi-mode attacks and failures (MMAFs) – events which disable the water distribution system and simultaneously ignite an urban fire. The consequences of MMAF scenarios are analyzed to determine the most serious

modes of infrastructure failure and urban fire ignition. Various methods to determine worst-case configurations of urban fire ignition points are also examined.

These MMAF scenarios are used to inform the design of potential mitigation measures to decrease the consequences of the urban fire. The effectiveness of mitigation methods is determined using the MUFS simulation tool. Novel metrics are developed to quantify the effectiveness of the mitigation methods from the time-series development of their consequences. A cost-benefit analysis of the various mitigation measures is conducted to provide additional insight into the methods' effectiveness and better inform the decision-making process of selecting mitigation methods.

Planned future work includes further refinement of the representation of fire propagation and suppression in MUFS and investigation of historical MMAF events to validate simulation predictions. Future efforts will continue development of appropriate optimization methods for determining worst-case MMAF scenarios.

This work should be of interest to water utility managers and emergency planners, who can adapt the methodology to analyze their communities' vulnerability to MMAFs and design mitigation techniques to meet their unique needs, as well as to researchers interested in infrastructure modeling and disaster simulation.

DEDICATION

This dissertation is dedicated with love and gratitude
to my first teachers: my parents.

You taught me to read and write, to walk and tie my shoes,
and the most important skill of all:
to learn.

Thank you.

ACKNOWLEDGEMENTS

The work presented in this dissertation would not have been possible without the help and support of the author's advisor, Dr. Kelly Brumbelow. For his constant patience and guidance, the author extends her sincerest gratitude.

This research was performed while the author was on appointment as a U.S. Department of Homeland Security (DHS) Fellow under the DHS Scholarship and Fellowship Program, a program administered by the Oak Ridge Institute for Science and Education (ORISE) for DHS through an interagency agreement with the U.S Department of Energy (DOE). ORISE is managed by Oak Ridge Associated Universities under DOE contract number DE-AC05-00OR22750. All opinions expressed in this paper are the author's and do not necessarily reflect the policies and views of DHS, DOE, or ORISE.

The research presented in this dissertation was also supported by an Engineering Dissertation Fellowship from the American Association of University Women Educational Foundation.

TABLE OF CONTENTS

Page

LIST OF FIGURES

FIGURE Page

FIGURE Page

LIST OF TABLES

1. INTRODUCTION

The study presented in this dissertation has three primary goals. The first is to develop a compound model of urban fire spread and suppression with a damaged water distribution system. The study's second goal is to use this model to examine the consequences of complex attacks or disasters which simultaneously disable a community's water distribution system and start an urban fire. Once the worst-consequence disaster scenarios are known, the study's third goal is to use the joint water distribution system/fire suppression model to test the effectiveness of mitigation and security strategies designed to protect communities from simultaneous failures of critical infrastructures which contribute to fire response.

Policymakers and researchers have long been aware of the importance of critical infrastructures to the health and integrity of modern societies. Many sources (Clinton 1998, USA PATRIOT Act [P.L. 107-56], Office of Homeland Security [OHS] 2002, President's Critical Infrastructure Protection Board [PCIPB] 2003) present lists of the infrastructures which are most critical to society's operation. The lists may vary slightly, but water distribution systems and emergency response (of which firefighting is a component) are common entries.

The increased focus on security after the events of September 11, 2001 prompted recognition of the complex interactions among critical infrastructures and the potential for cascading failures where these systems depend on one another. The *National Research and Development Strategy for Critical Infrastructure Protection* (Executive

---

This dissertation follows the style of *Journal of Infrastructure Systems*.

Office of the President, Office of Science and Technology Policy [OSTP] and U.S. Department of Homeland Security Science and Technology Directorate [DHS-S&T] 2004) states that:

> [A] coordinated attack by a small army of arsonists could wreak havoc on a community and completely drain water supplies needed to extinguish it, especially if those water supply networks were also attacked. (p. 32)

To counter the potential for this type of tandem attack, this strategy calls explicitly for advanced modeling and simulation efforts to provide better insight into the complex, nonlinear interactions of interdependent infrastructures. The strategy emphasizes the important benefits of developing advanced models of interdependent critical infrastructures by stating that:

> This capability can be used in a crisis response mode, and in an analysis and assessment mode to provide decision-makers with a better basis to make prudent, strategic investments and policy resolutions to improve the security of infrastructures. (p. 49)

This statement underlines the most important benefit of the joint water distribution system/fire suppression model and risk analysis methodology presented in this dissertation: to permit policymakers, utility managers, and emergency planners to examine the potential consequences of complex attacks or disasters in their own communities and to develop mitigation and response plans in advance of these disasters. These strategies will vary for each system, since each will be tailored to its specific community's conditions and needs. It is hoped, however, that the model and

methodology presented here may provide useful tools and guidance in crafting these strategies.

This research is presented and discussed in greater detail in the remaining seven sections of this dissertation. Section 2 presents an overview of the existing literature on the security of water systems and their interdependence with fire response. This section also presents existing literature on urban fire spread and suppression models.

Section 3 gives a detailed explanation of the technical workings of the Model of Urban Fire Spread (MUFS), a tandem model of fire spread and suppression run in conjunction with a hydraulic model of a damaged water distribution system, which was developed for this dissertation. MUFS is used to simulate the progress and suppression of urban fires under various scenarios of damage to a community water distribution network as part of an extensive vulnerability analysis against events which simultaneously damage a community's water system and start an urban fire. This type of situation is described generically as a multi-mode attack or failure (MMAF).

Section 4 presents the methodology for this coupled water system damage/urban fire vulnerability assessment. Section 5 includes the results of the MMAF vulnerability assessment and a discussion of the outcomes of the extensive MMAF simulations.

Based on the results of the vulnerability analysis and MMAF damage scenario simulations, mitigation strategies are developed and tested using the MUFS model. The methodology for modeling and testing the damage scenarios is presented in Section 6. The results of the MMAF damage simulations with mitigation measures in place are discussed in Section 7. The final section of the dissertation will present the conclusions

gained from the study and a summary of the suggested future work on this topic. This discussion will include planned improvements to the MUFS model and suggestions for future work on integrating models of interdependent critical infrastructures.

2. REVIEW OF RELATED LITERATURE

2.1. Vulnerability of Water Systems to Terrorist Attacks

National leaders have long been aware of the strategic importance of water systems to maintain the economy and stability of the United States. In *Presidential Decision Directive (PDD) 63* (Clinton 1998), President William J. Clinton formally designated water systems as part of the nation's critical infrastructure: "those physical and cyber-based systems essential to the minimum operations of the economy and government." In the same document, the President pointed out that these infrastructures' strategic importance makes them vulnerable to asymmetric attacks by nations or groups intent on harming the United States. *PDD 63* also presents a timeline for analyzing vulnerabilities of critical infrastructures and developing strategies to increase their security and robustness. Although this directive does mention terrorism as a motivation for critical infrastructure protection, its main emphasis lies on decreasing the impact of accidental mechanical and electrical failures due to the effects of the Y2K bug on the critical infrastructures' supporting computer systems.

The importance of protecting the nation's critical infrastructures from terrorism was reaffirmed in 2001 with the passage of the USA PATRIOT Act (PL 107-56). Section 1016 of this act, also known as the Critical Infrastructure Protection Act of 2001, explicitly named water systems as a component of the critical infrastructure and redefines this term to encompass "systems and assets, whether physical or virtual, so vital to the United States that the incapacity or destruction of such systems and assets

would have a debilitating impact on security, national economic security, national public health or safety, or any combination of those matters" (Title X, Section 1016e). This Act also established the National Infrastructure Simulation and Analysis Center to assist in threat assessment, risk mitigation, and counterterrorism activities.

This shift in attention from simple mechanical or electronic failures to premeditated, malicious attacks requires an accompanying shift in the types of vulnerabilities judged to be important. The Public Health Security and Bioterrorism Preparedness Act of 2002 (PL 107-88) states that "each community water system serving a population of greater than 3,300 persons shall conduct an assessment of the vulnerability of its system to a terrorist attack or other intentional acts intended to substantially disrupt the ability of the system to provide a safe and reliable supply of drinking water" (Title IV, Section 1433, a(1)). This Act established deadlines for the completion of the vulnerability assessments and promised future guidance on the types of attacks to be considered. Since this Act's institution, many different sources have published documents elucidating the types of threats that water systems may face.

The *National Strategy for the Physical Protection of Critical Infrastructures and Key Assets* (PCIPB 2003) cites four primary concerns for water systems' vulnerabilities: physical damage to water system components, contamination of the water supply, cyber-attack in information management systems used by the water system, and interruption of water services by another infrastructure's failure.

Mays (2004) closely echoes this assessment by presenting the following list of potential threats: cyber-based threats, physical threats, and contamination of drinking

water using biological or chemical means. Clark et al. (2004) expand on this by delineating the components of water systems which may be vulnerable to attack: raw water sources, raw water conveyance systems, water treatment facilities, inflow points to the water distribution system, pumping stations and valves, and treated-water storage facilities like tanks and reservoirs. Clark et al. present contamination as the most serious threat against water systems and state that, with few exceptions, physical destruction of water infrastructure may be expensive and inconvenient but does not present severe public safety risks.

The American Water Works Association has provided perhaps the most extensive list of potential threats in its guidance document for the security of water utilities (AWWA 2004). In addition to those listed by previous documents, the AWWA list includes such threats as arson against water facilities, release of toxic substances like chlorine gas from water treatment facilities, and the *threat* of water contamination to evoke public fear.

Terrorism vulnerability assessments for water systems are a relatively new concept, and data contributing to precise vulnerability quantifications are not widely available. Tidwell et al. (2005) present a methodology for modeling water system vulnerability to terrorist attacks using a variation of Markov chain modeling to incorporate the "latent effects" of security strategies and the utility's "company culture" regarding security.

Few sources directly examine multi-mode attacks or failures (MMAFs) involving water systems and fire response, but a recent article containing an interview of a

terrorism expert points out the possibility of this type of attack and the importance of water systems' preparation for it ("Taking Due Account of Terrorism," 2004).

Regardless of the precise listing of potential threats, it is clear that water systems occupy a strategic place in the nation's day-to-day operations and that their status as critical infrastructures makes water systems attractive targets for terrorist attack. Less comprehensively examined, however, is the extent to which water systems' interdependence with other critical infrastructures increases the vulnerability of these systems to intentional multi-mode attacks or collateral damage. Critical infrastructures' interdependence is discussed in the following section.

2.2. Interdependence of Water Systems with Other Critical Infrastructures

Extensive work has been done on exploring water systems' intrinsic vulnerability and predicting the direct threats against them. The very first modern work on critical infrastructure protection, *PDD 63*, points out another concern that has been less thoroughly studied. The nation's critical infrastructures are, in many cases, physically intertwined and operationally interdependent; therefore, while the consequences of water systems' incapacitation or contamination are grave, they may be even more so in light of their effects on other critical infrastructures.

Perrow (1984) introduces the concept of "normal accidents" in his book of the same title. A normal accident is one which is caused by unexpected system interactions, not by operator error or mechanical failure of a component. Such accidents, Perrow states, are unavoidable and cannot be mitigated by elaborate safety systems or

automation; indeed, these added systems create even more complex system interactions and tend to exacerbate the problem, not fix it. The system's interactive complexity, or its tendency for separate subsystems to interact in unpredictable ways, is one factor which contributes to normal accidents; the other factor named is "tight coupling," or the tendency of system processes to happen very quickly, with little opportunity for intervention. Some technologies' very nature makes them dangerous, Perrow states; in some cases designers can reduce the risk by decreasing the complex interactions and tight coupling of systems; in other cases, society must learn to accept a certain level of expected risk or be willing to abandon the technology altogether.

Zimmerman (2001) expands Perrow's thesis of complexity leading to unforeseen consequences, placing it in the context of recent terrorist attacks, natural disasters, and technological failures which led to significant infrastructure outages. She notes that interdependencies among infrastructures permit problems to propagate and examines two different types of infrastructure connections. These types are spatial interconnectedness, in which infrastructures are affected by the same events because they are located very close to one another, and functional interconnectedness, in which infrastructures are linked because one is directly dependent upon another for normal operations. Zimmerman proposes several strategies for overcoming the problems associated with interdependency: system redundancy, increased study of unpredictable system interactions, and improved technology for early detection of problems with the infrastructure.

Rinaldi, Peerenboom, and Kelly (2001) further develop this idea of various types of coupling among critical infrastructures by introducing six dimensions along which researchers may describe infrastructure interactions. The first, "Coupling and Response Behavior," echoes Perrow's notion of tight vs. loose coupling of system interactions. The other dimensions of this conceptual model characterize the infrastructures' characteristics: their state of operation (normal vs. stressed), the environment in which they operate, the types of interactions which may take place between them, and the types of failures which may arise from emergencies involving interdependent infrastructures. The authors propose this model in order to encourage other researchers and infrastructure managers to consider many different aspects of their systems when modeling the systems' interdependencies. The model they propose, therefore, is descriptive rather than quantitative.

Brown et al. (2004) present an algorithm for assessing vulnerabilities of water systems deriving from infrastructure interdependencies. This model is primarily concerned with natural disasters affecting water and electrical grids but presents a general framework which is adaptable to other infrastructure pairings. The algorithm begins with a "quick-look" assessment which uses whatever system information is readily available to identify potential risks. A conceptual model of the system is then developed to determine the probability and consequences of these risks, as well as the immediacy of the threats they pose. The threat scenarios are prioritized for urgency of mitigation efforts by plotting each potential risk on a two-dimensional graph, with the likelihood of the event on one axis and the magnitude of its consequences on the other

axis. The model they present can be used to approximate the economic and system – operations impact of various policy decisions as well.

Haimes and Jiang (2001) present the most quantitatively-based model of infrastructure interdependency examined here. This model is based on an economic technique called Leiontief Input-Output modeling for studying the equilibrium behavior of interconnected economic sectors; Haimes and Jiang adapted the methodology to apply to dynamic analyses of interdependent infrastructures. Given a failure in one or more infrastructures due to accidents, natural disasters, or terrorism, the model predicts the risk of inoperability for the other infrastructures. The model also takes into account "rescue" techniques used to repair damage to one or more affected infrastructures and the mitigative effects the efforts may have on related infrastructures. The main challenge in applying this model lies in constructing the matrices that describe the degree of infrastructure interdependence and the rate of propagation of cascading failures. The paper uses Hierarchical Holographic Modeling (Haimes 2004) to assist in building the matrices, though the paper is not explicit regarding the precise techniques used. The authors also present a series of illustrative examples of applying the interdependency analysis algorithm.

2.3. Computational Fire Spread Models

Infrastructure interdependence is a widespread condition, and infrastructure managers may legitimately be concerned with a variety of types of interdependencies. One relationship of particular importance to the water industry exists between municipal

water distribution systems and fire response services. Few investigators have yet examined the extent of this interdependence and modeled the potential consequences of cascading failure in this area. A good first step in examining this phenomenon is to study how fire spreads and how fire-response systems restrict fire. The literature presents several quantitative models of fire spread, and Friedman (1992) provides a comprehensive overview of early computer-based fire spread models. Most of these models focus on fire spread within a single room or a single multi-compartment building.

2.3.1. Compartment Fire Spread

Mitler and Emmons (1981) provide a good description of the physics of fire spread within a single compartment in their documentation for CFC V (Computer Fire Code, Version 5), an early single-room fire propagation model developed at Harvard University. The model tracks fire progress by calculating temperature in the room and by performing mass balance analyses between the two layers of the room's atmosphere: a lower layer containing air under normal conditions, and an upper layer containing smoke, soot, and other combustion byproducts at elevated temperatures. The mass and heat transfer equations are based on observations of controlled fires and will account for specific object placement within a room. This version, in an improvement over previous versions of the same model, permits the addition of ambient air through vertical vents in the compartment's ceiling.

CFC V was developed for the National Bureau of Standards, which later became the National Institute of Standards and Technology (NIST). NIST continued developing fire-spread models and later adopted CFAST, the Consolidated Model of Fire Growth and Smoke Transport (Peacock et al. 1988). Like CFC V, CFAST divides each room into an upper and lower zone based on air-layer properties; in an advance over previous models, however, CFAST supports multiple fires in multi-room buildings and will approximate fire travel through ventilation ducts between rooms.

Platt (1992) introduces a new approach to modeling multicompartment fire propagation: a stochastic model with probabilities of each type of fire spread derived from the properties of the surrounding materials. This model permits three means of fire spread between compartments: listed in order of decreasing probability, they are: spread through an open door, vertical spread between floors via flames projecting out windows, and horizontal or vertical spread through closed doors, walls, or ceilings.

Karlsson and Quintiere (2000) provide an excellent qualitative treatment of compartment fire development and mechanics as well as a good overview of recent developments in computer models of compartment fires.

Earlier fire spread models concentrated on single-room or single-building fire spread because there is less uncertainty in the expected conditions. However, the literature also includes several studies examining urban fire spread – that is, fire spread *between* buildings, rather than *within* buildings – and these models are valuable to any consideration of the interaction between water systems and municipal fire response services.

2.3.2. Urban Fire Spread

The seminal work in the study of urban fire spread was based on large urban fires following earthquakes in Japan (Hamada 1955, cited in Fujita 1975). Hamada's equations were derived empirically from historical earthquake-caused fires and relate velocity of fire spread to wind speed, plan dimension of a (square) building, and separation distance between the buildings. This model formed the foundation for many later models. Fujita (1975) combined Hamada's equations with a study of pedestrian evacuation from the fires to aid cities in creating effective emergency response strategies.

The Hamada equations also form the foundation for the post-earthquake fire module of HAZUS-MH (FEMA 2003a, 2003b), a software program designed by the U.S. Federal Emergency Management Agency to perform risk assessments and damage estimations for earthquakes, floods, and high winds. The post-earthquake fire module models fire spread and suppression and accounts for the time it takes residents to discover and report the fire as well as the potential for partially- or totally-disabled municipal water systems for firefighting. The density of fire ignition points is based on the intensity of the earthquake and is modeled empirically from historical post-earthquake fires. HAZUS-MH's Fire Following Earthquake module is discussed in greater detail in Section 3.2.

Other modern fire spread models have moved away from the approach specified by the Hamada equations. Himoto and Tanaka (2000) point out that the Hamada equations' applicability may have declined, since they were based on statistical data

involving building size, shape, layout, and construction which were valid in large cities in Japan half a century ago but may not be accurate after the advent of modern building materials and fireproofing techniques. Himoto and Tanaka present a more general physically-based model of post-earthquake fires that considers, building by building, the physics of fire propagation. The authors model fire spread between buildings through radiative heat flux and hot air plumes from already-burning buildings. Once a building has caught fire, its internal burning and contribution to heat flux in other buildings is modeled similarly to single-layer compartment fire models. This model, which is acknowledged in the paper to be incomplete and not yet ready to deal with realistic urban conditions, was tested on a few simple three-building configurations.

A physically-based urban fire spread model is also presented by Bertinshaw and Guesgen (2004). This model assumes that a city's firefighting capabilities have been disabled by some unspecified disaster. Given an ignition point for the fire, the GIS-based model calculates for each unburned building the heat flux from its burning neighbors. If the intensity of the heat transfer rises above a material-dependent threshold value, the unburned building ignites. This calculation is carried out for every unburned building at each time step. The model calculates heat flux following well-established laws of heat transfer. The most complicated calculation is the "configuration factor," an input to the heat transfer equation, which is a term that encompasses the sizes and distances of the faces of heat-emitting buildings. Bertinshaw and Guesgen outline a means of calculating the configuration factor for each building but caution that this is the most computationally-intense aspect of the fire-spread simulation. This model was

considered as a means of implementing the urban fire spread model for this research project; unfortunately, the model has never been tested against historical fire spread data, so its accuracy is unproven (Bertinshaw, personal communication, August 2005).

General mechanics of urban fire spread and water system needs to fight urban fires are dealt with by Mahoney (1980) and Eckman (1994). Eckman (1994) discusses basic needs for water systems to provide water for firefighting, including sufficient pressure, elevated water storage for firefighting, hydrant spacing, and water shuttle relay operations when adequate in-ground water supplies are not available. Mahoney (1980) presents a detailed guide to determining water pressure needs for the water distribution system under various topology and water requirement scenarios. This work includes a discussion of complex fire truck deployments, including supplying more than one fire stream with the same fire truck and connecting fire trucks in series to overcome the difficulties posed by a weakened water distribution system or unusual water needs imposed by topographic concerns.

2.4. Conclusion: Historical Multi-Mode Attacks and Failures

Review of historical literature also provides strong justification for continuing research into mitigation measures for multi-mode attacks and failures. History provides many examples of large-scale urban fires whose suppression efforts were hampered by a disabled water distribution system. Examples of historical MMAFs include the Great Earthquake and Fire of 1906 in San Francisco (Nolte 2006) and the Second Great Fire of London in 1940 (Johnson 1980).

3. METHODOLOGY: MODEL OF URBAN FIRE SPREAD

3.1. Introduction

The water distribution system vulnerability studies and mitigation assessment detailed later in this dissertation were conducted using the Model of Urban Fire Spread (MUFS), a numerical model of urban fire ignition, spread, and suppression which was developed specifically for this application. This section presents MUFS in detail; it begins with a discussion of the reasons a new model of urban fire spread is needed and a view of the main differences between MUFS and existing models of urban fire spread. The section then discusses the needed inputs to MUFS and presents the model's technical workings in detail. The section concludes with a discussion of MUFS's outputs and how they can be used to analyze urban fires and their consequences.

3.1.1. Overview of Model Operation

Before beginning a detailed discussion of MUFS's development and operation, it is useful to present a quick overview of the model and the stages in the simulation process. The main goal of MUFS is to determine the extent of the burned area resulting from a single- or multi-ignition urban fire with water for fire suppression coming from a water distribution system that may be partially or totally disabled. Coupled with information about the urban area's building layout and occupancy, the burned area reveals the number of people who are displaced when the fire damages their home or place of employment. The count of displaced people is used as the primary measure of

the consequences of the multi-mode attack or failure scenarios in the vulnerability assessment presented later in this dissertation.

The preliminary phase of the model requires the user to provide information about the urban area's layout, its water distribution system, and its fire response capabilities. MUFS requires more extensive inputs than many other urban fire spread models because MUFS's output is highly dependent both on the topology of the urban area and the status of the water distribution system. The required structure of these inputs is explained more thoroughly in Section 3.3.

The first step in the actual simulation process involves calculating the extent of unsuppressed fire spread in the time steps before the fire department arrives to begin fire suppression. All fires start unsuppressed, since it takes some time for the fire department to be notified of the fire and to deploy resources to fight the fire. The length of delay before the firefighters' arrival depends on the status of the urban area's communication and transportation infrastructures; this delay can be supplied as an input by the user or generated stochastically based on historical disaster response. After the time of ignition, MUFS calculates fire propagation at discrete time steps, the length of which are specified by the user.

For both unsuppressed and suppressed fire spread, MUFS begins the fire spread calculations at an ignition point (or set of points) specified by the user. At each time step, MUFS calculates the incremental distance covered by the fire during the time step in each of four cardinal fire spread directions determined relative to the dominant wind direction in the urban area: downwind, upwind, sidewind left, and sidewind right. The

polygons created by linking the coordinates of the burn fronts at any particular time step are therefore quadrilaterals (Figure 3.1a).

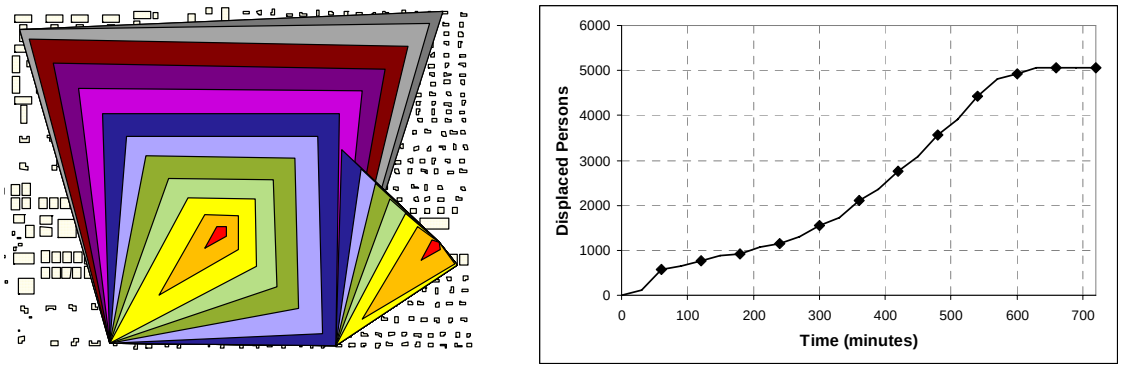

Fig. 3.1. Burned area quadrilaterals (3.1a, left) generated by MUFS and corresponding fire consequences (3.1 b, right) at 60-minute time step intervals.

After it has calculated the unsuppressed fire spread for the urban fire's initial period, MUFS conducts simulations of suppressed fire spread beginning at the time when the fire department arrives and continuing to the end of the user-specified simulation period. Firefighting efforts may completely stop the fire's progress in one or more of the fire spread directions (totally effective suppression), or they may merely slow the rate of the fire's spread (partially effective suppression). The effectiveness of the firefighting depends on the number of fire trucks and amount of water available, and a technical explanation of how MUFS determines fire suppression effectiveness is presented in Section 3.5. At each time step, the buildings encompassed by the final burn polygon are determined, and numbers of displaced persons are tabulated as a metric of the fire's consequences (Figure 3.1b). The output from MUFS's simulation process is discussed in detail in Section 3.6.

3.2. Comparison of MUFS and HAZUS-MH Fire Following Earthquake Module

MUFS was developed specifically for the vulnerability assessment and consequence analysis presented in this dissertation. In the original proposal for this study, the project plan stated that the vulnerability analysis would use the Fire Following Earthquake module of HAZUS-MH (FEMA 2003a, FEMA 2003b), a disaster analysis and planning tool developed by the U.S. Federal Emergency Management Agency that uses readily-available public data to predict the scope and consequences of a variety of natural disasters, including earthquakes and the urban fires they often ignite.

This project has several unique requirements which ultimately made it infeasible to use HAZUS-MH for the vulnerability analysis. HAZUS-MH's treatment of urban fires is based on the Hamada model of urban fire spread, with the inclusion of additional empirical data from recent post-earthquake urban fires and the incorporation of a model of urban fire suppression (FEMA 2003a). The basic framework of HAZUS-MH's urban fire spread and suppression model was preserved, although some modifications of the model were necessary to make it appropriate to this study and to make full use of the geographic data available. It is useful to consider the similarities and differences between HAZUS-MH's Fire Following Earthquake model and MUFS in three areas: fire ignition, fire spread, and fire suppression.

3.2.1. Fire Ignition

HAZUS-MH was designed as a tool to predict aggregate damage from earthquakes and other natural disasters. Under normal HAZUS-MH operation, the urban fire's ignition points are predicted based on a design earthquake event and geographically distributed automatically according to an empirical equation based on historical post-earthquake fires (FEMA 2003a). It does not permit the simulation of post-earthquake fires independent of the earthquake that caused them, and the user may not specify fire ignition points.

Simulating non-earthquake-caused urban fires calls for the ability to model fires with diverse ignition patterns, and for this reason it was necessary to improve the simulation of urban fire ignition. MUFS permits the user to specify the fire's ignition point(s), and the selection of these points depends on the type of MMAF being modeled. For example, a terrorist arson attack might center on local sites of importance, such as a museum or a school or City Hall, or it might focus on an area of the community where many people congregate, such as the central business district. An industrial accident which sparks an urban fire would be located the town's industrial district, and an urban fire begun by a domestic accident would begin in one of the town's residential districts. Allowing the user to specify the ignition point permits MUFS to look beyond fires caused by natural disasters and to simulate urban fires caused by a variety of incidents.

3.2.2. Fire Spread

There are many similarities between the basic urban fire spread model in HAZUS-MH and the one included in MUFS. Both models' fire spread calculations are based on the Hamada model of fire spread discussed in Section 2; accordingly, both models predict the spatial extent of urban fires through time as a function of urban layout and wind speed and direction. A major difference between the two models arises in how they determine building parameters as a function of urban topology. The original Hamada equations include simplifying assumptions about the urban area's layout and building spacing; they operate on an area composed of equally-sized, uniformly-spaced square buildings (Fujita 1975). Thus, the parameters in the Hamada equations which capture the size and spacing of the buildings may be generalized for the entire area.

Like the original Hamada model, HAZUS-MH uses average values for the urban area (FEMA 2003a). MUFS utilizes geographical information commonly available in modern GIS databases of urban areas to determine the topology-related building parameters separately for each individual building. This change allows for specific building footprints and urban development patterns to be considered in the fire spread simulation rather than an idealized building grid (Figure 3.2).

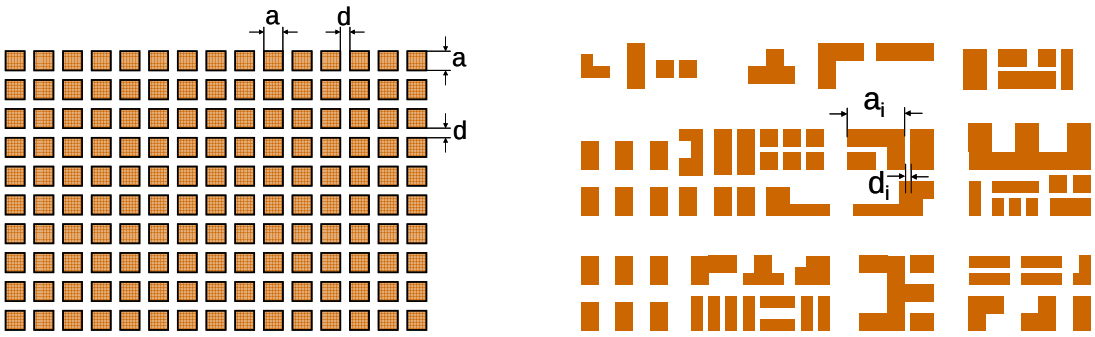

Fig. 3.2. Comparison of building grid of uniform size and spacing required by HAZUS-MH urban fire spread calculations (left) and nonuniform size, shape, and spacing permitted by MUFS (right).

3.2.3. Fire Suppression

The HAZUS-MH fire suppression model assumes that the fire burns uncontrolled for some initial period, representing the delay in fire response while the fire is discovered by building occupants or passersby, the fire is reported to the fire department, and the firefighters travel to the fire's location (FEMA 2003a). Each component of this initial delay is modeled empirically from historical urban fire events.

This approach is preserved in MUFS's timeline of urban fire development. The firefighters arrive at some time after the fire's ignition; the length of this delay can be specified by the user or modeled empirically as described above.

Once the firefighters arrive at the fire scene, their ability to control the fire's spread is dependent on the number of fire engines and the flowrate of water available from hydrants adjacent to the fire's location, as stated in Section 3.1. The *available* water and fire trucks are measured against the *needed* water and fire trucks in both HAZUS-MH and MUFS, but the models differ in how they determine the needed resources. The HAZUS-MH fire suppression model uses empirical relations to specify

the number of engines and amount of water needed to fight the fire based on the number of structures which have already been burned (FEMA 2003a). MUFS uses HAZUS-MH's approach to determine the number of needed fire trucks but calculates the amount of water needed based on building-specific parameters such as structure size, construction materials and fireproofing techniques, and the structure's contents. The equation MUFS uses to calculate the needed water and the method used for determining the time period over which this water must be applied (and thereby the needed rate of flow of water from the hydrants) are described in Section 3.5.3.2.

Perhaps the most significant difference between the models occurs in the precision of the reported results. Although HAZUS-MH can incorporate detailed information about urban layout and the water system, the results of its simulations are aggregated at the level of individual census tracts. Thus, investigating an urban fire's effect on a single building is not possible using HAZUS-MH. In contrast, MUFS does report fire consequences in terms of individual buildings, so a more detailed analysis of buildings affected by the fire is possible using MUFS simulation output.

The remainder of this section is devoted to presenting a detailed explanation of MUFS's simulation processes.

3.3. MUFS Data Requirements

Because the Model of Urban Fire Spread's calculations are highly tailored to the individual community being examined, the model is heavily dependent on user inputs of information about the system. Before beginning a detailed discussion of how the model

works, it is useful to present an overview of the inputs needed for the simulations and the format these inputs should adopt.

3.3.1. Urban Area Topology: Building Map and Building Properties

The most important input to the Model of Urban Fire Spread is detailed, building-specific information about the urban topology, including the coordinates of the vertices of each building. Other information necessary for the fire spread and suppression calculations includes the building's area and height, its usual number of occupants, and information about the building's fireproof construction and the fire hazard posed by its contents The building's Occupancy Hazard Classification (OHC) is an integer measure of the fire danger posed by the building's contents. OHC values are discussed in greater detail in Section 3.5. The building's Exposure Factor (EF) indicates whether the building is close enough to its nearest neighbors to pose an exposure hazard to surrounding buildings if it catches fire. This property has a value of 1 if the building is smaller than 100 ft^2 in footprint or more than 50 feet away from its nearest neighbors and would not pose an exposure risk to the surrounding area if it caught fire. Otherwise, the value of this parameter is 1.5 (Eckman 1994). The building's Construction Classification Number (CCN) represents the level of fireproof construction techniques employed in constructing the building. A value of 1.0 indicates general construction practices; lower values indicate fire-resistive or fireproof construction (Eckman 1994). Occupancy Hazard Classification, Exposure Factor, and Construction Classification

Number are used to calculate the amount of water required to extinguish a burning building; these values are used in the calculations described in Section 3.5.3.2.

Values for these parameters for some of the buildings in Micropolis are shown in Table 3.1 below. In the computer code developed for this study, the building information was stored in two ASCII files – one for building topology information and one for building properties – with information about buildings linked by unique building ID values.

3.3.2. Water Distribution System Information

In order to calculate the amount of water available for firefighting, MUFS must have detailed information about the layout and connectivity of the community's water distribution system. The study reported here used data from the hydraulic network modeling system EPANet (Rossman 2002).

The hydraulic model should include fire hydrant nodes, which MUFS uses to apply fire demands during the simulation of fire suppression. The fire hydrants should be installed with check valves which permit flow out of the hydrants but not into the system. This requirement is designed to prevent modeling inaccuracies in the fire suppression simulation and is related to how MUFS calculates the amount of firefighting water available. During the fire suppression simulation, if MUFS is unable to obtain the needed fireflow at firefighting pressure by simply imposing a fireflow demand, it changes the fire hydrant node from an ordinary junction node to an "emitter" node to determine how much water is available at firefighting pressure. If negative pressures

exist at the hydrant node (which can be caused by heavy damage or excessive demands on the water distribution system), an emitter will permit the simulated flow of water *into* the water distribution system, although no source of input water exists at the emitter node. Installing check valves immediately upstream of the fire hydrants prevents this inaccuracy from occurring.

MUFS uses the hydrants' coordinates to locate the closest hydrant to a burning building and accesses the water distribution system model at a precise location once it has located the correct hydrant for firefighting. This process is discussed in further detail in Section 3.5.2.

3.3.3. Fire Truck Availability Schedule

The final required input to the MUFS simulation is a schedule of when fire truck resources become available to the community. A community's own fire trucks are immediately available for deployment to a fire, even though there is some delay in fire response associated with travel time to the fire's location. Thus, the resources located in the community should be listed in the schedule as being available at the start of the simulation; actual firefighting does not begin until the delay in fire response specified by the modeler.

Many fire departments have mutual-aid agreements with the fire departments of surrounding communities. If the community's firefighting resources are overwhelmed, it may call on its mutual aid partners, who will deploy additional fire trucks. These fire trucks will arrive some time after the fire begins, because of the delay involved in the

target community's calling for mutual aid and the travel time between the donor and target communities. The delay before these additional firefighting resources become available is captured in the fire truck availability schedule. The fire truck availability schedule for "Micropolis," the model community used in this study, is shown graphically in Figure 3.3.

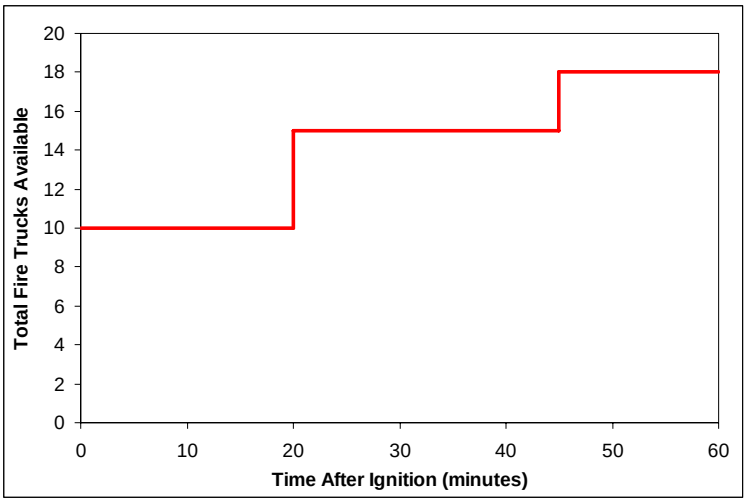

Fig. 3.3. Fire truck availability schedule for Micropolis.

3.4. Unsuppressed Fire Spread

Like the original Hamada model of urban fire spread, MUFS calculates the fire's propagation in four directions relative to the wind vector: downwind, the direction wind is blowing; upwind, the direction of the wind's origin; sidewind-left, the direction which is 90 degrees counter-clockwise from downwind or immediately to the left of a person facing in the downwind direction; and sidewind-right, which is offset 90 degrees clockwise from downwind.

The fire's progress in each of the four directions depends in part on the buildings' thickness along the fire spread direction (represented as *a*) and their separation from each other (*d*). The original Hamada equations assumed square buildings of uniform size and spacing, so a single set of values for the buildings' *a* and *d* parameters could be applied to the entire urban area. As shown previously in Figure 3.2, MUFS permits an added degree of realism by allowing buildings to vary in size, shape, and layout; thus, it is necessary to calculate each building's *a* and *d* values separately.

3.4.1. Calculating Building-Specific Urban Layout Properties

The first step in calculating unsuppressed fire spread is to find the buildings which lie along each of the four fire spread vectors and determine their a and d values. MUFS does this by searching for intersections between the fire spread vectors and every face of each building. With the exception of the ignition buildings – the buildings in which the ignition points lie – every building which lies on a fire spread vector has at least one entry and exit point. (The program distinguishes between entry and exit points based on their distance from the fire's ignition point.) For each building, the distance between the entry point and the exit point is the building's thickness along the fire spread vector, or its *a* value. Similarly, the distance from the building's exit point to the next building's entry point is the two buildings' separation along the fire vector, and this *d* value is assigned to the building the fire has just left. (Therefore, the last building the fire spread vector intersects before it leaves the urban area has no *d* value assigned, because the vector never enters another building.)

Because the fires start inside the ignition buildings, these buildings have an exit point in each fire spread direction but no entry point. The ignition building's *a* value, which can be different in each direction, is the distance between the ignition point and the fire vector's exit point. The ignition buildings' *d* values are calculated in the same manner as other buildings which intersect the fire spread vector. The *d* values for the ignition buildings may also be different in each fire spread direction.

3.4.2. Calculating Fire Spread Distance

Once it has calculated the *a* and *d* values for the buildings along the fire spread fronts, MUFS has all the information it needs to calculate the unsuppressed fire spread distance for each time step. Although fire suppression does begin at some user-specified time, the model calculates unsuppressed fire spread distance for each time step in the simulation. This is because the fire suppression calculations require a time period for each burning building over which the water for fire suppression must be applied. The unsuppressed burn duration of the building is the logical maximum period over which the firefighting water must be applied, because if the water is *not* applied over this time period the fire front will spread to the adjacent buildings. The water application time is calculated as the elapsed time between the fire front's entry into the building and its exit from the building. Therefore, it is necessary to run the unsuppressed fire spread calculations for the entire length of the simulation even though the unsuppressed burning period may be only a small fraction of the total simulation length.

The unsuppressed fire spread calculations proceed as follows. In each direction and for each time step, the model calculates each ignition point's incremental fire spread according to equations 3.1-3.3, which were preserved from the HAZUS Fire Following Earthquake model (FEMA 2003a) and adapted from the original Hamada model:

$$K_d = \frac{(a+d)}{T_d} - t \tag{3.1}$$

$$K_u = \left(\frac{a}{2} + d\right) + \frac{(a+d)}{T_u}(t - T_u) \tag{3.2}$$

$$K_s = \left(\frac{a}{2} + d\right) + \frac{(a+d)}{T_s}(t - T_s) \tag{3.3}$$

where K_d, K_u, and K_s are the incremental fire spread distances in meters calculated in the downwind, upwind, and sidewind directions, respectively. The variable a represents the thickness (measured in meters) of the building which the fire currently occupies projected along the direction of fire spread and d is the currently-burning building's separation in meters from the next building along the fire spread vector. The length of the simulation time step is represented by the variable t. The variables T_d, T_u, and T_s represent the amount of time the fire takes to spread, in each direction, throughout the length of one building plus the space separating it from the next building. In other words, T_d is how long the fire takes to spread the distance $(a + d)$ in the downwind direction, and T_u and T_s are similar measures of fire propagation time in the upwind and

sidewind directions. These propagation times are calculated by MUFS, following the techniques used by HAZUS-MH (FEMA 2003a), using equations 3.4-3.6 below:

$$T_d = \frac{1}{1.6(1+0.1V+0.007V^2)}\left[(1-f_b)\left(3+0.375a+\frac{8d}{25+2.5V}\right)+f_b\left(5+0.625a+\frac{16d}{25+2.5V}\right)\right] \quad (3.4)$$

$$T_u = \frac{1}{1+0.002V^2}\left[(1-f_b)\left(3+0.375a+\frac{8d}{5+0.2V}\right)+f_b\left(5+0.625a+\frac{16d}{5+0.2V}\right)\right] \quad (3.5)$$

$$T_s = \frac{1}{1+0.005V^2}\left[(1-f_b)\left(3+0.375a+\frac{8d}{5+0.25V}\right)+f_b\left(5+0.625a+\frac{16d}{5+0.25V}\right)\right] \quad (3.6)$$

where V is the wind velocity in meters per second and f_b is a numerical representation of the percent of the building which employs fireproof construction techniques. This variable is dimensionless and ranges in value from 0 to 1.

It is noted that equations 3.1-3.3 and 3.4-3.6 have different forms for each direction. This is due to the wind's effect on the rate of fire spread, which is different for each direction. Fire spread in the downwind direction is driven by the wind, so higher wind speeds contribute to a greater rate of fire spread. Conversely, fire spread in the upwind direction goes against the wind in order to make progress, so higher wind speeds contribute to lower rates of fire spread. Sidewind-direction fire spread is intermediate in speed, so the sidewind-left and sidewind-right directions use a third fire spread equation.

In this model it is assumed that the community has a single prevailing wind direction and a constant wind speed. In reality, both wind speed and direction may vary

spatially and temporally. This ability is not currently incorporated into MUFS because of practical limitations on computational complexity; however, enabling the simulation of fire spread under changing wind speed and direction is a topic for future research.

Each of the six equations listed above uses a, d, and f_b values for the building in which the fire resides at the beginning of the time step. If the fire front moves into a new building or buildings during the time step, then MUFS recalculates fire spread using values of the building-specific parameters averaged over the relevant buildings in the time step.

After MUFS has calculated the fire spread for each ignition point and each time step, it determines the time at which the burn front enters and exits each building in order to calculate the buildings' burn durations (represented as T_{burn} in later equations).. When an urban fire simulation includes multiple ignition points and more than one ignition point's fire front intersects a building, the burn front which reaches the building first is used to calculate its burn duration. This is reasonable because an area cannot burn twice; therefore, the fire front which reaches an area first will be the front which actually ignites the area.

3.5. Suppressed Fire Spread

Once the program has run the unsuppressed fire spread calculations and determined the buildings' burn durations, MUFS is ready to begin simulating fire spread under suppression efforts. Once the firefighters arrive at the scene of the fire, there are two possible outcomes of the fire suppression effort, If the firefighters have enough fire

trucks and water at adequate pressure and flowrate to extinguish the fire, then the firefighters achieve totally effective fire suppression and the fire's progress halts in that direction. Because MUFS simulates fire suppression under disaster conditions, however, the fire department and water distribution system may not be able to provide sufficient resources for totally-effective fire suppression. In this case, MUFS calculates a reduced rate of fire spread based on the ratio of available resources to needed resources.

The main task of the suppressed fire spread module is to allocate fire trucks and water for firefighting at each time step. This process begins with the deployment of fire trucks to the burning buildings.

3.5.1. Fire Truck Assignment

The number of fire trucks available is a user input to MUFS, and this value can change over time to reflect the arrival of additional fire trucks after a short delay, in fulfillment of mutual aid contracts between the target community and other nearby jurisdictions. MUFS checks at each time step to see if any new fire trucks have arrived.

At each time step, the buildings currently burning are sorted in order of firefighting priority. MUFS currently allows the user to choose whether to prioritize firefighting by the building's number of occupants or the flammability of its contents, which is represented by the building's Occupancy Hazard Classification ("OHC"; Eckman 1994). OHC numerical values are inversely related to firefighting priority. Buildings with highly flammable contents (e.g., flour mills, lumber yards, textile factories, etc.) are high priority assignments for fire truck assignment and have low OHC

values; buildings with lower quantities of flammable contents (e.g., apartments, schools, hotels, etc.) are lower priority assignments and have high OHC values. Typical values of OHC, determined by the building's use and typical contents, are presented in Table 3.1. As discussed below, the OHC also is used to calculate the volume of water required to extinguish fire in a building.

Table 3.1. Typical Occupancy Hazard Classification Values (Adapted from Eckman 1994)

OHC	Description	Example Buildings
3	Severe Hazard Occupancies	Explosives storage, lumberyards, baled straw or hay storage, plastics manufacturing
4	High Hazard Occupancies	Building materials storage, Department stores, Auto repair garages, Warehouses
5	Moderate Hazard Occupancies	Libraries, Restaurants, Abandoned Buildings
6	Low Hazard Occupancies	Churches, Gas Stations, Funeral Homes
7	Light Hazard Occupancies	Residential Dwellings, Hotels, Schools

Starting with the highest-priority burning building, MUFS assigns one fire truck per building until all trucks are assigned. Once a fire truck arrives at its target building, it locates the nearest serviceable fire hydrant. This is the fire hydrant closest to the building vertex nearest to the burn front. However, to protect the safety of the firefighters, the target fire hydrant must not lie inside the polygon which defines the burning area. In addition, the fire hydrant must be located within 1000 feet of the

building vertex nearest to the burn front: a practical limitation imposed by the excessive friction loss caused by laying long suction lines from the hydrant to the fire truck (Eckman 1994).

3.5.2. Water Distribution System Interface

When each fire truck has been assigned a target building and fire hydrant, MUFS accesses the water system to determine the available fire flow. To do this, MUFS uses the EPANet hydraulic model (Rossman 2002) to impose a firefighting demand of 1000 gallons per minute (gpm) for each target fire hydrant, which is a typical flow rating for a fire engine's onboard pump (Mahoney 1980). If more than one fire truck is assigned to a hydrant, multiple fire demands may be imposed. Using the EPANet software, MUFS then checks the pressure at each of the target hydrant nodes. Water for firefighting must be delivered at the hydrant at a minimum pressure of 20 pounds per square inch (psi) (NFPA 2006). If the pressure at the target hydrant is greater than or equal to 20 psi, the hydrant is able to supply the needs of the fire truck(s) connected to it and the truck or trucks receive the full 1000 gpm.

If the water distribution system is unable to supply the needed firefighting demand at the minimum pressure, due to excessive demands on or damage to the system, MUFS determines how much water the system can provide at the minimum firefighting pressure. To do this, the model removes the fire flow demands from the insufficient-pressure hydrant nodes and converts them to emitter nodes, which behave in the hydraulic model like uncontrolled orifices through which water flows at a rate

determined by the opening size and water pressure. (Hydrants which can provide fire flows at adequate pressures are not converted to emitters, but their fire flow demands are left in place for the length of the time step.) The elevation of each emitter node is increased by 46 feet, which is the elevation head equivalent of a pressure of 20 psi. This step guarantees that any flow the emitter can provide will exit the emitter at a pressure of 20 psi. The node's emitter coefficient is set to 1850 gpm/psi$^{1/2}$, which is appropriate for a fire hydrant with a ten-inch orifice (derivation of this value is shown in Appendix 1). The program then re-runs the hydraulic analysis; the flow from the emitters, if any, represents the flow that the hydrants can provide at a pressure of 20 psi. This flow is supplied to the fire trucks, and if more than one truck is connected to a hydrant the available flow is divided evenly among the connected trucks.

It was determined during model testing that the EPANet model of the water distribution system should include check valves in the pipes connecting the hydrants to the water system, because if the hydrant nodes experience negative (suction) pressures during firefighting operations, the emitters will simulate water flow *into* the water distribution system. This is not consistent with actual physical circumstances, and installing check valves at the hydrants permits water to flow out for firefighting but prevents flow into the system due to negative pressures.

3.5.3. Factors in Fire Suppression Effectiveness

Once MUFS has assigned the fire trucks and tapped the water distribution system to determine the available fire flow, the model has half of the information it needs to

calculate suppression effectiveness: the number of fire trucks and amount of water which are actually *available*. These values must be compared, however, to the number of trucks and amount of water which are *needed* to suppress the fire.

3.5.3.1. Trucks Needed

HAZUS-MH prescribes an empirical formula for determining how many fire trucks are needed based on the total number of burned buildings (FEMA 2003a). MUFS calculates the number of buildings burned at the beginning of each time step at the same time the currently-burning buildings are determined. Both operations are based on the previous time step's burn polygon. Currently-burning buildings are those with some (but not all) vertices inside the burn polygon; the tally of burned buildings includes buildings with any number of vertices inside the burned area. This total count of burned buildings is the basis for determining the number of fire trucks needed based on the relationship adopted from HAZUS-MH, shown in Figure 3.4.

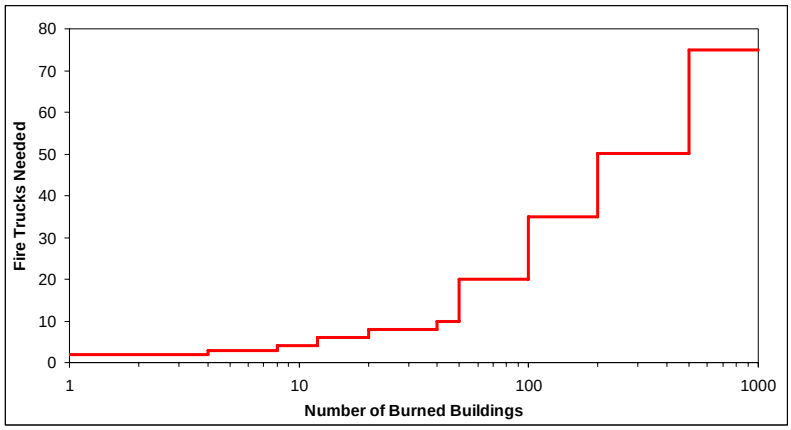

Fig. 3.4. Number of fire trucks needed to extinguish an urban fire based on how many buildings are burned. Adapted from FEMA (2003a).

For multi-ignition fires, MUFS calculates the number of trucks needed separately for each ignition point, and the number of fire trucks assigned to each ignition is tabulated separately as well.

3.5.3.2. Water Needed

The amount of water needed to extinguish a burning building is calculated separately for each building. The total volume of water needed is recommended by the National Fire Protection Association (NFPA 1993 cited in Eckman 1994) as:

$$TWS = \frac{Vol}{OHC} \cdot CCN \cdot EF \qquad (3.7)$$

This formula uses common and readily-available information to calculate the volume of water needed. In the equation above, *TWS* is the total water supply in gallons needed to suppress the fire. *Vol* refers to the volume of the structure in cubic feet. *OHC*, the structure's Occupancy Hazard Classification, is a dimensionless indicator of a building's hazardous or inflammable contents. OHC values are integers ranging from 3 (for high-hazard buildings like explosives storage facilities) to 7 (for low-hazard buildings like homes, fire departments, and schools). *CCN*, the structure's Construction Classification Number, is a dimensionless indicator of the burning structure's fireproofing: a minimum *CCN* of 0.5 indicates a fire-resistant structure made of fireproof materials and designed to withstand fire, whereas a maximum *CCN* of 1.5 indicates a wood frame building. The final parameter in the above equation *EF* is the building's Exposure Factor, is a

multiplier to incorporate the extra water supply needed when a burning structure is located close to other structures and poses an exposure risk to its unburned neighbors. This parameter is 1.0 when buildings present no particular exposure risk; its value is 1.5 when other buildings are located less than 50 feet from the burning structure.

It is important to note that the water *needed* for firefighting is specified as a volume of water, whereas the water available for fire fighting is calculated as a volumetric flow rate. In order to compare the two values, it is necessary to express them on the same basis; one way to do this is to convert the volume of water needed for fire suppression into the required flow rate by dividing the volume by an appropriate application time.

As explained above in Section 3.4, this needed application time is the motivation for calculating the unsuppressed burn duration of each building which could possibly be touched by the fire. The reason for using this time is that it represents a logical maximum period over which the firefighting water can be applied – because if the fire is not suppressed within this time period, the fire front will move on and consume adjacent buildings. Thus, the minimum flow rate required for effective fire suppression is given by dividing the needed water volume (equation 3.7) by its maximum possible application time length (equation 3.8):

$$Q_{needed} = \frac{TWS}{T_{burn}} \tag{3.8}$$

where Q_{needed} is the volumetric flow rate in gallons per minute (gpm) needed to extinguish the building; TWS is the amount of water (in gallons) needed to suppress the

fire, as calculated in Equation 3.7; and T_{burn} is the unsuppressed burn duration (in minutes) calculated for the building.

3.5.4. Fire Suppression Effectiveness: Adjusting Fire Propagation Rate for Available Fire Suppression Resources

When MUFS has determined the needed and available firefighting resources, the next step is to adjust the normal (unsuppressed) rate of fire spread to account for partially- or totally-effective fire suppression. Following the fire suppression algorithm contained in the Fire Following Earthquake module of HAZUS-MH (FEMA 2003a), MUFS calculates the ratio of available water and fire trucks to the needed resources:

$$R_{truck} = \frac{N_{Trucks,\,available}}{N_{Trucks,\,needed}} \tag{3.9}$$

$$R_{water} = \frac{Q_{available}}{Q_{needed}} \tag{3.10}$$

where $N_{trucks,needed}$ is the number of fire trucks predicted to be needed to suppress the ignition point's fire based on the number of burning buildings; $N_{trucks,available}$ is the number of fire trucks actually assigned to the ignition point; Q_{needed} is the volumetric flow rate (in gpm) prescribed to extinguish the fire at a specific building; and $Q_{available}$ is the volumetric flow rate (in gpm) actually available for firefighting from the water distribution system.

Next, the program calculates the incremental unsuppressed fire spread distance in each fire spread direction for each ignition point. It is necessary to re-run these calculations for the current time step, even though they were run previously for the entire simulation length, because the unsuppressed fire spread calculations rely on building-specific characteristics and the time step's building data may have changed due to fire suppression in an earlier time step. The incremental unsuppressed fire spread distance is calculated as described in Section 3.4, using equations 3.1 – 3.6.

The unsuppressed fire spread distance is a baseline fire spread distance for the time step: a maximum distance which can be reduced based on the success of the firefighting efforts. The reduction factor, adopted from the HAZUS-MH fire suppression algorithm (FEMA 2003a), is calculated using Equation 3.11 below, which requires the truck and water ratios calculated using Equations 3.9 and 3.10:

$$P_{effective} = \max\left\{(R_{truck} \cdot R_{water})^{0.7},\ 0.33 \cdot R_{truck}\right\} \tag{3.11}$$

In Equation 3.10, $P_{effective}$ is a unitless reduction factor ranging in value from 0 to 1. It has a minimum value of one-third the value of R_{truck} calculated in equation 3.9.

Using methodology derived from HAZUS-MH (FEMA 2003a), this reduction factor is used to adjust the incremental fire spread distance according to Equation 3.12:

$$K_{d,\text{sup pressed}} = K_{d,non-\text{sup pressed}} \cdot (1 - P_{effective}^{0.7}) \tag{3.12}$$

In this equation, $K_{d,suppressed}$ is the incremental fire spread distance under fire suppression and $K_{d,non\text{-}suppressed}$ is the incremental distance the fire would spread if it were totally

unsuppressed. $K_{d,non\text{-}suppressed}$ is calculated as described in Section 3.4.2 using Equation 3.1, 3.2, or 3.3 (depending on the fire spread direction).

If the fire department has all the resources it needs for totally effective fire suppression – i.e., R_{truck} and R_{water} are both equal to 1 – then the reduction factor calculated in Equation 3.10 above is also equal to 1 and the suppressed incremental fire spread distance is zero. In this case, the fire's progress in that direction halts and does not re-start at a later time step. Since the reduction factor is calculated separately in each fire spread direction, the fire may halt in some of an ignition point's fire spread directions and continue to progress in other directions.

If either R_{truck} or R_{water} is less than 1, the fire undergoes partially effective suppression. This means that the fire's progress slows and the time step's incremental suppressed fire spread distance is less than its unsuppressed value, but the fire's progress does not halt. The reduced fire spread distance is calculated using Equation 3.11 above.

It is important to note that R_{truck} and R_{water} are calculated separately for each ignition point and for each time step, and the values may change over time and between ignition points. R_{truck} may be different for each ignition point in a multi-ignition fire even within the same time step, and this is likely in cases where one ignition point is located in an area which receives high priority for fire suppression (due to a concentration of buildings with high population or low OHC) and another ignition point is located in an area with lower fire suppression priority. If there are not enough fire trucks to meet the needs of every burning building, then the high-priority ignition point will receive more fire trucks and will consequently have a higher R_{truck} value than the

low-priority ignition point. All fire spread directions within the same ignition point have the same R_{truck} value; this is because the number of fire trucks needed is determined for the entire ignition point and cannot be resolved to the level of individual buildings or fire spread directions. The heuristic rule used to determine how many fire trucks are needed at an ignition point was adopted from HAZUS-MH, which does not determine fire suppression effectiveness at the level of individual buildings. Using fire suppression effectiveness metrics which were designed for different scales of spatial resolution may introduce some uncertainty into the fire suppression calculations. Development of building-scale recommendations for fire truck assignment would improve the accuracy of the calculations, and integrating more precise fire truck assignment recommendations is a goal of future model development.

The methodology used to calculate the amount of water needed for fire suppression was adopted from the National Fire Protection Association (NFPA 2006) and is applicable at the level of individual buildings. Therefore, the value of R_{water} may vary between fire spread directions associated with the same ignition point. Buildings are assigned to the nearest fire spread direction for the purpose of calculating R_{water}. For each burning building, the nearest fire spread direction is the one whose front point is nearest to the building vertex which is closest to the fire front.

The process of assigning fire trucks, imposing firefighting demands, determining R_{truck} and R_{water}, and calculating the fire suppression effectiveness is repeated for each time step from the beginning of fire response until the end of the simulation.

3.6. MUFS Simulation Results

3.6.1. Burn Front Coordinates

MUFS converts the fire spread vectors calculated using the Hamada fire spread equations to X-Y coordinates using a straightforward application of vector mathematics. For each fire spread vector, MUFS uses the vector's total length at each time step and the vector's angle to decompose the vector into its X and Y components. These components, when added to the X-Y coordinates of the ignition point, yield the X-Y coordinates of the fire front points.

3.6.2. List of Burning Buildings

Once the coordinates of the fire front boundary points are known, MUFS determines which buildings are totally burned or in the process of burning at the end of the simulation. The list of burned and partially-burned buildings is an important output because the consequences of the multi-mode attack and failure simulations conducted with MUFS are recorded as the number of people who are displaced – that is, people who lose their home and/or place of employment – because of the fire. To calculate this value, MUFS must know which buildings are partially or totally destroyed.

MUFS locates the burning buildings by checking each building in the urban area to see whether some or all of its vertices are inside the burn polygon. Currently, the list of burned buildings does not distinguish between partially-burned buildings (some, but not all, vertices inside the burned area) and totally-burned buildings (all vertices inside the burned area), but this distinction is possible if it is desired in the future.

If any of a building's vertices are inside the burned area, the building is counted as a burned building in the determination of the urban fire's final consequences.

4. METHODOLOGY: ANALYZING VULNERABILITY TO MULTI-MODE ATTACKS AND FAILURES

4.1. Introduction

Understanding the potential consequences of a multi-mode attack or failure (MMAF), an attack or disaster which simultaneously disables one or more support infrastructures for fire response and ignites an urban fire, is the first step in designing mitigation strategies to prepare for and lessen the impact of this type of event.

Several different methods are presented as alternatives for exploring the potential consequences of an MMAF in an example community. The relative advantages of each technique are discussed as well, and the results and interpretation of each technique will be presented in Section 5. The process of designing and testing mitigation strategies based on these results will be presented in Section 6.

4.2. Overview of Vulnerability Analysis

The main goal of the multi-mode attack or failure vulnerability assessment is to provide a detailed understanding of the progress and expected consequences of a disaster involving an urban fire with disabled water system and/or other support infrastructures. Simulating this type of event across a wide variety of attack and disaster scenarios yields insight into the most frequent and worst-case consequence profiles.

It is useful to examine each mode of a multi-mode attack or failure separately before discussing the consequences of the modes' joint action. Sections 4.3.1 through

4.3.6 will present the procedure for modeling damage to a community water distribution system. Sections 4.3.7 through 4.3.9 will discuss the methodology for modeling damage to the communications or transportation infrastructures, which can impede fire response.

Section 4.4 contains a scenario-based method used to determine ignition points for the urban fire aspect of the multi-mode attack or failure. The overall procedure for modeling MMAF scenarios – a synthesis of the support infrastructure damage scenarios covered in Section 4.3 and the urban fire scenarios covered in Section 4.4-- is discussed in Section 4.5

Conducting scenario-based simulations of multi-mode attacks or failures is only one potential method for determining the possible range of consequences of this type of disaster. A complementary method for determining the worst-case fire ignition points based on optimization is presented in Section 4.6.

Once each mode of the multi-mode attack or failure is specified, the facets of the disaster are combined and simulated together using the Model of Urban Fire Spread (MUFS), which was described in Section 3. The results of the multi-mode attack and failure simulations will be presented and discussed in Section 5.

4.3. Damage Scenarios: Water System

Water distribution networks are complex systems, and the types of vulnerabilities they may face are numerous. In order to model attacks on water systems and recommend protective strategies, it is necessary to identify the most likely modes of attack on the water system. Indeed, water utilities across the United States have already completed

this process as the first step in hardening the nation's water infrastructure., as required by the Bioterrorism Preparedness Act (PL 107-88).

The first step in this project's vulnerability analysis for multi-mode attacks and failure scenarios is to select a small set of attack/failure scenarios centered on the community's water distribution to disable its fire response The selection process focuses both on the physical ease of access required to the system and on the probable magnitude of the resulting damage.

Without a specific water system for consideration, however, it is impossible to provide more than a general listing of potential vulnerability types. Due to heightened security concerns after the 9/11 terrorist attacks, it is difficult to obtain a sufficiently detailed electronic model of a real community water system and publish the results of an in-depth vulnerability analysis. Therefore, a detailed "mock city" water system model was used to conduct the vulnerability analysis and explore the effect of a multi-mode attack/failure on a realistic city without presenting a security risk to a real community. The Micropolis model (Brumbelow et al. 2006), developed at Texas A&M University, is a detailed and realistic model of a fictional small town (pop. 5,000) implemented in geographic information system (ArcGIS 9) and hydraulic modeling (EPANet) software.

Micropolis obtains its water from two sources, a surface-water reservoir and a small community wellfield. Water from these sources is combined and treated at a single water treatment plant. After the water treatment plant, three identical high-service pumps operating in parallel convey the water to the distribution network.

Pipe diameters for water mains range from two inches (original cast iron mains located primarily in the central business district) to twelve inches (modern ductile-iron mains located primarily in the outlying regions of the city). Under peak normal or fire demands the system experiences considerable head loss in regions with low-diameter mains. The city has a single elevated storage tank, located in the central business district, with a maximum storage volume of approximately 50,000 cubic feet.

4.3.1. Damage Profile A: Long-Term Damage to High-Service Pumps

A series of attack and damage scenarios affecting the Micropolis water distribution system were modeled in the hydraulic modeling software, EPANet. The first category of attacks/failures involves the long-term incapacitation of one or more of the high-service pumps which supply water to the city. This situation could arise from a variety of causes: sabotage against the water system, long-term power failure, or an accident or natural disaster which destroys or does serious damage to the pumps and cannot be repaired within a few hours. The affected pumps were shut down for the duration of the simulation; this condition is modeled in EPANet by setting the status of the affected pump(s) to "Closed," which can be done easily through the EPANet user interface. Damage profile A01 featured all three high-service pumps permanently out of service. Damage profile A02 damaged two of the three high-service pumps but left one still operational. Damage profile A03 reflected damage to one pump, with the other two pumps still operating. Because the pumps are identical and are operating in parallel, the

number of pumps in service is important but the identity of the specific individual pump(s) sustaining damage has no bearing on the scenario's consequences.

4.3.2. Damage Profile B: Short-Term Power Outage to Pumps

Like Scenario A, Scenario B examines the consequences of pump incapacitation during a multi-mode attack or failure. The damage profiles modeled in this category, however, involve short-term damage to the system's pumps, and the pumps are restored to operation after a period of incapacitation. This scenario was intended to model the effects of power outages, in which the pumps stop operating when they are not supplied with electric power (if the water system has no backup generator) but come back online when power is restored.

This condition was modeled in EPANet by operating the system pumps on simple time-based operation patterns. EPANet permits the user to enter operation levels for each hour of the day. The patterns used to model the conditions represented in this category had a value of "0" (totally inoperable) during the pumps' down time and a value of "1" (fully operational) at all other times. This pattern was applied to all pumps in the system, because the high-service pumps are located close to the smaller pumps which supply water from the reservoir and wellfield to the water treatment plant. Because of the pumps' close spatial grouping, it was assumed that they all operated from the same power feed.

Damage scenario B01 features a loss of power for two hours at the beginning of the simulation. After two hours, power is restored and all pumps operate normally

thereafter. Damage scenario B02 imposes a four-hour power loss at the beginning of the simulation. In damage scenario B03, the pumps operate normally at the beginning of the simulation, but they lose power after two hours for a duration of two hours, and then regain power for the remainder of the simulation.

The proposal for this dissertation called for a damage profile C, which involved the destruction of the pipe which runs from the high-service pumps to the distribution grid. In the Micropolis water system, this pipe is the only conduit from the water treatment plant to the distribution grid, and it is located immediately downstream from the system's three high-service pumps. Because of the topology of the Micropolis water system, this damage scenario is identical in impact to Scenario A01 (destruction of all three high-service pumps). Therefore, damage profile C was judged to be redundant and not modeled separately.

4.3.3. Damage Profile D: Destruction of Elevated Storage Tank

Damage profiles A and B examine the effects of compromising the city's firefighting by restricting the flow of water into the system. During times of peak demand or firefighting need, however, the city has another source of water at its disposal: water contained in the system's elevated storage tank. Many cities use their elevated storage tanks to provide surge capacity: the tanks drain during the high-demand portions of the day and refill at night. Tanks also provide the extra water needed for extinguishing large fires. Damage profile D examines the consequences of an attack or

disaster which destroys (or otherwise depletes) the city's elevated storage tank and cuts off the community's access to this surge capacity.

Scenario D01 makes the tank unavailable from the start of the simulation. This is modeled in EPANet by setting the status of the pipe which runs from the tank to the distribution grid to "Closed," so no water can enter or leave the tank. Scenario D02 cuts off access to the tank after one hour of simulation time. In both these scenarios, the system's pumps are left fully operational. Modeling a compound damage profile which destroys both pumps and storage tank, thereby limiting or eliminating all the city's sources of water for firefighting, is discussed in the next section.

4.3.4. Damage Profile AD: Destruction of Pumps and Elevated Storage Tank

Two of the model scenarios studied in this project involve a coordinated attack or severe disaster which disables the water system's pumps and the elevated storage tank. This compound damage profile combines elements from damage profile A and damage profile D. In Scenario AD1, all three high-service pumps are disabled at the beginning of the simulation. The tank is disabled after one hour of simulation time. This scenario cuts off all sources of water for firefighting after the tank is destroyed, but it is assumed in MUFS that the fire department has some fire suppression capacity even if the water system cannot provide any water. This partially-effective suppression accounts for firefighting tactics that do not rely on the water distribution system, such as drafting from alternative water sources or the use of fire-suppressing foam. Eckman (1994) describes these measures in detail.

Scenario AD2 disables only two of the three high-service pumps. These cease functioning at the beginning of the simulation and remain inoperable for the entire duration. The elevated storage tank is disabled after one hour of simulation time. The third high-service pump, along with the booster pumps serving the surface reservoir and wellfield, remain in operation for the length of the simulation.

4.3.5. Damage Profile E: Water Main Breaches

Even with adequate supply of water, a water distribution system must be able to provide water at sufficient pressure for firefighting to provide totally effective fire suppression. By causing sudden drops in pressure, a water main breach could impair a system's ability to respond to firefighting demands. The scenarios modeled in damage profile E examine this possibility.

In theory any main may be breached, but this damage profile considers the sections of water main which are most vulnerable to damage. In many communities, including Micropolis, water mains run under the streets. In locations where the roads cross streams, the pipes are above ground and attached to the underside of bridges. This comparative exposure may make the water mains more vulnerable to a deliberate attack or to a natural disaster like a flood or earthquake destroying the bridge and the attached pipes.

Four different water main breach scenarios were modeled in this study. Micropolis has seven bridges. Three of the damage scenarios involve single bridge failures; damage scenarios E01, E02, and E03 involve the destruction of the furthest

downstream, the most-used, and the furthest upstream bridge/pipe pair. Damage scenario E04 involves the simultaneous destruction of the furthest downstream and highest-use bridge/pipe pairs. In each case, the destruction of the bridges occurs at the start of the simulation. The location of the water main breaches are shown in Figure 4.1.

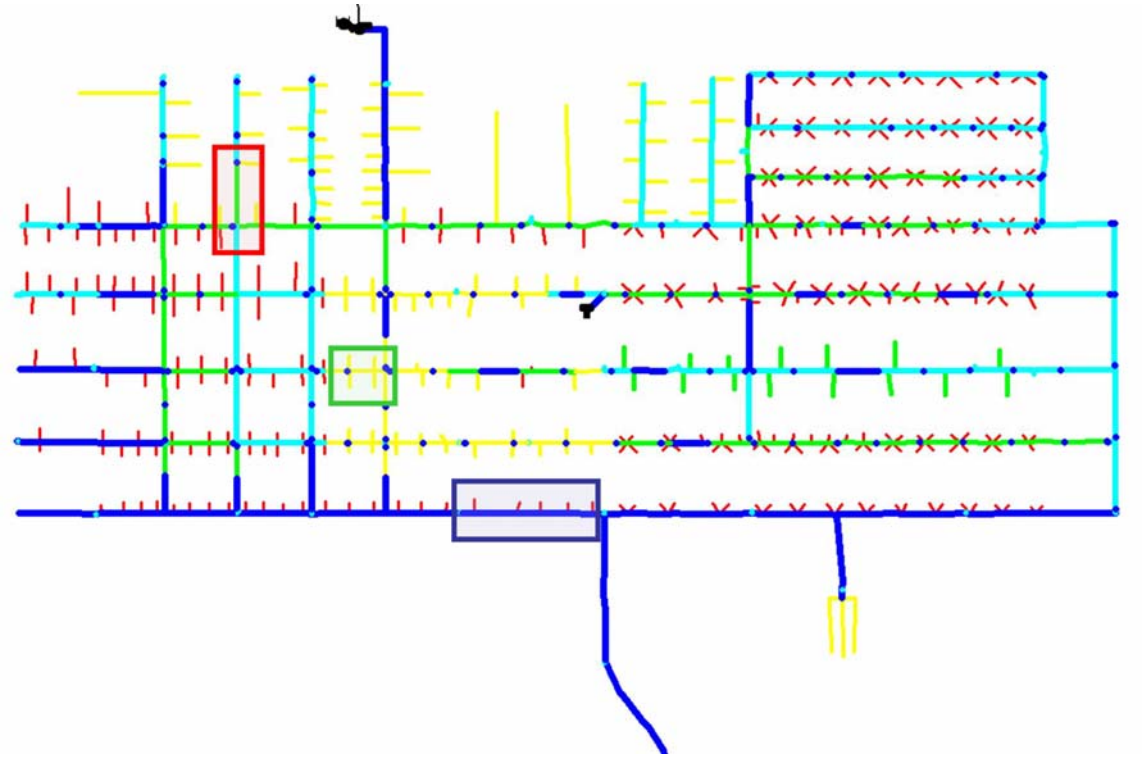

Fig. 4.1. Location of water main breaches modeled for damage profile E. The blue-shaded area is the furthest-downstream bridge and is modeled as damage scenario E01. The green-shaded area is the heaviest-traveled bridge and is modeled as damage scenario E02. The red area is the furthest-upstream bridge and is modeled as damage scenario E03. A dual breach affecting the blue and green shaded areas was modeled as damage scenario E04.

After the destruction of the bridge and the accompanying pipe breach, water flows freely from both sides of the breach for fifteen minutes of simulation time. This delay represents the water utility's efforts to control the water loss through the breach.

Flow through the open pipe ends is modeled in EPANet as an emitter at either end of the breached pipe. In EPANet, an emitter is a hydraulic device which regulates outflow through an orifice based on the area of the orifice and pressure at the emitter's location (Rossman 2002). In simple terms, this represents flow through a hole which is open to the environment. After fifteen minutes, the isolation valves on either side of the breach are closed using a simple time-based control embedded in the EPANet input file. In the Micropolis water distribution system model, there are 197 manually-operated gate valves which can be used to restrict or redirect flow in the event of a water main breach or contamination event (Brumbelow et al. 2006). Closing the isolation valves on either side of the breach cuts off the flow through the pipe breaches and restores pressurized flow to the system.

4.3.6. Damage Profile F: Isolation of Water Contamination

The final damage profile involves the water utility voluntarily isolating sections of the water distribution system in order to contain an accidental or deliberate contamination. Contamination of water distribution systems has long been a concern in the field of water systems security, and isolating the contamination as soon as possible after its discovery is often recommended as a security strategy (AWWA 2004; EPA 2002; EPA 2004). In some cases the isolated contaminated water cannot even be used for firefighting, since it may pose an inhalation or cutaneous contact hazard (Department of Homeland Security [DHS] and Texas Engineering Extension Service [TEEX] 2004).

The simulations of damage profile F investigate the effects that isolation of areas of the water distribution system may have on firefighting efforts.

Five different contaminant isolation scenarios were simulated. For each scenario, the isolation valves at all points of inflow and outflow to the contaminated areas were closed at the beginning of the simulation. In addition to cutting off flow to the hydrants in the affected areas, in many cases this forced the water for firefighting at non-contaminated locations to take alternate routes which involved higher energy loss, thereby decreasing the pressure of any water arriving at firefighting hydrants. This decreased pressure sometimes resulted in decreased available flow at the minimum required pressure.

Scenario F01 involves the isolation of a large-diameter main on the southeast side of the water distribution system. This pipe supplies water to the wastewater treatment plant and is a major conduit for water flow to the east side of town. The area affected by the isolation is shaded in red on Figure 4.2 .

In Scenario F02, the city's central business district is isolated. This scenario cuts off water flow to the center of the city, where many of the government and heavy-use buildings used as ignition points in urban fire spread simulations (described below in Section 4.4) are located. The affected area is show in Figure 4.3.

Scenario F03 simulates the response to the contamination of the water in the elevated storage tank by isolating the tank and the pipes in its immediate vicinity. This prevents firefighting efforts located elsewhere in the city from using the tank to supply firefighting water, forcing the other hydrants to rely instead upon the water which can be

supplied by the water treatment plant and high-service pumps. The isolated area for Scenario F03 is shown in Figure 4.4.

Scenario F04 models isolation of a contamination of the water supply to city's highest-density residential area. Approximately half of the city's residents live in or near the affected area; therefore, a reliable water supply to this area for drinking and firefighting is very important. The affected area is shown in Figure 4.5.

The final scenario modeled in damage profile F involves the contamination and isolation of the northwest corner of town, which is a low-population-density, high-value residential area. The affected area is indicated in Figure 4.6.

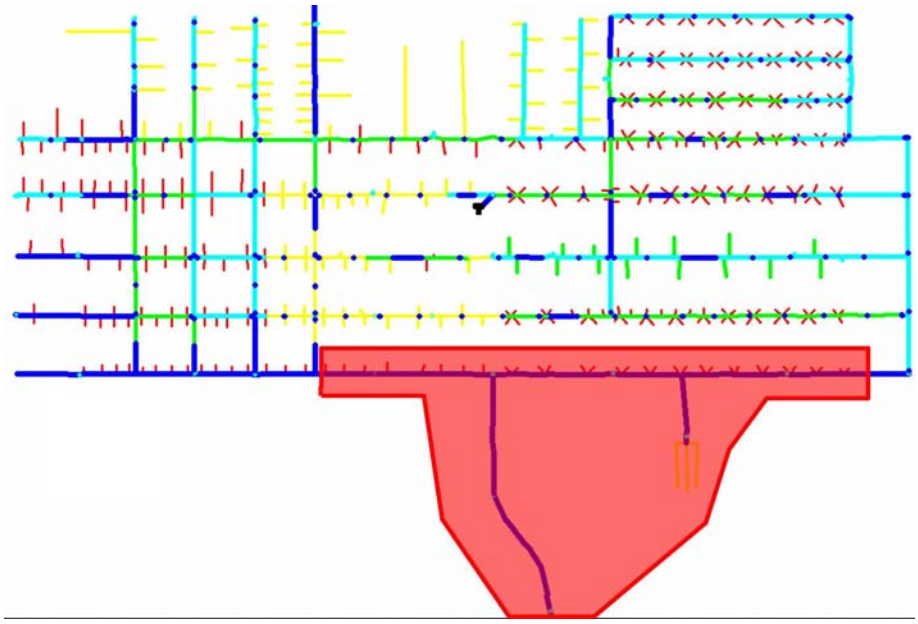

Fig. 4.2. Zone of water distribution system affected by damage scenario F01. Pipes in the water distribution system are color-coded by diameter: red pipes are 2 inches or less in diameter; yellow pipes are 4 inches; green pipes are 6 inches; cyan pipes are 8 inches; and dark blue pipes are 12 inches. Thus, the isolated zone for this damage scenario restricts passage through a section of large-diameter main which normally transmits high volumes of water to the east side of town.

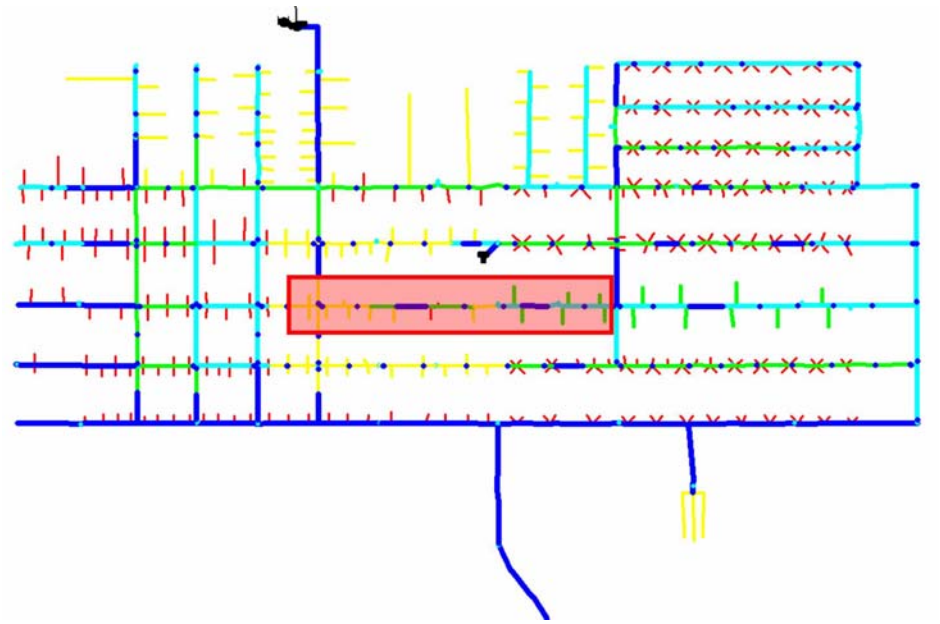

Fig. 4.3. Zone of water distribution system affected by damage scenario F02. This scenario isolates the Central Business District of Micropolis from the rest of the water distribution system.

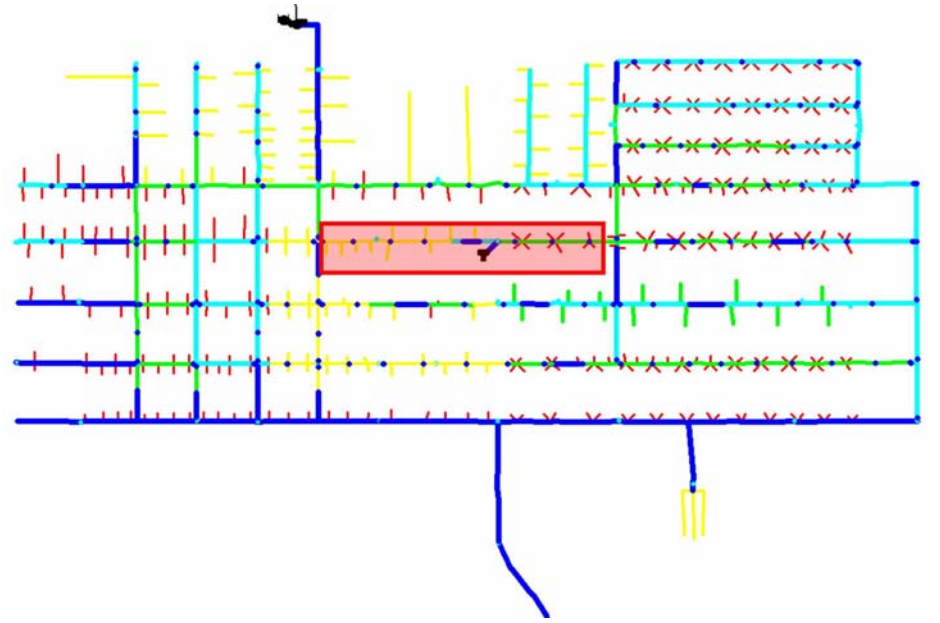

Fig. 4.4. Zone of water distribution system affected by damage scenario F03. This scenario isolates the city's elevated storage tank and the nearby water mains from the rest of the water distribution system.

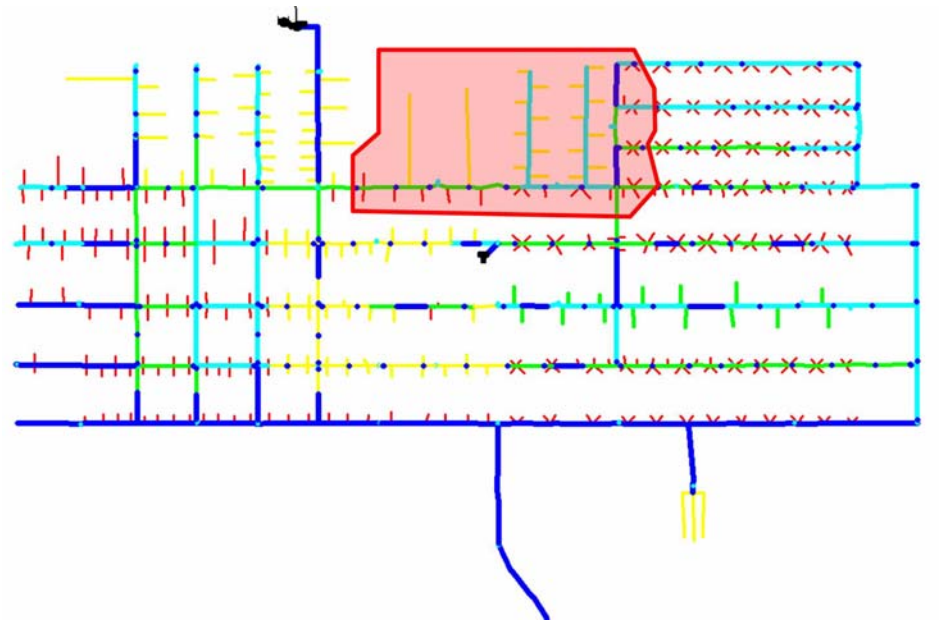

Fig. 4.5. Zone of water distribution system affected by damage scenario F04. This scenario isolates a high-population-density residential area from the rest of the water distribution system.

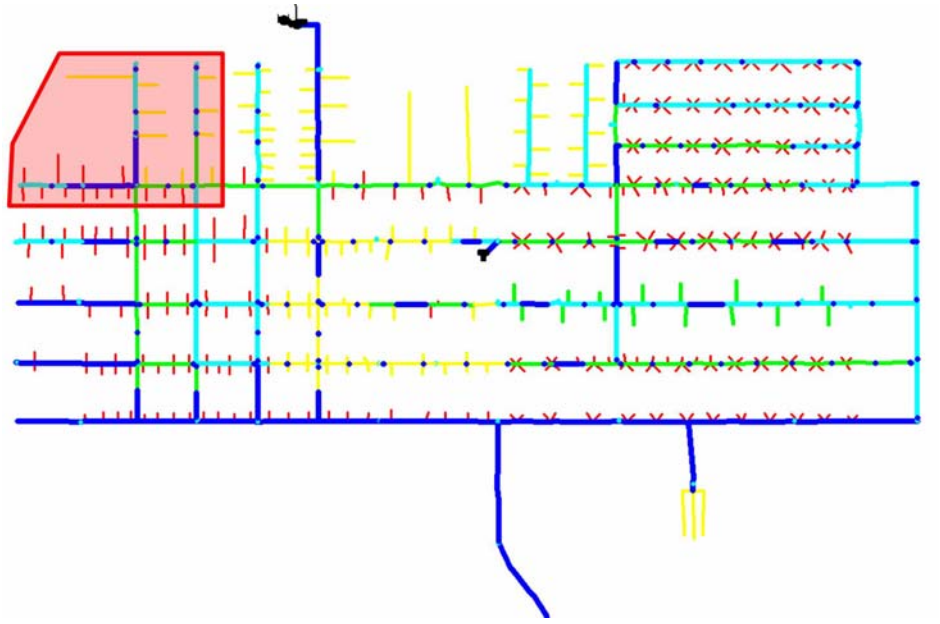

Fig. 4.6. Zone of water distribution system affected by damage scenario F05. This scenario isolates a high-value, low-density residential area from the rest of the water distribution system.

4.3.7. Damage Profile G: Transportation System Disruption

This analysis of interdependent critical infrastructures affecting fire response is not confined to the water distribution system. In damage profile G, the effect of damage to the city's transportation grid is examined. This is an important consideration because damage to the community's street network could impede firefighters' travel to the fire site.

Scenario G01, the only scenario modeled in damage profile G, operates on an undamaged water distribution system; however, the transportation network has sustained nonspecific damage which delays firefighters' arrival at the fire ground. The fire response delay for Scenario G01 is 30 minutes, a threefold increase from the 10-minute delay assumed in the other scenarios. This delay is not dependent on the relative location of the fire station and the ignition point or the location of the damage to the road network. Because of this, a more detailed analysis of the effect of transportation network damage on fire response effectiveness which takes route analysis and specific damage profiles into account would be an excellent topic for future research.

4.3.8. Damage Profile H: Communications Network Disruption

Because citizens generally use the telephone network to report a fire to the fire department, an attack or disaster which disables the city's communications network has the potential to delay fire response efforts, since residents must then report the fire by walking or driving to the nearest fire station instead of reporting it by telephone. HAZUS-MH permits the user to specify whether the communications network is

damaged and to model the delay in fire response randomly (FEMA 2003a); MUFS permits random communications delays based on HAZUS-MH's model, or the user may specify a deterministic delay in response.

Scenario H01 models the effect of a communications disruption on fire response using an undamaged water distribution system model and a delay in fire response of 20 minutes. This is longer than the normal fire response delay of 10 minutes used in most of the other damage scenarios, but shorter than the transportation-related delay of 30 minutes specified in Scenario G01.

4.3.9. Damage Profile BH: Pump and Communications Failures Caused by Power Outage

If the power failure modeled in damage profile B is extensive enough, it potentially could affect more than just the water distribution system's pumps. If a power outage affected the communications system as well, the outage could have a compound effect on fire suppression – both by delaying fire response and by interfering with the water system's ability to provide water for firefighting.

Scenario BH1 is simulated with the same water system model as B01, which involves a power outage which disables the water system's pumps for two hours. After two hours, the pumps are restored to operation. In addition to the temporarily-disabled pumps, the delay in fire response is 20 minutes, which is consistent with the communication failure modeled in damage profile H. Scenario BH2 uses the hydraulic model from Scenario B02, in which the pumps are disabled for four hours and then

return to operation. Like scenario BH1, this scenario combines the temporary water system damage from scenario B02 with a delay in fire response of 20 minutes.

4.4. Urban Fire Ignition Points

The disasters modeled in this study involve multiple modes of infrastructure attacks/failures, so it is necessary to specify not only the type of damage inflicted on the water distribution system but the distribution of ignition points for the urban fire which accompanies the water system damage. As was stated earlier in Section 3, the ability to specify the fire's ignition point or points is one major difference between the Model of Urban Fire Spread (MUFS) and the Fire Following Earthquake module of HAZUS-MH. There are many possible strategies to determining the ignition points to consider in the vulnerability analysis. Emergency planners may study data on historical terrorist attacks in order to develop a list of the *most likely* targets based on known trends in vandals' and terrorists' prior targets. This approach has the benefit of relying on extensive historical data and expert guidance as to the most frequent modes of terrorist attack. It is not possible, however, to predict the potentially infinite variations on the most likely group of attacks which may occur. In addition, natural disasters may start fires in random patterns which do not conform to terrorist target profiles. A valuable addition to scenario-based vulnerability assessments is to find the *worst-case* target arrangement without consideration for the specific cause of the fire. Optimization can be a helpful tool in determining this worst-case ignition point profile.

This dissertation adopts both approaches to MMAF vulnerability analysis. The current section addresses the process of choosing a variety of urban fire scenarios meant to simulate specific types of attacks or disasters. Section 4.5 presents the methodology for using optimization methods to determine the worst-case ignition point profile.

Creating the ignition point profiles for the urban fire simulations requires the modeler to consider the ideological and cultural value of the buildings in the community and to choose the most likely targets for attack. Although it is impossible to predict every potential terrorist target or attack, terrorist groups' motivations are well-studied and often conform to specific criteria (Seger 2003). In particular, the *National Strategy for Homeland Security* enumerates some of the threats inherent in an open and free society: "Americans congregate at schools, sporting arenas, malls, concert halls, office buildings, high-rise residences, and places of worship, presenting targets with the potential for many casualties" (OHS 2001, pp. 7-8). With these trends in mind, five damage profiles were selected for study in the scenario-based urban fire modeling. The emphasis during this process was on the targets chosen, not necessarily on the actors committing the attacks. Thus, the actors could be domestic (also called "homegrown") groups or international terrorist groups, but the modeling approach adopted here is similar for both because their effect on the community's infrastructure is the same. The identity, ideology, and origin of the groups committing the attacks are important to this analysis only because they may affect the group's choice of targets. The targets in these profiles were chosen to mimic common arson and terrorist bombing targets. A comprehensive database enumerating and describing historical terrorist attacks is

available at the Terrorism Knowledge Base (Memorial Institute for the Prevention of Terrorism (MIPT) 2006).

The first target profile centered on the area's houses of worship and was intended to mimic an attack by religious extremists. An actual recent example of this type of event includes the bombing of the Golden Mosque, a Shi'ite shrine in Iraq, and retaliatory arson attacks against Sunni mosques throughout Iraq (Knickmeyer and Ibrahim 2006). This profile, abbreviated CHU, has three ignition points, and the locations of these ignition points are shown superimposed as pink triangles on a building map of Micropolis in Figure 4.7.

Potential targets for an ecoterrorist arson attack were considered next, and this attack profile was abbreviated as ECO in the simulation results. Actual examples of ecoterrorist arson attacks are numerous, including the Earth Liberation Front's alleged 1998 arson against a Vail, Colorado, ski lodge and three ski lift buildings (Caldwell 2006) and the same group's 2004 arson attack against a West Jordan, Utah, lumber storage facility (Canham 2004). The two ignition points chosen to model this type of attack in Micropolis were a lumberyard and a printing press, both located in the industrial area on the east side of town. The locations of the ignition points are shown as green stars in Figure 4.7.

Government and community buildings composed the targets for the third attack profile. A prominent actual example of this type of attack is the 1995 bombing of the Alfred P. Murrah Federal Building in Oklahoma City, Oklahoma (Johnston 1995). The Micropolis government and community buildings selected as targets for simulated arson

attacks included City Hall, which houses most of the city's government offices; the city post office; the community center; and a historic rail depot museum dedicated to the community's history. All four of these targets are located in the city's central business district near the center of town. This target profile was abbreviated GOV in the simulation results. The targets in the GOV profile are shown as blue squares in Figure 4.7.

The community's three school buildings were the targets for the next attack profile, which is abbreviated SCH in the simulation results. A real example of this type of attack on an area's schools is the 2004 Beslan school siege by Chechen separatists (BBC 2004), although that attack was a hostage seizure, not an arson attack. Micropolis has an elementary school, located near the Central Business District, and a middle school and high school, which are located in the southwest corner of town. These buildings are denoted by the red circle markers in Figure 4.7.

The final target profile considered in this study is a collection of high-population gathering places within the community. The most prominent example of this type of event is the 9/11 attacks on the World Trade Center (National Commission on Terrorist Attacks upon the United States (NCTAUS) 2004). The high-population target profile, which is abbreviated as POP in the simulation results, has five ignition points: City Hall, the city's three school buildings, and a movie theater located in the central business district. This target profile's distribution of ignition points is shown with orange stars in Figure 4.8. A separate building map was needed to show this target profile clearly because it repeats some of the targets from the SCH and GOV target profiles.

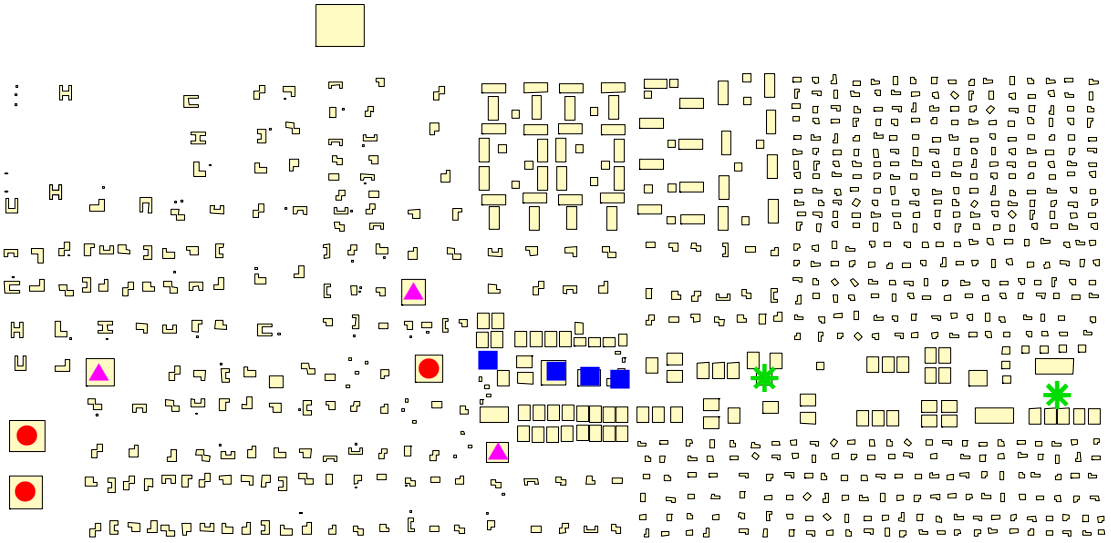

Fig. 4.7. Ignition points for CHU, ECO, GOV, and SCH urban fire target profiles. CHU ignition points are shown by pink triangles (3); ECO ignition points are shown by green stars (2); GOV ignition points are shown by blue squares (4); and SCH ignition points are shown by red circles (3).

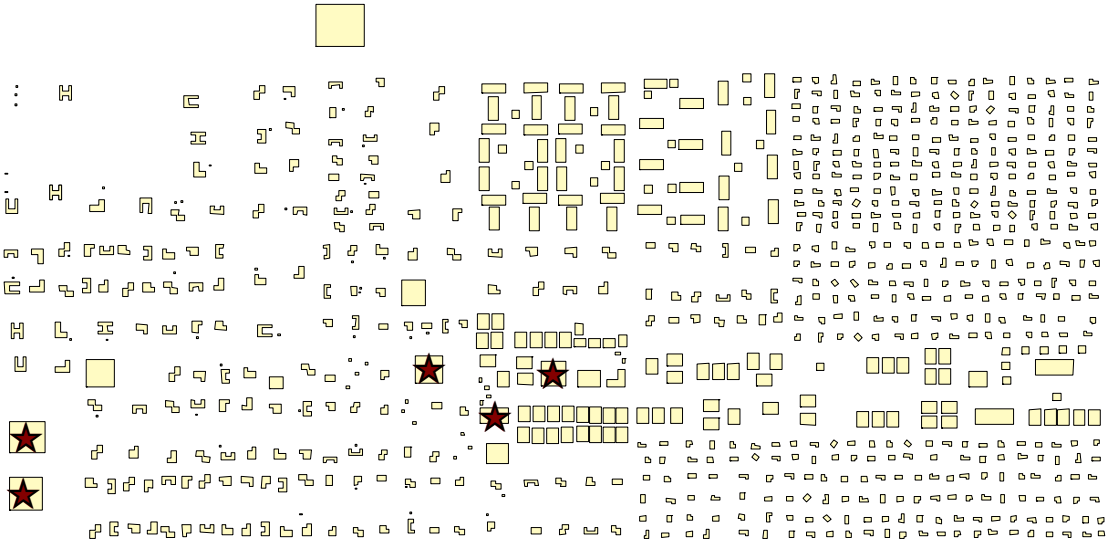

Fig. 4.8. Ignition points for POP urban fire target profile. POP ignition points are shown by maroon stars.

The selection of targets for each damage profile was highly subjective, and this phase of the vulnerability assessment underlines the importance of a broad understanding of the potential threats against the community. Other common targets for arson attacks include facilities like abortion clinics, police facilities, construction projects and/or business headquarters, transportation hubs, telecommunications hubs, and diplomatic facilities (MIPT 2006). Because the range of potential targets is diverse, the selection of targets for MMAF simulation should be completed in consultation with experts familiar with the community, its mechanisms of emergency response, and its potential vulnerabilities.

4.5. Simulation of Scenario-Based Urban Fires

Using the water damage and urban fire scenarios described in Sections 4.3 and 4.4, a wide variety of multi-mode attack and failure scenarios were simulated using the Model of Urban Fire Spread presented in Section 3 to provide insight into the possible range of consequences from this type of disaster.

MUFS incorporates a great deal of information about the physical environment contributing to the urban fire, so in addition to a characterization of the water system damage and the urban fire ignition points, it was necessary to specify the prevailing wind speed and direction. The original plans for this phase of the simulation called for a range of wind speed inputs, but preliminary results indicated that wind speed had a marginal effect on the consequences predicted by a long-term simulation. Therefore, the wind speed was held constant at 10 mph (approximately 4.47 m/s) for all simulations. A

variety of wind directions were considered, since the magnitude of the urban fire's spread distance depends on the prevailing wind direction. In MUFS, wind directions are specified as the wind's destination direction (not its origin direction, which is common meteorological practice) and due east is designated as 0 degrees, with directions increasing in the counter-clockwise direction. Eight wind directions were considered in the simulations: the four cardinal directions 0 degrees (east), 90 degrees (north), 180 degrees (west), and 270 degrees (south) and the four secondary directions (north-east, north-west, south-west, and south-east) offset 45 degrees from the cardinal directions). This convention is not consistent with standard meteorological practice; it is adopted to facilitate the vector mathematical operations used in model computations. Future versions of the computer code written to facilitate simulation will conform to standard wind direction conventions.

The scenario-based simulations varied three simulation parameters: wind direction, water system and other infrastructure damage profile, and ignition point target profile. Thus, each simulation was specified as a unique direction/damage/target "triplet." This creates the potential for 880 unique damage scenarios, but the actual range of scenarios was limited somewhat to prevent redundant simulation of nearly-identical scenarios and make the required simulation time more manageable The average computation time for one direction/damage/target scenario, assuming an urban fire duration of 12 hours, was about one hour (using standard desktop personal computers); therefore, early efforts to decrease the required simulation time by eliminating nearly-redundant direction/damage/target triplets led to a considerable

savings in computational needs. The direction/damage/target triplets actually simulated after elimination of redundancies are presented in Table 4.1. For clarity, the infrastructure damage scenario component of the target profile/wind direction/infrastructure damage triplet is omitted from the table below. Every infrastructure damage profile was simulated for each target profile/wind direction pair listed in Table 4.1. This resulted in the simulation of 788 unique target profile/wind direction/infrastructure damage scenarios. (In addition, four simulations failed at runtime due to computer problems; this small number of simulation failures, equivalent to about one-half of one percent of the total simulations, was deemed to be negligible.)

Table 4.1. Target Profile/Wind Direction Combinations Simulated in Scenario-Based Vulnerability Analysis

Target Profile	Wind Directions
CHU	45, 90, 135,180, 225,270,315
ECO	All
GOV	All
POP	0, 45, 90, 180, 225, 270, 315
SCH	0, 45, 90

Each of the direction/damage/target scenarios specified above were simulated using MUFS, following the process presented in Section 3. The results of these simulations, including the range of damages predicted by the urban fire simulations and the process used to analyze the consequences and determine the most serious results, are presented in Section 5.

4.6. Optimization of Fire Ignition Points

The work presented so far in this section used urban fire simulations based on clearly-delineated damage scenarios to predict the potential range of consequences of an attack or failure affecting fire response and one or more of its supporting infrastructures. The main disadvantage to this approach of simulating likely attack or disaster scenarios is that the success of the analysis depends heavily on accurate selection of the ignition points for the urban fire. The experts selecting the ignition points may overlook some valid attack or disaster scenarios (including errors in execution of a correctly predicted terrorist attack). Furthermore, it is impossible for any expert to predict *every* potential multi-mode attack and failure scenario which might affect a community. Scenario-based vulnerability assessments of the type explained earlier in this section are useful because they provide insight into the range of possible consequences, but they may not be sufficient to describe the worst-case attack or disaster scenario.

The possibility of overlooking a high-consequence multi-mode threat against the community prompted the use of an alternative method of determining the distribution of urban fire ignition points. Several methods of optimization were tested as a means to find the highest-consequence distribution of fire ignition points. Unlike the approach described in Section 4.4, this approach does not consider the likely mechanism of ignition; it makes no difference to the calculations whether the fires were caused by accident, arson, or natural disaster. The goal of the optimization process is simply to find the spatial distribution of ignition points which causes the maximum damage; this is

important because insight into the worst-case scenario can help community leaders plan to avoid worst-case damages.

Ideally, this type of analysis would consider each building in the urban area as a potential ignition point. However, the amount of time required to run the full fire spread and suppression simulations for even a small number of simultaneous ignitions if the possible ignition locations are totally unrestricted is prohibitively high. Preliminary calculations indicated that the optimization process for selecting only three ignition points from the 868 buildings in Micropolis would require many *years* of computation time. Clearly, some simplification of the problem was needed in order to make it computationally feasible.

The first measure taken to simplify the optimization problem involved imposing some restrictions on the potential ignition points. In actual practice, it may not make much difference in the simulation results if a large urban fire starts in one building or one of its immediate neighbors. It is possible to reduce the scale of the problem by generalizing groups of buildings to a single representative structure. The Micropolis buildings were represented by a grid of ten potential ignition buildings spaced approximately evenly: about 1000 feet apart. These representative buildings were chosen based on their location and their similarity to other buildings in their immediate area.

Because the fire spread and suppression simulation can be time-intensive, a sensitivity analysis was conducted on the level of detail included in the optimization calculations. The purpose of the sensitivity analysis was to provide an understanding of

the tradeoff between model completeness and the computational resources required. Three different optimization methods were investigated in this phase of the project.

4.6.1. Optimization Method 1: Dynamic Programming with *a priori* Damage Counts

The first set of simulations used a dynamic programming algorithm to maximize the consequences of a three-ignition urban fire (with ignition points restricted to the ten possible ignition buildings described above). For this option, the consequences of a fire starting at any given ignition point were determined individually for each possible ignition point *before* the optimization process. This *a priori* determination of each ignition point's consequences greatly improved the speed of the optimization calculations; each optimization run took only minutes on a desktop personal computer instead of hours or days to complete. The consequences were determined using an unsuppressed fire spread simulation in the Model of Urban Fire Spread. A medium-duration (two hours) single-point urban fire was simulated separately for each ignition point, and the resulting list of burning buildings was saved as an input for the optimization model. The fire spread simulations included only unsuppressed fire spread because, during normal simulation of a multi-ignition urban fire, fire suppression activities for one ignition point affect the resources available for suppressing the other ignition points' fires. The "costs" of fighting ignition points are not necessarily linearly additive; therefore, it is not possible to predict a multi-ignition fire's response to fire

suppression by simulating each ignition point's fire spread and suppression separately and later summing the results.

The consequences of *unsuppressed* urban fires can be added linearly, however, as long as care is taken to prevent double-counting buildings which lie in two or more ignition points' burn polygons. To accomplish this, a short postprocessor function was implemented in Visual Basic 6 code to combine any number of ignition points' burning building lists (generated automatically by MUFS as a simulation output), remove any redundant entries, and calculate the total number of displaced people from the combined building list. The function determined which buildings appeared more than once based on each building's unique ID number, which was part of the input information included in the building properties table described in Section 3.

The worst-case distributions were determined by using a dynamic programming algorithm to optimize the placement of the ignition points to maximize the consequences of the resulting fire. Dynamic programming is an optimization technique which considers a problem as a series of "stages," or successive decisions. In this problem, there were ten stages: one for each potential ignition point. For each stage, the decision to be made was a simple yes/no choice of whether or not to ignite a fire at that ignition point. In the equations below, the stage is indicated by the subscript k.

The dynamic programming problem is formulated in a series of equations as follows:

$$\text{Find } u_k,\ k = 1,2,3 \ldots 10 \tag{4.1}$$

which

$$Max\ J_{damage} = \sum_{k=1}^{N} g_k - \alpha(x_{\max} - x_N)^2 \tag{4.2}$$

where

$$g_k = \sum_{bldg} b_{bldg} \cdot v_{bldg} \tag{4.3}$$

Subject to: $x_0 = 0$ (4.4)

$$x_{k+1} = x_k + u_{k+1} \tag{4.5}$$

$$x_{max} = 3 \tag{4.6}$$

where u_k is the decision variable for each stage, with possible values of 0 or 1; J_{damage} is the total consequences of the combination of ignition points selected as described above; α is a weight on the penalty for incomplete deployment of resources (i.e. some number of ignitions different from the desired number); g_k is the stagewise running gain; b_{bldg} is a binary indicator of whether or not a building is burned by an ignition point combination's fire polygon; v_{bldg} is the value (number of occupants) of a building; and x_k is the state variable for stage k.

In dynamic programming terminology, the method for scoring the "goodness" of each set of decisions is called the "objective function." For this application, the objective function (equation 4.2) for any set of fire ignitions is a count of the people

displaced by the fires (J_{damage}). Its value is calculated using the ignition points' associated burned building lists and the postprocessor function described above. From the attacker's perspective, higher values of the objective function are better than lower values, and the attacker's goal is to get the highest possible value of the objective function (i.e. to maximize the consequences of the attack).

The total number of "yes" decisions is constrained by the resources of the attacker; in this case, the attacker was assumed to have only three incendiary devices, so the maximum number of fires the attacker could ignite was limited to three (as shown in Equation 4.6). In theory, the attacker could choose to set fewer than three fires. Failure to use all of the available resources would not produce an optimal outcome, however, since the attacker is trying to maximize the damage inflicted by the multi-ignition fire. A human being with common sense would see this fact intuitively; to force the computer program to follow this logic, the program is instructed to impose a very large penalty (represented by α in Equation 4.2) for any final decision which does not use all the available resources.

As the attacker considers, for each stage, whether or not to place the incendiary device at that location, the decision is affected by how many incendiary devices have already been placed at stages the attacker has already considered. The count of how many fires have been ignited at any particular stage (including the fire set at the current stage, if applicable) is known as the "state," and the state has a range of feasible values for each stage. For example, for stages 3 through 10, the possible state values are 0, 1, 2, and 3. (The state value cannot be greater than 3 because the attacker can only set a total

of three fires.) At the earliest stages, the range of potential values is narrower; for example, at stage 2 the highest possible value for the state is 2, because the attacker cannot have set three fires at the two locations already considered.

One of the main goals in designing and testing this method was to determine whether emergency planners can predict the relative severity of an urban fire event based on the results of medium-term unsuppressed fire spread calculations. This approach is extremely fast but may involve an unacceptable simplification of the behavior of urban fires. In addition, this approach is not intended to be used alone to predict the consequences of the worst-case fire scenario, but rather as a tool to identify the worst-case scenario so that emergency planners can devote their time to studying that one scenario in more depth. The main question under consideration in this step is: is an optimization process based on this type of extreme simplification of the multi-mode attack or failure actually capable of accurately pinpointing the worst-case distribution of urban fire ignition points? The results of the dynamic programming optimization process and the answers to these questions about this technique's useful application will be discussed in Section 5.

4.6.2. Optimization Method 2: Dynamic Programming with Fire Suppression Included in Damage Calculations

A fundamental assumption involved in using optimization method #1 is that it is possible to predict the suppressed severity of a multi-ignition urban fire based on *a priori* "snapshots" of the individual fires' unsuppressed behavior. The allocation of

resources for fire suppression is a complex process, however, so accurate prediction of the fires' suppressed behavior based on their unsuppressed behavior may not actually be possible. Optimization method #2 was implemented to test the validity of this assumption. This method is considerably more time-consuming than optimization method #1, because the optimization procedure uses suppressed fire spread equations to calculate the damages of each ignition point, and the fire spread and suppression simulations must be run during the course of the dynamic program solution procedure. (Suppressed fire spread simulations cannot be run *a priori*, because the precise configuration of ignition points makes a difference in the final results of the simulation.) As a tradeoff for the added time and complexity required to solve the dynamic program, this optimization process is informed by more accurate and complete information about the urban fire and may produce more accurate results than optimization method #1. The results of this procedure were compared with the results from optimization methods #1 and #3 to provide insight into the tradeoff between expediency and accuracy.

The dynamic program formulation for this optimization method was set up in a similar manner to the formulation described in Section 4.6.1 for optimization method #1. The only difference between the two model formulations is the methodology used to calculate the running gain function, which is the marginal number of displacements added to the total number of displacements by an ignition at the current stage. The equation for the running gain for this model formulation is the same as the equation for the previous method (Equation 4.3), but the value of b_{bldg}, an input to the running gain

equation, is determined using a MUFS simulation including the configuration of ignition points under consideration.

Like the previous method, this problem was formulated as a ten-stage dynamic program: in other words, a series of ten decisions (one for each potential ignition point) of whether or not to ignite an urban fire at each possible ignition point. The attacker's resources were assumed to be the same as for optimization method #1, so each stage has three possible states (corresponding to the number of fires set at all stages already considered, including the current stage). The only difference between this method and the previous one is in the evaluation of the objective function, which is akin to a scorecard of each potential solution's fitness. For optimization method #1, the value of the objective function was determined by using the postprocessor function described in Section 4.6.1 to construct a combined burned building and calculate a combined damage count from the separate burn polygons of each of the ignition points under consideration. Optimization method #2 determines the value of the objective function by running a suppressed fire spread simulation in MUFS for each combination of ignition points considered by the dynamic programming algorithm. Note that dynamic programming does not consider every potential combination of ignition points; the dynamic programming solution process guides the user away from combinations which are clearly sub-optimal. Thus, this process is not equivalent to a total enumeration of all possible combinations of ignition points; this method will be discussed in Section 4.6.3.

Because this method accounts for damage to the water system in its allocation of resources for fire suppression, it was necessary to specify a water system damage

scenario to use in the fire suppression simulations. The dynamic program was solved using water system damage scenario D01 (destruction of the system's elevated storage tank), which is described in detail in Section 4.3.3. A wind speed of 10 mph, blowing due east, was specified for all related simulations. To test the correctness of the solution, the dynamic program was solved six separate times varying the order of the stages; a correct solution algorithm will produce the same solution no matter what stage order is used.

Solving the dynamic programming problem using full fire spread and suppression simulations to evaluate the objective function took much longer than using the *a priori* fire extent polygons; optimization method #2 required approximately twelve hours to deliver a solution running on a desktop personal computer. In contrast, as mentioned in Section 4.6.1, optimization method #1 required only a few minutes to deliver a solution. The methods' respective results and accuracy are discussed in Section 5.

4.6.3. Optimization Method #3: Total Enumeration of Possible Solutions

By far the most time-consuming method of determining the most damaging configuration of urban fire ignition points is to consider each possible combination of three ignition points (from ten potential locations), simulate the fire resulting from each combination, tabulate the results, and choose the combination with the most serious damage. This procedure was implemented as optimization method #3, a third alternative means of determining the worst-case urban fire scenario. The main advantage to this

approach is that it is guaranteed to produce the worst-case combination of the potential ignition points. The main disadvantage is that this method is computationally expensive; five days of continuous simulation on a desktop personal computer were required for this approach to deliver a solution. The results of this optimization method are presented and discussed in Section 5, along with suggestions for future research into other possible optimization methods to expedite the solution of this problem.

5. RESULTS AND DISCUSSION: ANALYSIS OF VULNERABILITY TO MULTI-MODE ATTACKS AND FAILURES

5.1. Results of Scenario-Based MUFS Simulations

The vulnerability analysis described in Section 4 required the simulation of a large number of multi-mode attack and failure (MMAF) scenarios to provide insight into the range of potential damages resulting from this type of attack or disaster. Seven hundred eighty-eight distinct combinations of wind direction, infrastructure damage, and fire ignition point profiles were simulated for the scenario-based vulnerability analysis. The results of these simulations are summarized as a results matrix in Figure 5.1a.

The numbers in Figure 5.1a reflect the number of people predicted to lose their home or place of employment because of the multi-mode attack or failure simulated in each scenario. As an aid to interpreting the matrix, the cells are color-coded. Figure 5.1a consists of eight sub-matrices: one for each wind direction included in the simulations. The wind direction is noted in the white cell at the upper-left corner of each sub-matrix. The gray cells in the top row of each sub-matrix hold the abbreviations for the 23 water system or other support infrastructure failure scenarios described in Section 4. (In addition to these infrastructure damage scenarios, a twenty-fourth infrastructure damage profile was simulated as a basis for comparison, using an undamaged model of the Micropolis water distribution system with normal communications and transportation systems. The abbreviation used to refer to this scenario is “UND,” for “undamaged”.) The gray cells in the first column of each sub-matrix in Figure 5.1a include the

abbreviations for each urban fire ignition point profile. These ignition point profiles are explained in further detail in Section 4. In order to avoid modeling redundant scenarios, not all ignition point profiles were modeled for every wind direction. For example, the SCH target profile, which involves ignition points at each of the three school buildings, was only simulated for wind directions 0, 45, and 90.

The cells containing the numerical results of the simulations are color-coded based on their severity. Red cells represent scenarios producing consequences in the 95th or greater percentile of all simulations, which displaced 5,005 or more people from their homes and/or businesses. These high-consequence scenarios are especially prevalent for the ECO ignition point profile with wind directions of 225 and 315 degrees. Figure 5.1a shows that the highest damage level encountered for any scenario was 5,069 displaced persons, and this consequence value was shared by several wind direction/infrastructure damage/ignition point profiles. (A displacement count of higher than 5,000 is possible, even though the population of Micropolis is 5,000, because people who lose both their home and place of employment because of the MMAF event are counted twice. The maximum possible damage count is 6,999 displacements.) Orange cells represent scenarios with consequences in the 75th or higher percentile (which displaced between 3,298 and 5,004 people each). Yellow cells show scenarios with consequences in the 50th or higher percentile, with damages ranging from 2,210 to 3,297 displaced people. Blue cells contain the scenarios in the 25th or higher percentile, displacing 1,243 to 2,209 people each. Green cells contain the least severe scenarios, with consequences below the 25th percentile in magnitude (displacing 1,242 or fewer people).

0	UND	A01	A02	A03	AD1	AD2	B01	B02	B03	BH1	BH2	D01	D02	E01	E02	E03	E04	F01	F02	F03	F04	F05	G01	H01
ECO	826	2042	826	826	2060	826	1980	2041	826	2488	2494	816	826	572	826	572	572	826	852	826	826	826	1153	911
GOV	1701	1878	1561	1655	1878	2249	1878	1878	1655	1655	1655	3777	1655	1113	1107	884	1113	1828	1206	1806	1601	1655	1958	1655
POP	1983	2512	1987	1987	2512	1987	2512	2512	1983	2512	2512	2492	1983	2487	2009	1983	2487	2487	2487	2490	2490	1983	2514	2009
SCH	1245	1615	1759	1759	1615	1759	1615	1615	1759	1619	1619	1612	1759	1759	1759	1245	1759	1759	1759	1612		1245	1083	739

45	UND	A01	A02	A03	AD1	AD2	B01	B02	B03	BH1	BH2	D01	D02	E01	E02	E03	E04	F01	F02	F03	F04	F05	G01	H01
CHU	2607	3231	2667	2667	3232	2667	3231	3231	2607	3231	3231	2667	2607	2607	2607	2607	2607	2607	2564	2667	2607	2607	2271	1998
ECO	5000	5032	5000	5000	5032	5000	5032	5032	5000	5069	5069	5000	5000	5014	5000	1278	5010	5000	5000	5000	5000	5000	5037	4155
GOV	3435	1922	3425	3435	3484	3425	1922	1922	3435	4494	4494	4864	3435	3494	3435	3389	3494	1932	3484	2002	3425	3435	4250	4494
POP	2671	2671	2671	2671	2671	2671	2671	2671	2671	2818	2818	3440	2671	2671	2671	2671	2671	2671	2671	2671	2671	2671	2816	2818
SCH	1290	3118	1326	1325	3118	3118	3118	3118	1290	3000	3118	1421	1421	1290	1206	1325	1206	1290	1206	1421	2253	1290	1301	1291

90	UND	A01	A02	A03	AD1	AD2	B01	B02	B03	BH1	BH2	D01	D02	E01	E02	E03	E04	F01	F02	F03	F04	F05	G01	H01
CHU	412	668	622	412	896	562	665	668	421	886	893	581	421	422	562	422	571	412	701	581	412	412	473	470
ECO	1350	2490	1350	1350	2507	2430	2486	2486	1350	2458	1325	2430	2430	1368	1350	1358	2393	1360	2390	2387	1350	1350	1853	1352
GOV	1394	2334	1892	1394	2334	1898	2334	2334	1404	2342	2342	3783	1394	1628	1848	1618	1593	2347	2334	1913	1913	1390	1750	1928
POP	1774	2341	1765	1765	2401	2362	2341	2341	1767	2178	2178	2371	2332	2278	1765	1765	2278	2280	2336	2262	2268	1767	2308	2128
SCH	1044	1395	1062	1044	1395	1274	1066	1236	1146	877	935	1291	1291	1120	1081	1054	1180	1044	1363	1236	1054	1044	955	775

135	UND	A01	A02	A03	AD1	AD2	B01	B02	B03	BH1	BH2	D01	D02	E01	E02	E03	E04	F01	F02	F03	F04	F05	G01	H01
CHU	751	3079	696	751	3159	696	3079	3079	751	2993	3079	944	696	696	751	773	775	696	1327	944	696	751	929	1378
ECO	5037	3326	5037	5037	3326		3326	3326	5037	3326	3326	3324	5037	3324	5037	5045	3324	5037	5037	3324	2359	5037	3326	3326
GOV	1227	1158	1222	1222	1158	1216	1158	1158	1222	1227	1227	1118	1216	1158	1222	4473	1158	1118	1158	1173	1222	1222	2381	1227

Fig. 5.1a. Results of scenario-based MMAF simulations.

180	UND	A01	A02	A03	AD1	AD2	B01	B02	B03	BH1	BH2	D01	D02	E01	E02	E03	E04	F01	F02	F03	F04	F05	G01	H01
CHU	287	1415	1017	960	1415	1063	1415	1415	535	1415	1415	1075	1063	970	287	287	287	960	495	1060	287	287	1049	1158
ECO	528	1292	528	528	2472	528	1292	1292	528	2664	2664	778	528	589	528	559	711	778	1738	778	528	528	1495	1141
GOV	1053	2294	1696	1053	2294	1696	2294	2294	1053	1562	1562	2234	1053	1547	1053	2190	1569	1547	2294	2190	1053	1053	905	1971
POP	1774	1784	1774	1774	1784	1784	1784	1784	1774	1797	1797	1784	1784	1779	1769	1772	1779	1784	1784	1774	1774	1774	1723	1774

225	UND	A01	A02	A03	AD1	AD2	B01	B02	B03	BH1	BH2	D01	D02	E01	E02	E03	E04	F01	F02	F03	F04	F05	G01	H01
CHU	2488	2955	2426	2488	2956	2252	2956	2955	2488	2956	2955	2426	2488	2338	2089	2353	2338	2338	2236	2426	2338	2353	2580	865
ECO	486	5069	486	486	5069	486	5069	5069	486	5069	5069	5041	486	5041	486	1578	5041	5041	1539	5041	992	486	5041	1297
GOV	3421	4469	3421	3421	4876	3850	4469	4469	3421	4469	4469	3853	3850	3569	3421	3424	3568	3563	4469	3562	3421	3421	4364	4444
POP	3298	3312	3298	3298	4002	3988	3312	3312	3298	3302	3302	3988	3988	3298	3298	3298	3298	3298	3298	3298	3298	3298	3282	3288

270	UND	A01	A02	A03	AD1	AD2	B01	B02	B03	BH1	BH2	D01	D02	E01	E02	E03	E04	F01	F02	F03	F04	F05	G01	H01
CHU	1022	1404	1029	1022	1404	1219	1404	1404	1022	1407	1407	1219	1220	1021	1220	1220	1220	1022	1220	1021	1022	1022	1251	1045
ECO	1037	2506	1037	1037	2538		2496	2500	1037	2446	2538	2501	1037	2434	1037	919	2447	2552	1037	2498	1037	1037	2465	1013
GOV	3828	3830	3828	3828	3830	3828	3830	3830	3828	3830	3830	3830	3828	3830	3828	3828	3830	3830	3830	3830	3828	3828	2310	3830
POP	1825	2327	1825	1825	2327	1822	2327	2327	2327	2333	2333	1825	1822	1825	1822	1822	1825	1825	2327	1825	1825	1825	1830	1828

315	UND	A01	A02	A03	AD1	AD2	B01	B02	B03	BH1	BH2	D01	D02	E01	E02	E03	E04	F01	F02	F03	F04	F05	G01	H01
CHU	2210	3060	2238	2210	3145	2321	3060	3060	2247	3060	3060	1570	2256	2247	2210	2210	2210	2210	2210	2261	2210	2210	2708	2665
ECO	949	5069	1010	1016	5069		5069	5069	1016	5069	5062	5005	2099	5005	1010	549	5005	5005	1010	5005	1010	1016	5005	1596
GOV	3946	3863	3544	3544	3863	3544	3863	3863	3544	3863	3863	4199	3544	4228	3544	4228	4228	3544	3863	3866	3544	3544	3863	3866
POP	3370	3370	3370	3370	4178	4178	3370	3370	3370	3370	3370	4178	4178	3370	3370	3370	3370	3370	3370	3370	3370	3370	3346	3348

Fig. 5.1a (Continued).

Figure 5.1a clearly shows the relative severity of the scenarios' results categorized by wind direction and fire ignition point profile. To provide additional insight into the infrastructure damage scenarios' consequences, the number of displaced people averaged over all ignition point profiles are presented for each damage scenario in Table 5.1, arranged in order of decreasing severity.

It is not surprising that the three most damaging entries in the list are infrastructure damage scenarios that involve compound failures: Scenario AD1, for example, includes damage both to the water system's pumps and the elevated storage tank, and Scenarios BH1 and BH2 involve short-term pump inactivity and fire response delays caused by failures in the communications infrastructure.

Table 5.1. Average MMAF Scenario Consequences by Infrastructure Damage Profile

Scenario Name	Average Consequences (Displaced People)	Scenario Name	Average Consequences (Displaced People)
AD1	2848	F02	2260
BH1	2781	AD2	2223
BH2	2758	D02	2164
A01	2692	H01	2054
B02	2687	A02	2042
B01	2680	B03	2009
D01	2650	A03	2005
G01	2411	E03mod	2002
F03	2367	F04	1990
F01	2344	UND	1978
E04	2331	E02	1976
E01	2306	F05	1962

It is also interesting to compare the average results for infrastructure damage scenarios which are similar except for a few key variables, in order to assess those variables' effects on the consequences of the urban fire. For example, Scenarios G01, H01, and UND all use the same hydraulic model of an undamaged water distribution system; the only difference is in the delay in fire response (30 minutes, 20 minutes, and 10 minutes, respectively). The large difference in consequences between Scenarios G01 and UND underlines the importance of cities' providing for speedy fire response even in the case of disaster.

Even more striking is the difference in consequences between Scenario A01 (which involves the destruction of all three of the water distribution system's high-service pumps) and Scenario A02 (which models the destruction of two of the three high-service pumps). Keeping only one pump on-line reduces the average consequences of the urban fire by 650 displaced people: a reduction of nearly 25% from Scenario A01's damage level. This suggests that one important MMAF mitigation strategy for Micropolis to consider may be to provide for backup pump capacity so that the likelihood of at least one high-service pump remaining in service is increased. The similarity of the average consequences of Scenarios A01, B02, and B01 – all of which involve the incapacity of all three high-service pumps, but for varying durations – shows that it is very important for Micropolis's water utility not to allow its pumping capacity to cease completely even for a short time, particularly in the fire's early stages. (Scenario B03, which takes the pumps offline temporarily two hours into the MMAF

simulation, is significantly less damaging than Scenarios A01, B02, and B01, which take the pumps offline at the beginning of the MMAF simulation.)

A final observation on the relative importance of Micropolis's two sources of water for firefighting (water supplied by the high-service pumps or stored in the elevated storage tank) suggests another possible mitigation measure to improve the city's resistance to MMAFs. It is interesting to note that the three scenarios (A01, B02, B01) which involve the initial incapacity of all of the high-service pumps are all more damaging on average than Scenario D01, which involves the destruction of the elevated storage tank at the beginning of the MMAF simulation. This result was counter to preliminary predictions, because Micropolis's water distribution system was designed to meet base-level, day-to-day water needs with the high-service pumps and use the elevated storage tank to provide surge capacity during high-use periods. It seemed reasonable to expect that Scenario D01, which removes the fire department's access to this surge capacity, would be one of the most damaging infrastructure failure scenarios. While this is not the case, Table 5.1 does show that the difference in average consequences between Scenario D01 and Scenario A01 (42 more people are displaced on average in Scenario A01 than Scenario D01) is not great in magnitude considering the overall effects of the disasters. Therefore, Scenario D01 should still be considered a serious mode of infrastructure failure. This finding suggests that another potential way to mitigate the effects of MMAFs involving urban fires and water utility damage would be to build redundant storage capacity in Micropolis's water distribution system. Micropolis has only one elevated storage tank; thus, if the tank is destroyed the system

loses all of its storage capacity at once. Building a second tank, even a smaller one, at a different location could be one possible way to decrease Micropolis's vulnerability to this type of attack or failure.

Table 5.1 yields one final insight into potential mitigation measures to protect Micropolis from urban fire MMAFs. Slightly further down the list of infrastructure damage scenarios ranked by average damage levels is a block of scenarios (F03, F01, E04, E01, F02) which involve the isolation of key sections of water main, either because of a water main breach or because of contamination of the water in the mains. Isolation of zones within the water distribution system has two main effects on the system's ability to handle fire suppression. First, any fire hydrants within the isolated zone are cut off from outside water sources, which affects their ability to provide water for firefighting. Second, water that would normally pass through the isolated area must take an alternate route, which causes greater head loss and may decrease the pressure available at hydrant nodes downstream of the isolated area. While the zone isolation scenarios are not the most serious infrastructure failure scenarios tested, their consequences are still significantly higher than the MMAF scenario modeled with an undamaged water distribution system. This raises the possibility that a mitigation measure designed to bridge the isolated zones, both to bring water to the isolated hydrants and to lessen the need for alternate routes around the zones, could help decrease the consequences of this type of event. This potential mitigation measure will be discussed further in Section 6, along with the other possible mitigation measures described in this section.

5.2 Selection of Attack Scenarios for Mitigation

Section 5.1 includes suggestions for mitigation measures based on the most serious infrastructure failure scenarios, but it is still necessary to select the wind direction/infrastructure damage/target profile scenarios used to test the mitigation measures. The main goal of this project is to identify water and other support infrastructure mitigation measures to protect the community against urban fire MMAFs; water utilities and emergency planners are presumed to have a much higher degree of control over the water distribution system and other support infrastructures than over the targets chosen by terrorists or the wind direction at the time of the attack. Therefore, it is advisable to test the mitigation measures against the most damaging combinations of target profile and wind direction to verify their effectiveness.

Figure 5.1a provides some idea of the relative severity of the various scenarios, but in order to identify the most damaging target profiles and wind directions it is advisable to examine the simulation results differently. Figure 5.1b shows the results of this parallel analysis. The consequences of the MMAF simulations are plotted on the vertical axis, and each combination of target profile and wind direction are contained in a separate data series. (Thus, each row in Figure 5.1a is a separate data series in Figure 5.1b.)

The scenarios within each wind direction/target profile category are sorted in order of increasing magnitude, so that the horizontal scale in Figure 5.1b reflects each scenario's percentile ranking within its direction/target category. (Scenarios plotted

further to the right are higher in magnitude than scenarios plotted further to the left *on the same line*.)

Plotting all this data on one set of axes yields a complicated graph, but it does permit the analyst to identify several distinct "tiers" of wind direction/target profile category damages. The data series plotted in Figure 5.1b were interpreted to fall into three horizontal bands, and this separation between the damage levels was used to select the most damaging wind direction/target profile combinations to test the mitigation strategies in the next phase of the project. The top band in Figure 5.2 is relatively narrow and contains data series with a large number of scenarios resulting in more than 5,000 displacements. Four wind direction/target profile categories fall into this band: ECO 45 (that is, the combination of the ECO group of ignition points with a wind direction of 45 degrees), ECO 135, ECO 225, and ECO 315.

The next natural grouping of wind direction/target profile categories occurs for the series whose scenarios cause approximately 3,300 to 4,000 displacements. This second tier includes six additional wind direction/target profile categories: GOV 45, GOV 225, GOV 270, GOV 315, POP 225, and POP 315.

Below the second tier the graph becomes significantly more jumbled and individual categories are more difficult to characterize in terms of overall damage levels. However, this analysis technique was helpful in identifying the ten categories in the top two tiers. Scenarios in these high-consequence categories were used to test the effectiveness of the proposed mitigation strategies, and this process is explained in further detail in Section 6.

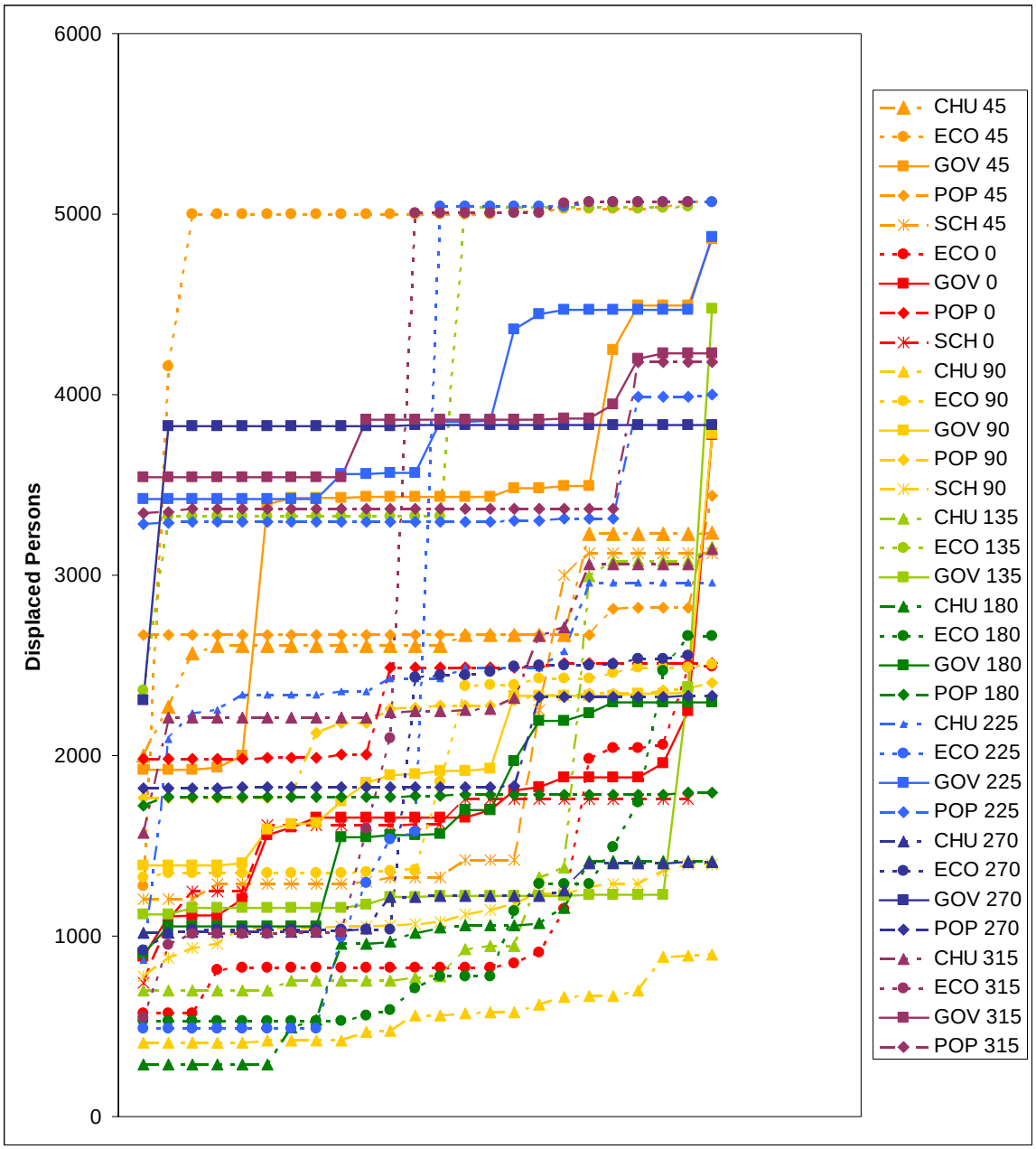

Fig. 5.1b. Graph of MMAF simulation results separated by target group/wind direction.

5.3. MMAF Fire Spread Profiles: Visualizing Burned Area Extent

Characterizing MMAF scenarios' severity in terms of the number of people displaced by the fire is a useful metric, but this is by no means the only way to describe the scenarios. Plotting the fires' progress over time provides insight into the fire's behavior and the success of firefighting efforts at various locations in the urban area.

Figures 5.2 through 5.6 show the differences in fire behavior for a range of high-consequence and low-consequence MMAF scenarios. Figure 5.2 shows the progress of the urban fire over time for the ECO target profile with wind blowing into the southwest and infrastructure damage scenario B01. This scenario, which displaced 5,069 people, is one of the most damaging MMAF scenarios modeled in this phase of the vulnerability analysis and is listed as one of the red-shaded scenarios in the 95th percentile of consequences in Table 5.1. It may be surprising that an urban fire started by an ignition point profile with a relatively low number of ignition points – two ignition locations, in contrast to the four points modeled using the GOV target profile or the five points modeled using the POP profile – but several factors contribute to the high level consequences of this MMAF scenario. First, the ECO targets are located in an area of high building and population density, so there is more fuel to burn and more people to be affected by the fire than if it were located in the less-dense eastern half of town. Both ECO targets are located in the town's industrial district, where many of the buildings have low Occupancy Hazard Classification values (i.e., high hazard for fire). Thus, a fire which consumes the buildings in the industrial district may require more than twice as much water to extinguish as one which burns residential or government buildings

which are comparable in size. In addition, Table 5.2 shows that water system damage profile B01 is one of the more serious water system damage scenarios. The combination of low-OHC buildings near the ignition points and high-consequence water system damage means that the stressed water distribution system can supply only a limited amount of water for firefighting, and the suppression is not as effective as it would be in a residential or commercial section of town.

Comparing the unsuppressed and suppressed burn profiles shown in Figure 5.2a and Figure 5.2b provides insight into the effectiveness of the fire suppression at various times. The suppressed and unsuppressed fire areas at the end of the simulation are the same; for this infrastructure damage scenario, the fire is never fully suppressed, and fire progress stops only when the fire reaches the boundaries of the urban area in all of its fire spread directions. However, the time it takes to cover the full burn area is considerably longer in the suppressed case. With the exception of the red innermost polygon, which shows the fire's extent before the fire department begins fighting the fire, the polygons are spaced at equal sixty-minute intervals. The wider bands of color visible at each time step in the unsuppressed case mean that the fire is moving considerably faster – that is, covering more area in the same amount of time – than in the suppressed case. Because of this, the suppressed fire takes longer to consume the affected area, which gives emergency managers longer to evacuate the buildings on the outer reaches of the affected area.

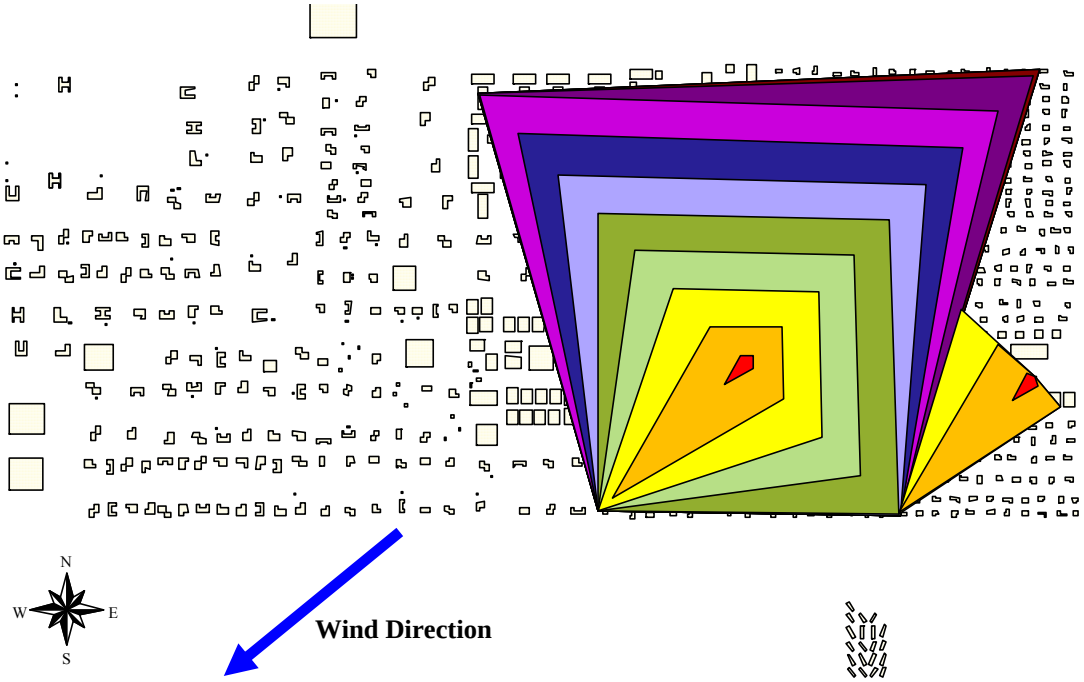

Fig. 5.2a. Unsuppressed fire area, ECO target profile, wind 10 mph at 225 degrees.

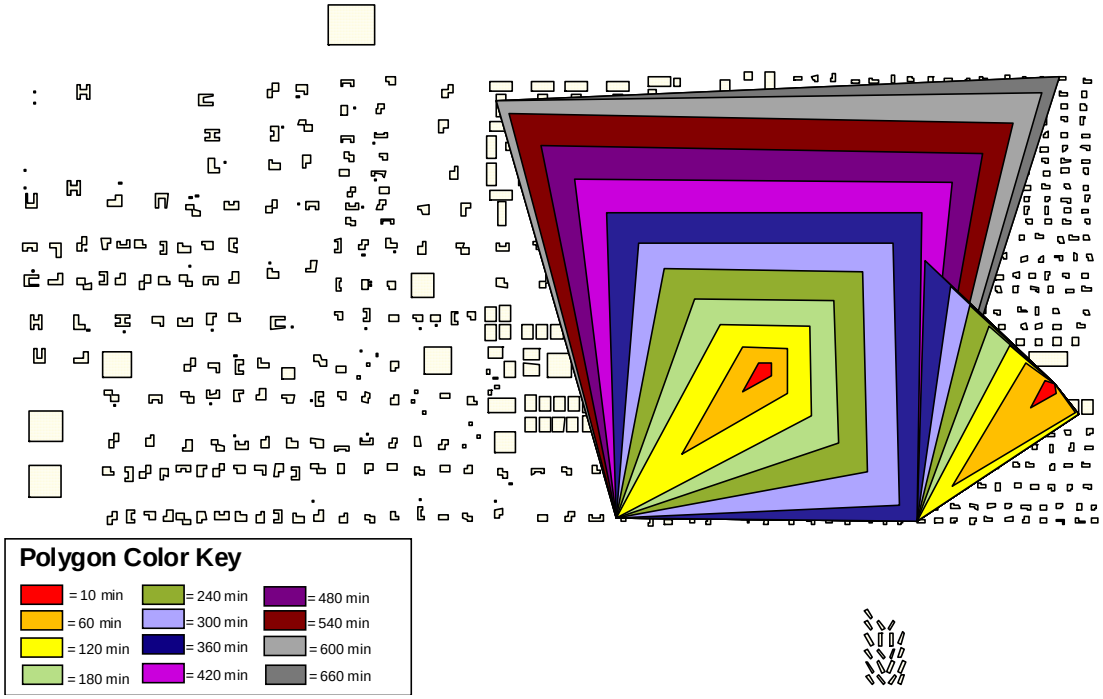

Fig. 5.2b. Suppressed fire area, ECO target profile, wind 10 mph at 225 degrees, water system damage scenario B01.

Figures 5.3a and 5.3b show another example of an urban fire which was ultimately stopped not by fire suppression but by the boundaries of the urban area; this example was selected from the orange-shaded scenarios in the 75th percentile of damages shown in Table 5.1. This MMAF scenario involved an urban fire started in four of the government buildings located in the town's central business district (GOV ignition profile), with wind blowing into the northeast and damage to the city's elevated storage tank (infrastructure damage profile D01). This scenario's burned area progress through time also shows that, while the partially-effective fire suppression never stops the fire, it slows it down and provides added time for building evacuation. Figure 5.3b gives an interesting graphical demonstration of differences in the sectors' ability to fight fires effectively. The northwest part of the burned area in Figure 5.3b shows much higher effectiveness in the fire suppression – that is, the bands of color are narrower and the fire takes longer to reach the end of the urban area – than the southeastern portion of the burned area in Figure 5.3b. Some additional information about the functioning of the Micropolis water distribution system can explain the differences in fire suppression effectiveness. The northwestern part of the burned area is served by the main trunk line of the distribution system, and this is one of the highest pressure zones in the distribution system because the water has just left the high-service pumps downstream of the water treatment plant and has not yet lost much of its energy to friction. In addition, fire hydrants are plentiful in this area, so there are ample locations for the fire trucks to get the water they need to fight the fire. In contrast, the southeastern part of the burned area is supplied with water at a lower pressure because the water loses energy to friction on

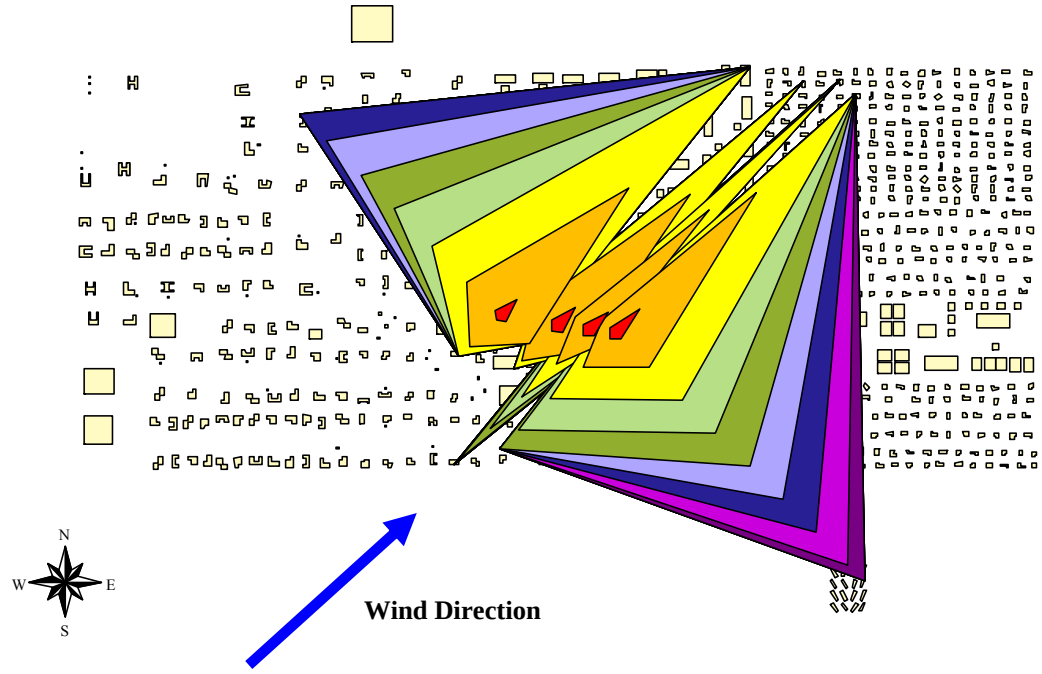

Fig. 5.3a. Unsuppressed fire area, GOV target profile, wind 10 mph at 45 degrees.

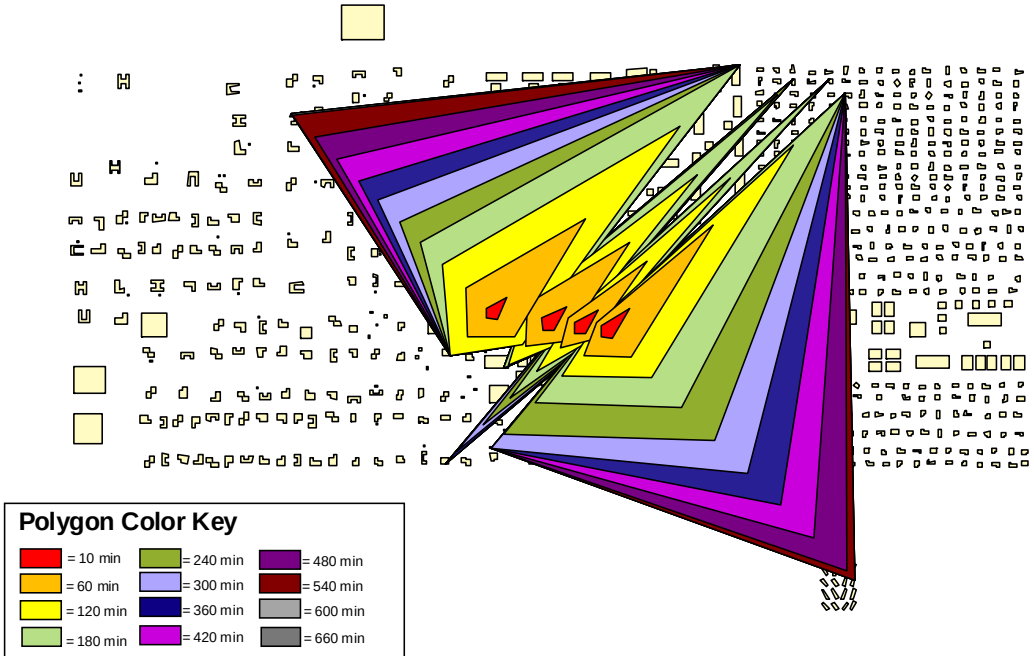

Fig. 5.3b. Suppressed fire area, GOV target profile, wind 10 mph at 45 degrees, water system damage scenario D01.

the circuitous path it must take from the water treatment plant to the fire hydrant. In addition, fire hydrants are comparatively sparse in that area of the city, placing a greater strain on the hydrants that are available. The result of these differences in the state of the water distribution system at the two locations is that the northwestern sector has more water available for firefighting, and it experiences more effective fire suppression. The southeastern sector has less water available at pressures adequate for firefighting, so the firefighting activity is less effective at reducing the fire's rate of spread.

Figures 5.4a and 5.4b show a moderate-consequence urban fire; this scenario was chosen from the yellow-shaded 50th damage percentile and caused the displacement of 3,118 people. This MMAF scenario involved an urban fire starting at the city's three school buildings, with wind blowing at 10 mph into the northeast. Because this scenario's infrastructure damage profile was long-term damage to all three of the water system's high-service pumps, the only source of water for firefighting is the city's elevated storage tank. Figure 5.4b clearly shows the effects of this limited water supply. Examining the fire polygons originating from the ignition point closest to the center of town shows that the fire suppression is effective at slowing the rate of the fire's spread in the early hours of the simulation. Particularly after 240 minutes, however, the bands of incremental fire area for each time step grow wider, which means the rate of fire spread increases. Examining the hydraulic output of the water distribution system model for this scenario shows that the elevated storage tank is completely empty by 255 minutes, so it is reasonable to conclude that the change in fire spread rate is caused by exhausting the supply of water for firefighting.

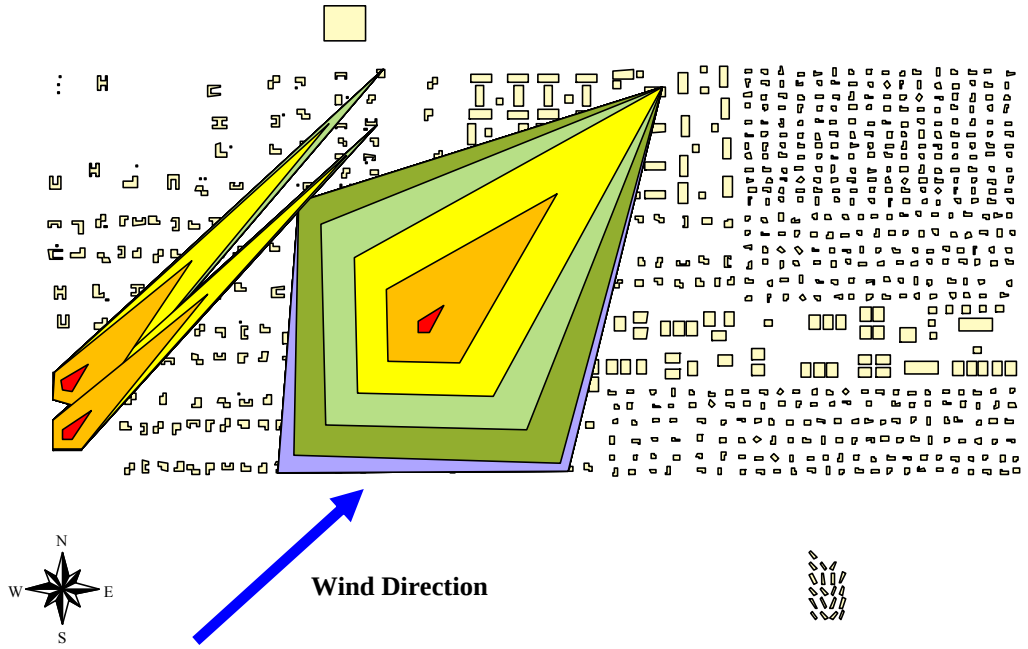

Fig. 5.4a. Unsuppressed fire area, SCH target profile, wind 10 mph at 45 degrees.

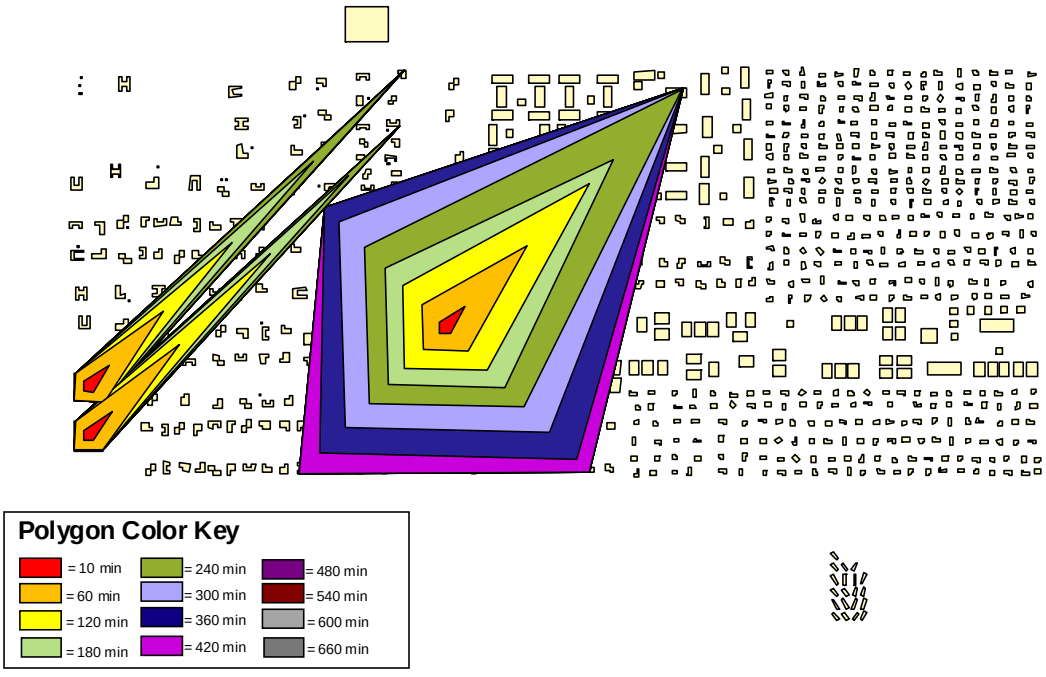

Fig. 5.4b. Suppressed fire area, SCH target profile, wind 10 mph at 45 degrees, water system damage scenario A01.

Figures 5.5a and 5.5b show the urban fire resulting from ignition points at the area's greatest population centers, with the wind blowing at 10 mph into the east. This scenario is a relatively low-consequence scenario, selected from the blue-shaded (25^{th} damage percentile) category in Table 5.1. This scenario displaced 1,983 people. Figure 5.5b clearly demonstrates the impact of effective fire suppression early in the disaster. The figure shows that the easternmost fire ignition point's fire is completely suppressed in the downwind direction after one hour. This early suppression saves almost the entire industrial district – the area covered by the unsuppressed burn polygon associated with that ignition point -- from being burned. Totally effective suppression is achieved after two hours of simulation time for the urban fire associated with the middle school, which is on the western edge of the urban area. While the fire's suppression does not ultimately save the adjoining residential area from being burned – it is eventually reached by the fire from another ignition point – this early suppression pushes back the damage by about seven hours, giving area residents additional time to evacuate.

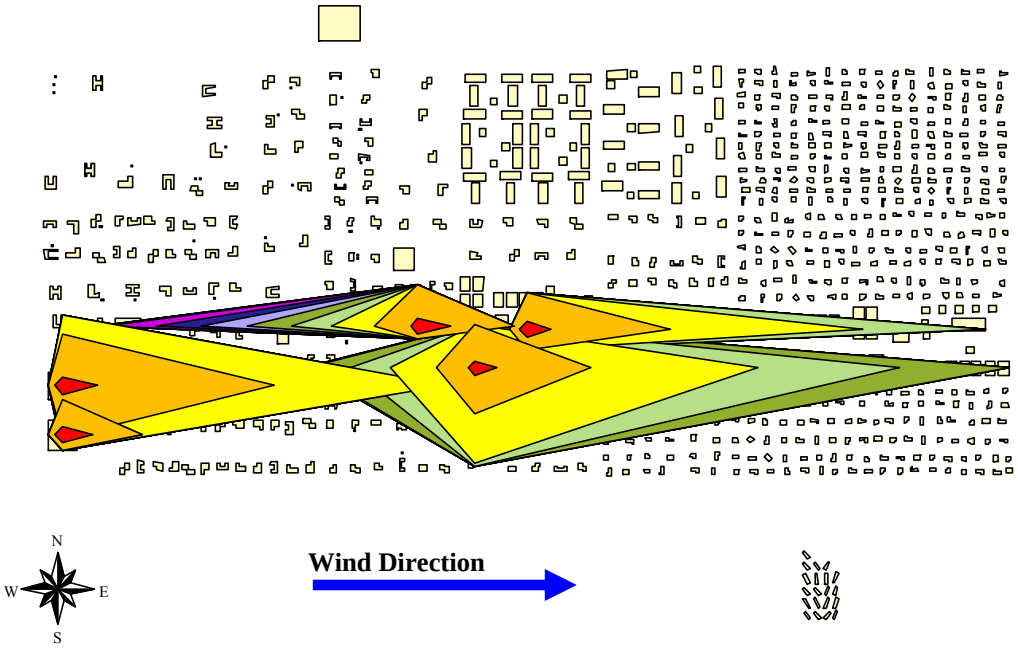

Fig. 5.5a. Unsuppressed fire area, POP target profile, wind 10 mph at 0 degrees.

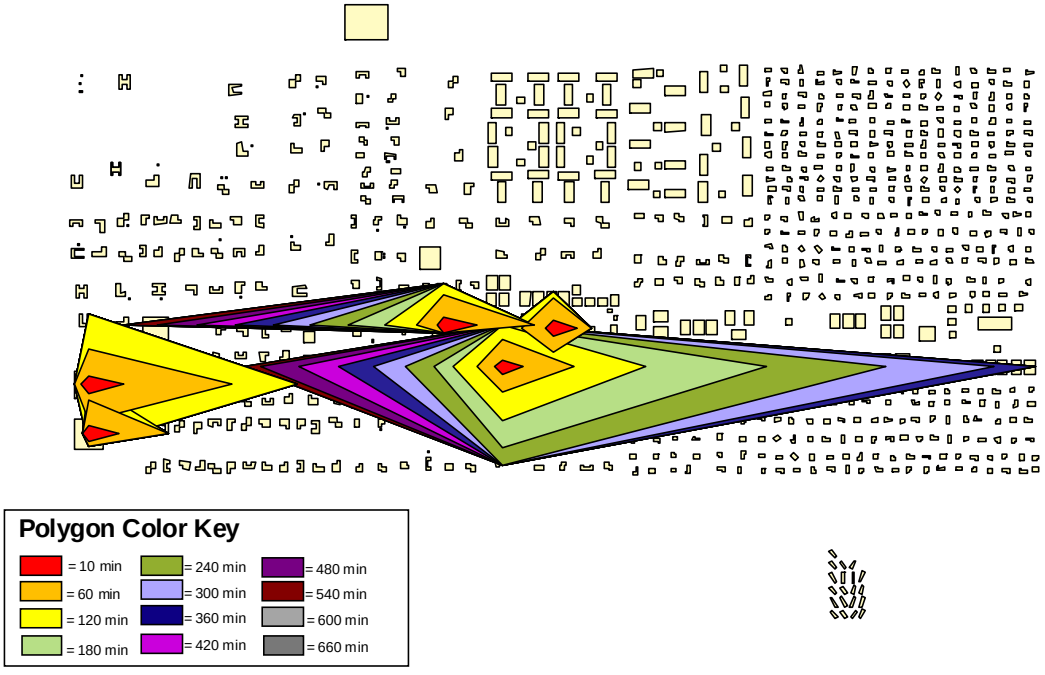

Fig. 5.5b. Suppressed fire area, POP target profile, wind 10 mph at 0 degrees, water system damage scenario D02.

Figures 5.6b, another low-consequence MMAF scenario, provides even more examples of the benefit of early totally-effective suppression. This scenario features an attack on the area's houses of worship with wind blowing at 10 mph into the northwest. It was selected from the green-shaded scenarios in Table 5.1, and this scenario displaced 696 people. As Figure 5.6a shows, the unsuppressed burned area is quite large and stretches into the highest-density residential area in the north-central part of town. However, totally-effective suppression halted the fire's spread in the sidewind-right direction for all three ignition points, cutting off the fire's potential to threaten the high-density residential area and the high-density central business district. Totally effective suppression in the sidewind-left direction for the westernmost ignition point kept that target's fire from engulfing the middle school, another high-consequence building. Effective suppression kept the fire away from high-population-density areas, which is the reason for the scenario's low overall consequences and the dramatic reduction in area between the unsuppressed and suppressed fire spread simulations.

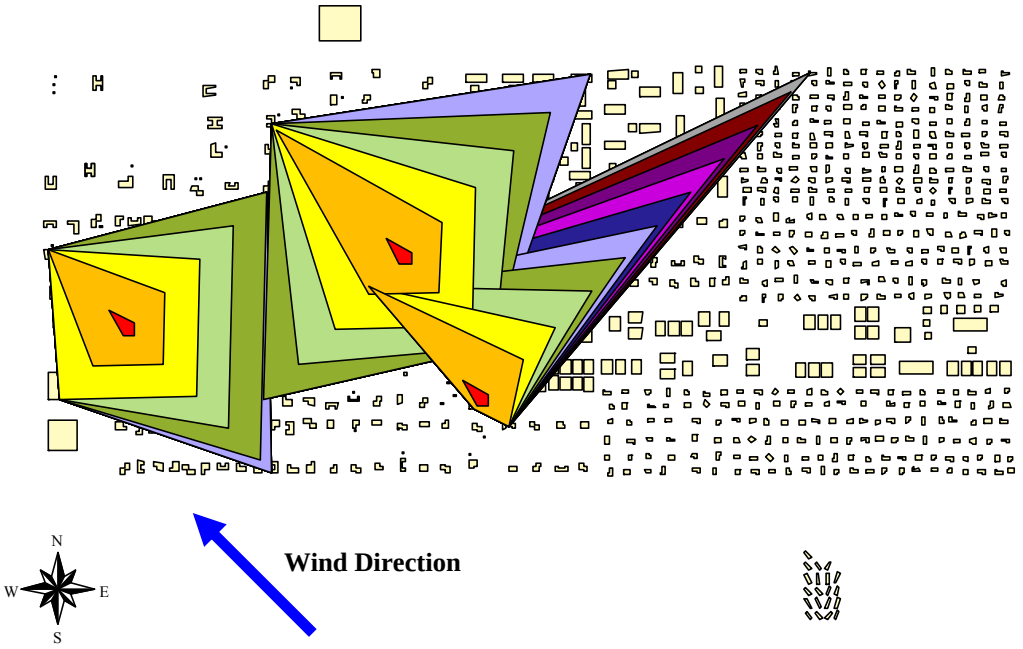

Fig. 5.6a. Unsuppressed fire area, CHU target profile, wind 10 mph at 135 degrees.

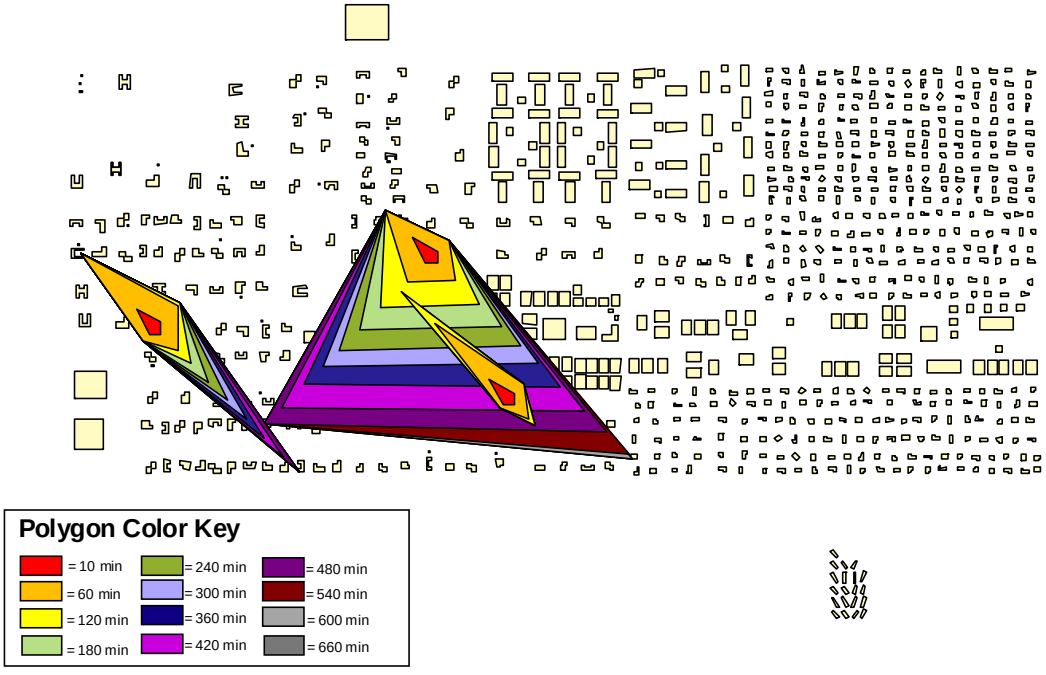

Fig. 5.6b. Suppressed fire area, CHU target profile, wind 10 mph at 135 degrees, water system damage scenario E01.

5.4. Using Dynamic Programming to Find Worst-Case Ignition Point Placement

Applying the technique of dynamic programming to the placement of urban fire ignition points to determine the worst-case MMAF scenario was more complicated than was originally anticipated. The fact that the burned-area polygons may overlap, but buildings may only burn once, means that the incremental damage caused by choosing to place an incendiary device at any particular ignition point depends not only on the number of incendiary devices already placed (the state) but *where* they were placed (the decision history). It is difficult to account for this added level of complexity with the traditional dynamic programming technique.

A modified form of dynamic program could be developed to solve this type of problem, where the incremental gain is defined explicitly *a priori* for each possible combination of burn polygons. Figure 5.7 on page 91 helps illustrate this technique. Instead of determining before the solution that the incremental value of starting the fire that causes burn polygon 5 (purple polygon) is a single value – for example, 250 people displaced – the algorithm could be instructed to use an incremental gain value of 225 if an incendiary device has already been placed at point 4, or a value of 230 if one has been placed at ignition point 3, or a value of 210 if one has already been placed at ignition point 6. Since two incendiary devices may already have been placed when the algorithm reaches ignition point 5, the analyst would similarly need to determine the incremental damage caused by setting a fire at point 5 if fires have already been started at all possible two-ignition-point combinations of point 3, point 4, and point 6 – these are all of the polygons that intersect polygon 5 in Figure 5.7. This process would have to be repeated

for every potential ignition point to construct a conditional incremental-gain table to be used in calculating the running gain during the dynamic programming solution. The considerable added effort involved in conducting this analysis defeats the purpose of using dynamic programming and *a priori* damage calculations to simplify the optimization process, so this technique is not recommended for use in determining the worst-case placement of urban fire ignition points.

5.5. Optimizing Ignition Point Placement by Enumeration

The total enumeration optimization method described in Section 4.6.3 successfully located the worst-case arrangement of urban fire ignition points for wind blowing into the east at 10 mph and infrastructure damage scenario D01, which involves the destruction of the elevated storage tank at the beginning of the simulation. The worst-case ignition point placement, shown in Figure 5.8 on the next page, displaces 6,778 people, which is greater than the population of Micropolis because many of the disaster victims lose both their home and their workplace to the fire. This scenario is particularly damaging because the fire ignition points are located mainly in the high population density areas of town and in areas where the route of water from the treatment plan to the local hydrants is impeded by low-diameter pipes. This limits the effectiveness of fire suppression, although the suppression is still partially effective at decreasing the rate of fire spread. The extent of the burned area over time is shown in Figure 5.9a and 5.9b.

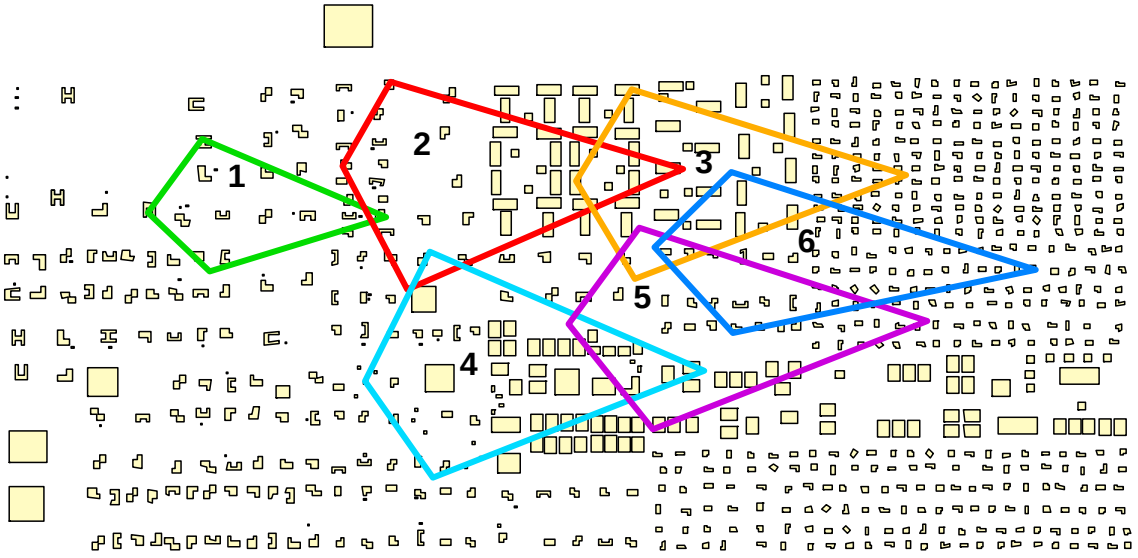

Fig. 5.7. Illustration of challenges of solving the ignition point placement problem using dynamic programming techniques.

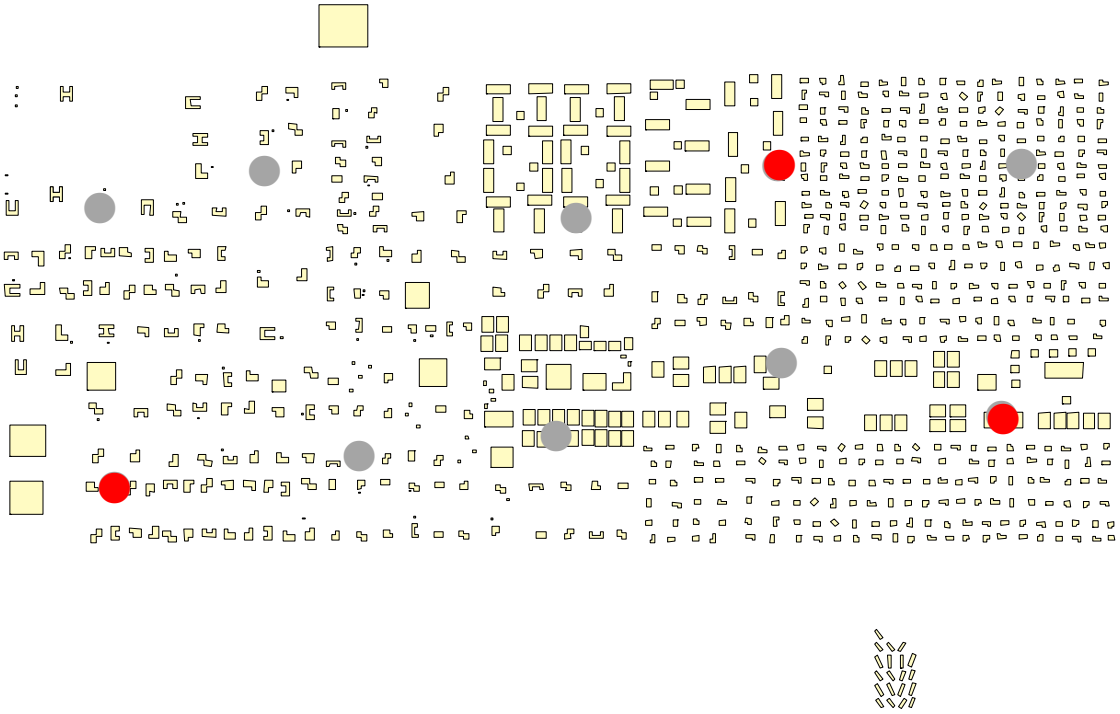

Fig. 5.8. Location of the worst-case ignition point arrangement. Ignition points are indicated by red circles. Non-optimal ignition points are indicated by gray circles.

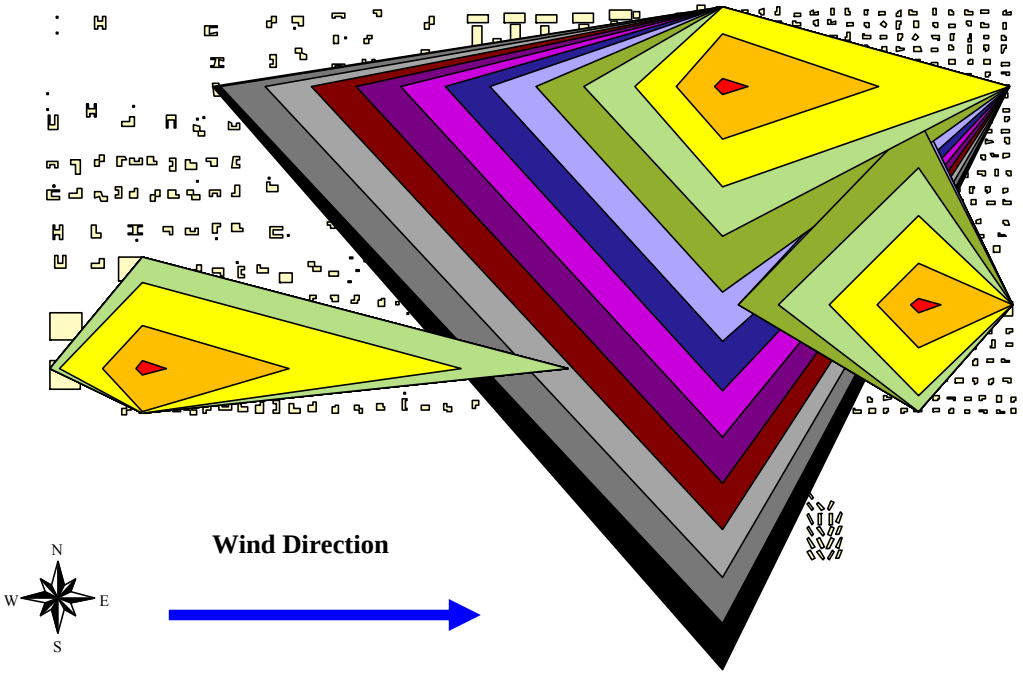

Fig. 5.9a. Unsuppressed fire area, optimized ignition points, wind 10 mph at 0 degrees.

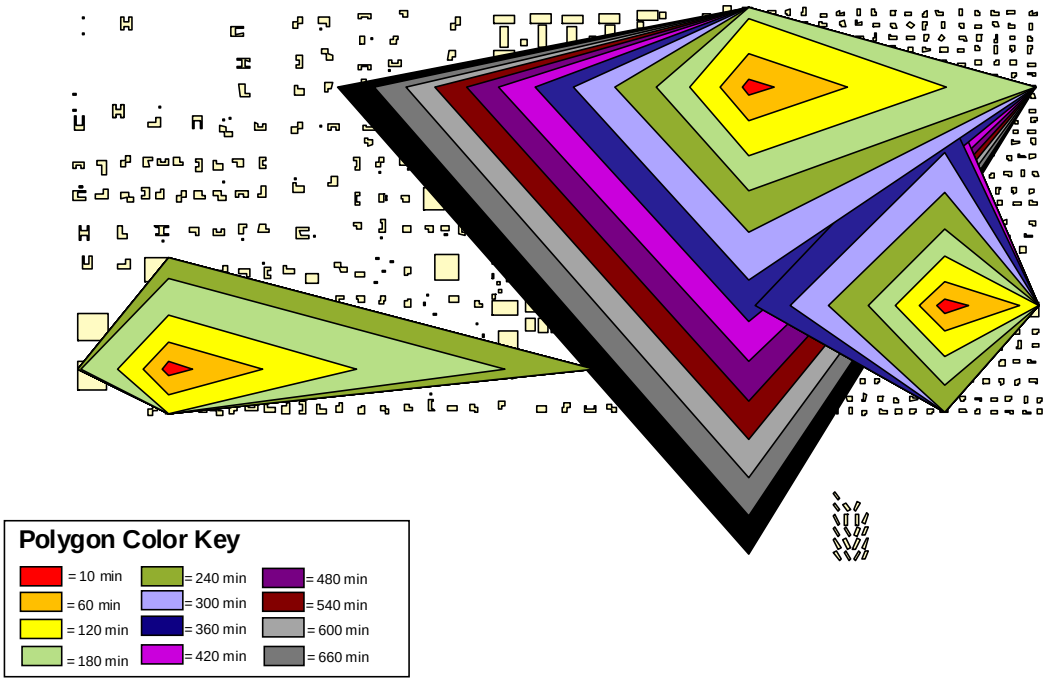

Fig. 5.9b. Suppressed fire area, optimized ignition points, wind 10 mph at 0 degrees, water system damage scenario D01.

5.6. Conclusion

The results of the extensive MMAF damage scenarios provide good insight into the possible scope of an attack or disaster involving an urban fire with damage to one or more community infrastructures. The severity of many of these MMAF scenarios clearly indicate the need for measures to mitigate the damage against the water systems and other support infrastructures, thereby increasing their ability to function in disasters even under heavy damage. The results of this analysis also suggest a variety of possible mitigation measures, as shown in Table 5.2 and discussed in Section 5.1. This discussion of potential mitigation measures continues in Section 6, which addresses the methodology of designing potential measures and testing their effectiveness against multi-mode attacks and failures.

6. METHODOLOGY: MITIGATING MULTI-MODE ATTACKS AND FAILURES

6.1. Introduction: Importance of Mitigating Infrastructure Damage

The primary goal of the study presented in this dissertation is to develop and test measures to mitigate damage to the support infrastructures which contribute to effective fire response, especially the water distribution system. Mitigating potential multi-mode attacks or failures (MMAFs) is an important step in protecting communities against complex attacks and disasters. In general, mitigation techniques provide passive protection against attacks or failures, minimizing the damages and disruption of services which accompany disasters by increasing infrastructures' physical resistance to damage (Tierney, Lindell, and Perry 2001). Mitigation complements traditional security measures like guards, fences, and security cameras around important system assets. These traditional measures decrease the likelihood of a successful attack against support infrastructures; the mitigation measures modeled here decrease the consequences of an attack or failure which thwarts the traditional security measures and actually takes place.

The mitigation measures studied in this phase were designed based on the most serious modes of infrastructure damage revealed by the unmitigated MMAF simulations described in Sections 4 and 5. This section presents seven potential mitigation measures and the methodology used to test their effectiveness against MMAFs. The results of this analysis are presented in Section 7.

6.2. Design of Mitigation Measures

Table 5.2, which identifies the most damaging support infrastructure damage scenarios, can help suggest mitigation measures to counter the effects of the most serious damage scenarios. These most serious damage modes were incorporated into the design of the mitigation measures presented in this section. In addition, common impediments to effective firefighting (e.g. loss of pressure caused by inadequately-sized water mains, lack of sufficient fire trucks, etc.) were also considered in the mitigation design process. Seven mitigation measures were developed and tested for their effectiveness against the MMAF scenarios described in Section 4.

6.2.1. Mitigation Method M01: Enlarging All Water Mains

Hydraulic simulations of the Micropolis water distribution system under fire flow demands show significant pressure loss when water must pass through low-diameter mains, particularly the system's 2-inch and 4-inch diameter mains. This pressure loss is caused by increased friction with the pipe walls in small-diameter pipes, and lost water pressure in the water distribution system can cause a decrease in the amount of water available at firefighting pressures. To decrease friction-caused pressure loss, the first mitigation method investigated the effect of replacing with 12-inch ductile iron pipe all water main sections with a diameter of less than 12 inches, which is the largest pipe diameter present in the Micropolis water distribution system. This measure requires the replacement of about 38,000 feet of pipe, at an estimated cost of $1.8 million for the materials and labor involved in excavating, replacing, and backfilling the pipe sections.

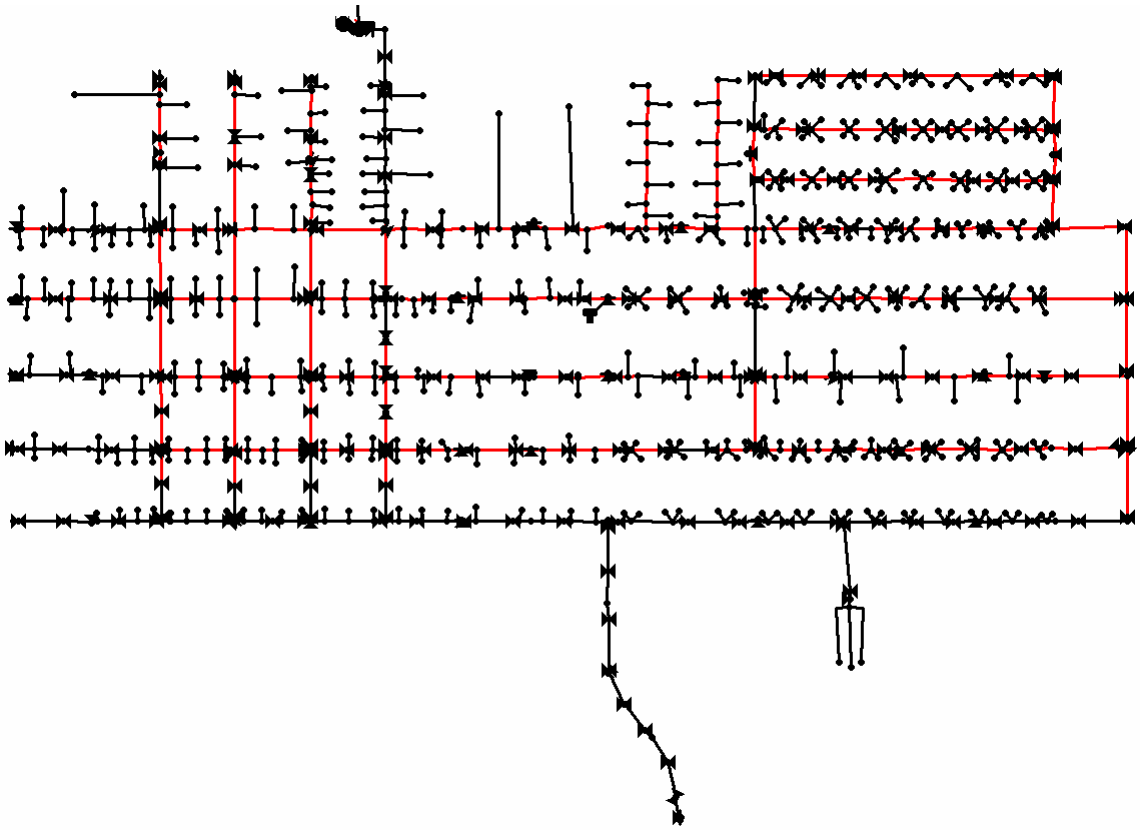

Fig. 6.1. Water mains to be replaced in mitigation method M01. Red lines show mains which are less than 12 inches in diameter; these are replaced by 12-inch ductile iron pipes in the M01 scenario.

This estimate is presented in 2005 dollars and is derived from cost data from *Mechanical Cost Data 1997*, also known as the Means Manual (R.S. Means Company 1996), with costs adjusted for inflation. The water mains affected by this proposed mitigation measure are shown in a schematic diagram of the water distribution system's hydraulic model in Figure 6.1.

6.2.2. Mitigation Method M02: Enlarging 2-Inch Water Mains

The high cost of implementing mitigation method M01 raised the concern that water utilities would be unable to finance such an extensive water main replacement project even if it were shown to be highly effective at improving the water distribution system's ability to resist multi-mode attacks and failures (MMAFs). A lower-cost alternative is to replace only the smallest mains in the water distribution system, since these pipes are the ones which cause the most energy loss in the system. Accordingly, mitigation method M02 was designed to test the effectiveness of this strategy. The Micropolis water distribution system includes about 4.300 feet of 2-inch diameter cast iron pipe, located mainly in the central business district and the residential areas immediately adjacent. This area contains the city's oldest buildings, and the small-diameter cast iron pipes are artifacts of the city's original water distribution installed circa 1910 (Brumbelow et al. 2006), before modern water system design and firefighting practices were developed. Mitigation method M02 involves replacing the 2-inch water mains with 12-inch diameter ductile iron mains, which are the standard water mains used in the city's most recent water distribution systems expansions. The cost of this mitigation method is estimated at approximately $200,000 in 2005 dollars (R.S. Means Company 1996). The water mains affected by this mitigation measure are shown in Figure 6.2.

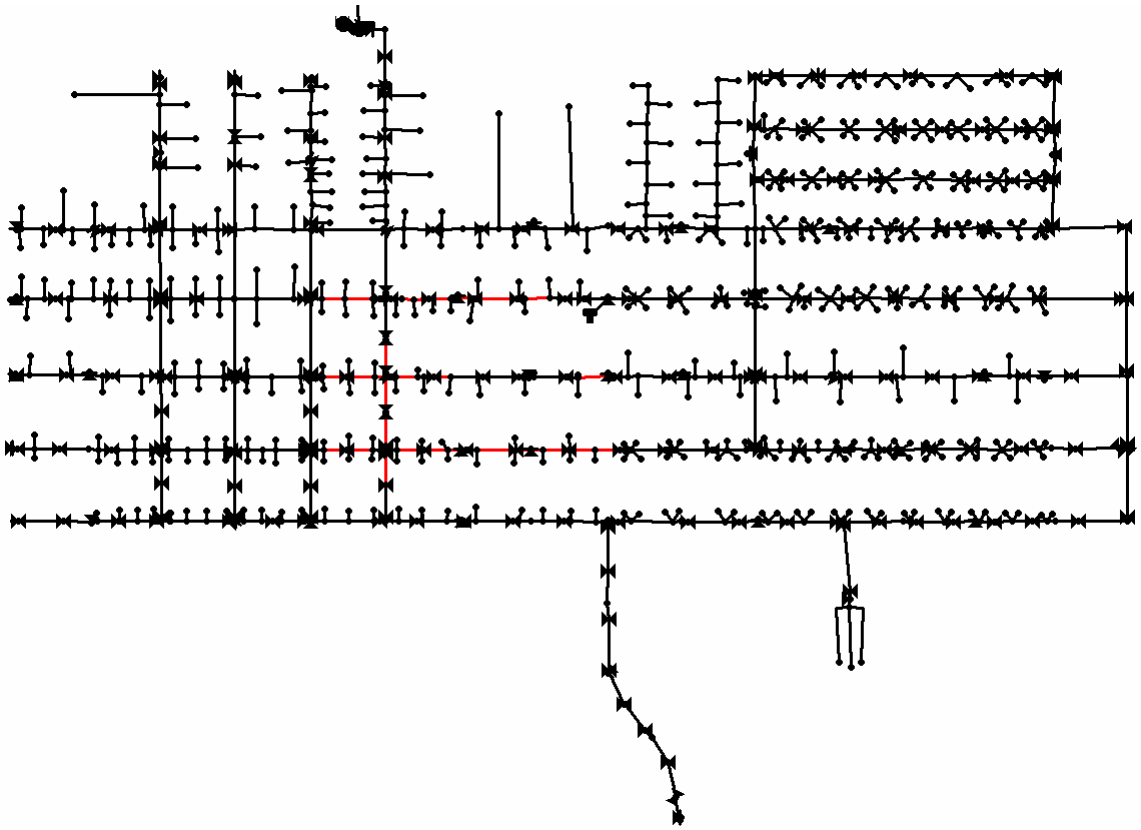

Fig. 6.2. Water mains to be replaced in mitigation method M02. Red lines show mains which are 2 inches in diameter; these are replaced by 12-inch ductile iron pipes in the M02 scenario.

6.2.3. Mitigation Method M03: Voluntary Water Conservation

Fire flow demands are large compared to a typical household's or business's base-level water usage. The large number of households and businesses in Micropolis compared to the possible number of fire demands raises the possibility that the water used for base-level demands may decrease the water available for fire fighting during high-demand periods. Mitigation measure M03 was designed to test the impact of base-level demands on the water system's ability to provide water for fire fighting and the effect of a voluntary water-conservation order during the disaster response period.

The water-conservation order was assumed to reduce all base-level demands to half their pre-conservation levels. This mitigation measure does not include any physical change to the water distribution system, but it is assumed that a successful conservation order must be prefaced by a public education campaign explaining the reason for emergency conservation measures and their potential benefit. This education campaign may include measures like television advertisements, paid advertisements in local newspapers, and inserts in water utility customer bills. In addition to the cost of producing these items, one or more city employees' time would be required to draft these materials. The cost of this education campaign is estimated very roughly at $50,000.

6.2.4. Mitigation Method M04: Auxiliary Elevated Water Storage Tank

The analysis of the most serious water infrastructure damage scenarios presented in Section 5.1 highlights the importance of the surge capacity provided by the water distribution system's single elevated storage tank in helping the fire department meet fire flow demands. Several of the support infrastructure damage scenarios involve the destruction of the elevated storage tank, however, and the damages associated with this profile were often high. Many other damage scenarios preserved the fire department's access to the storage tank, but their consequences increased when the tank was drained as a result of prolonged fire fighting demands. Mitigation measure M04 investigates the benefits of additional water storage capacity for use in fire response.

Mitigation scenario M04 includes a second elevated storage tank, approximately half the size of the main tank, located on the eastern edge of town. The auxiliary tank is located away from the main tank so that an event which compromises one tank may not affect the other tank. The eastern side of town was chosen as the auxiliary tank's location because hydraulic simulations of the water distribution system indicate that the residential areas on the east side are most likely to experience lowered water pressure during peak demand periods. These zones are the most hydraulically distant from the water treatment plant and high-service pumps, so loss of pressure caused by friction with pipe walls is most pronounced in this area.. Thus, the auxiliary water tank may present a dual benefit: increased water for firefighting during emergencies and improved service quality during non-emergency usage.

The auxiliary tank's location is shown in Figure 6.3. The tank's capacity is approximately 375,000 gallons. The estimated cost of constructing the tank is $475,000 in 2005 dollars, based on construction cost estimates from *Mechanical Cost Data 1997* (R.S. Means Company 1996) and adjusted for inflation.

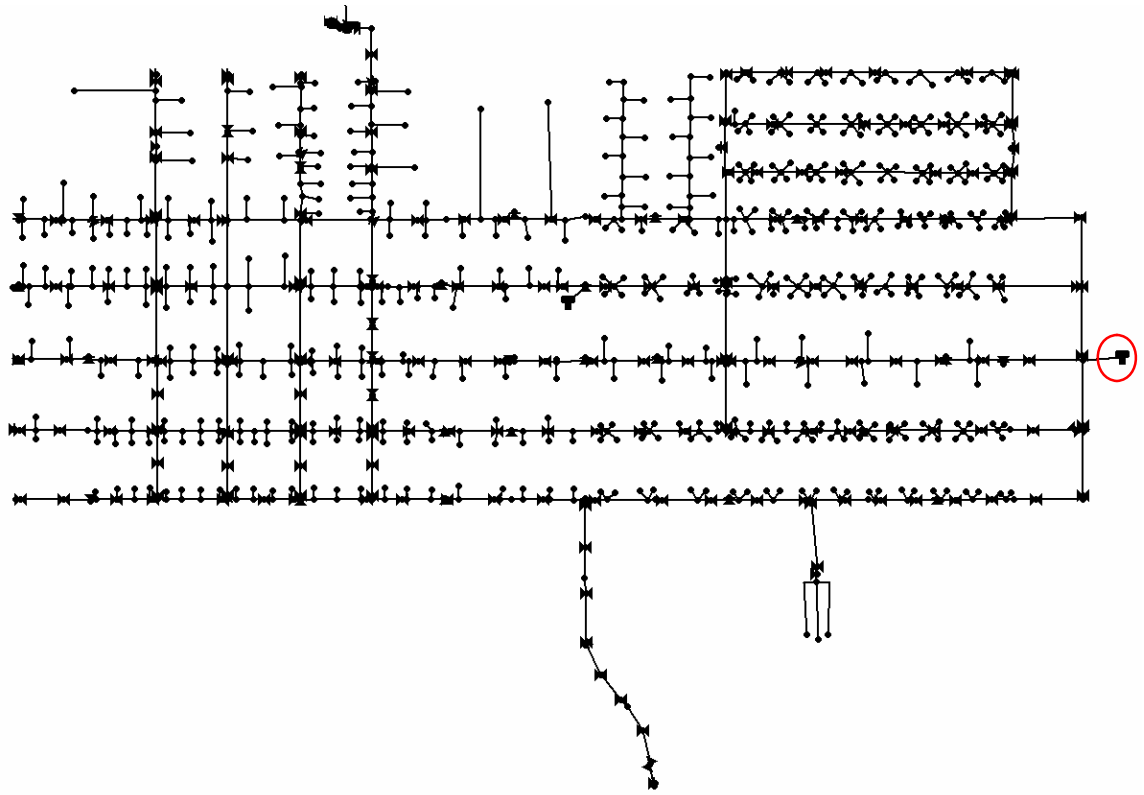

Fig. 6.3. Location of auxiliary elevated water storage tank for mitigation method M04. The auxiliary tank is circled in red and is located on the eastern edge of town.

6.2.5. Mitigation Method M05: Additional Mutual Aid Fire Response

Fire departments typically plan in advance to deal with fires that overwhelm their own resources by creating mutual aid contracts with nearby communities. (Eckman 1994) Accounting for resources arising from mutual aid is why the Model of Urban Fire Spread uses a time-varying number of available fire trucks. Since MUFS uses two different types of firefighting resources – available fire trucks and water – to calculate the effectiveness of the fire suppression, it is possible that securing additional fire trucks

through mutual aid contracts could help more effectively contain the urban fires resulting from high-consequence multi-mode attacks and failures.

Mitigation measure M05 was designed to investigate the effect of additional mutual aid resources on fire suppression effectiveness for the MMAF scenarios studied here. This mitigation measure doubles the number of fire trucks available through mutual aid contracts. The number of trucks available immediately (the community's own firefighting resources) does not change. A time series of the fire trucks available over time for this mitigation measure is shown in Figure 6.4. This mitigation measure is assumed to have negligible cost of implementation.

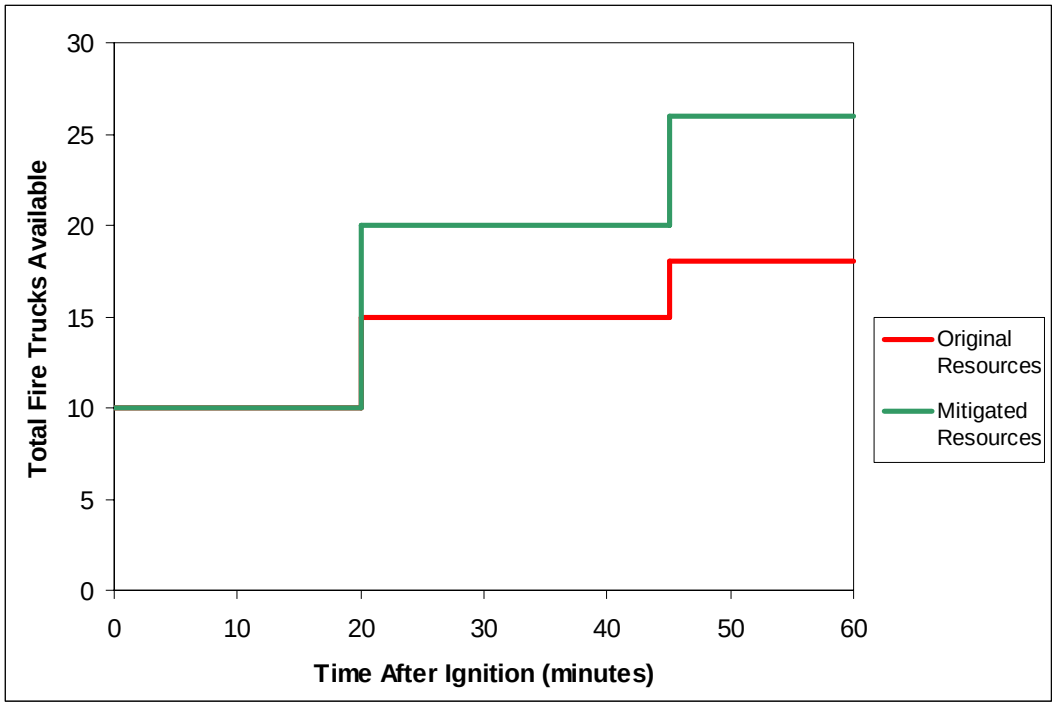

Fig. 6.4. Time series of fire trucks available in Micropolis using mitigation measure M05**.**

6.2.6. Mitigation Method M06: Auxiliary High-Service Pump Station

The analysis of most serious water infrastructure damage scenarios presented in Section 5.1 highlighted the importance of the water utility maintaining at least one high-service pump operating during the fire fighting operation. The system's three high-service pumps are all located at the same site, however, so an attack or failure which compromises one pump is more likely to affect all three pumps than if they are located separately.

Mitigation measure M06 installs a fourth high-service pump located far away from the three main pumping stations as part of an auxiliary water supply connection. The pipeline is 5,700 feet long and is constructed of 12-inch diameter ductile iron pipe, which is the standard large-diameter pipe used in Micropolis's most modern water supply lines. The auxiliary pump is identical to the three primary high-service pumps. The installation cost of the pipeline and pumping station are estimated at $240,000 in 2005 dollars (Abelin, Pritchard, and Sanks 2006). The locations of the pump and pipeline are shown in Figure 6.5. Water in this auxiliary supply line runs from the water treatment plant along the north edge of town to the pump and connection to the water distribution system, which are located in the residential area in the northeastern quadrant of Micropolis.

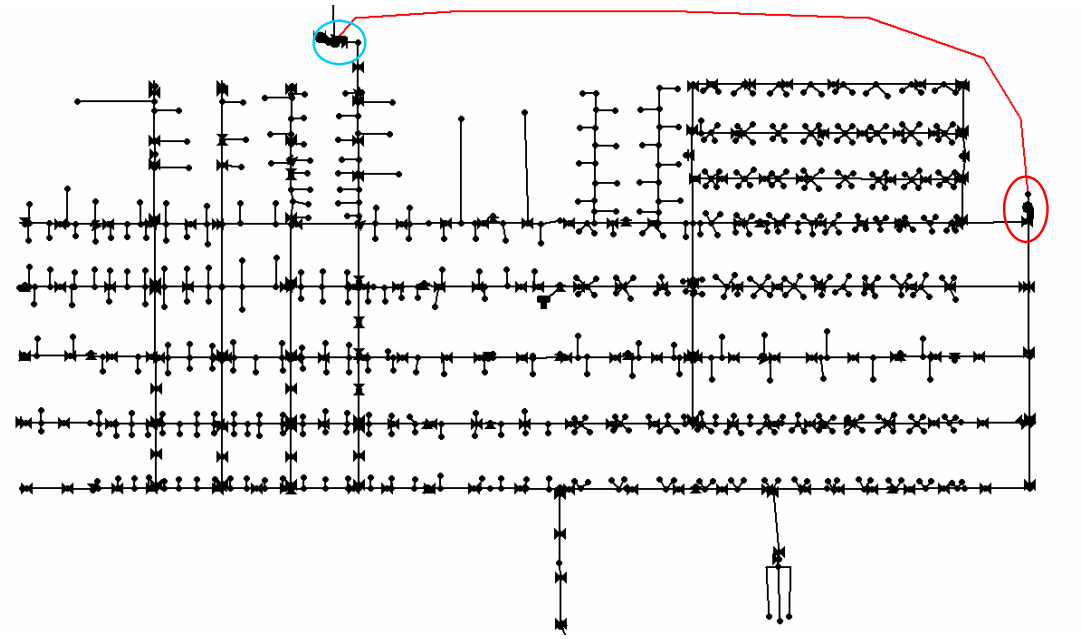

Fig. 6.5. Auxiliary water supply pipeline and pump for mitigation method M06. The auxiliary pipeline is shown as a red line. The auxiliary high service pump is circled in red. The location of the three primary high service pumps is circled in blue.

In addition to providing backup pumping capacity for fire response in case the primary pumping station is damaged, this mitigation measure has the dual benefit of improving water pressure in the northeastern quadrant of town. As discussed in Section 6.2.4, that area of Micropolis is the most likely to experience lower water pressure during periods of peak demand, because the water must travel long distances, often through low-diameter pipes, to reach the area. The auxiliary supply line, which provides a more direct route (through a large diameter pipe) from the water treatment plant to the northeastern residential zone, serves as a bypass to this circuitous route and decreases the likelihood of unsatisfactory water pressure during daily high-demand periods.

6.2.7. Mitigation Method M07: Portable Above-Ground Emergency Water Mains

The final conclusion of the analysis of the most serious support infrastructure damage scenarios in Section 5.1 was that the scenarios which involve isolation of areas of the water system (damage profiles E and F from Sections 4.3.5 and 4.3.6) present a dual impediment to effective fire response. The isolation denies water to any fire hydrants located in the isolated zone, preventing them from contributing to fire response. In addition, damage scenarios like F01 that block heavy-use water mains force water traveling to other areas to take a circuitous alternate route, increasing the loss of energy due to friction with pipe walls and potentially decreasing the available flow of water at the pressure needed for fire fighting.

One potential solution to the problems raised by isolating sections of the water distribution system is for communities to run temporary, portable water mains above the ground to serve as alternate paths for water which would normally pass through the isolated area. These temporary water mains could also be run from working hydrants to hydrants inside the isolated area to provide a source of water for fire fighting if needed. This solution is modeled here as mitigation measure M07.

The temporary pipelines are modeled as running between fire hydrants, because fire hydrants are easily accessible from above ground and serve as convenient access points to the water distribution system. The temporary mains were modeled as 10-inch diameter hoses with rubber interior walls, since it was hypothesized that extended lengths of large-diameter fire hoses could be used for this purpose. This mitigation measure is assumed to have a negligible implementation cost, since it involves the

temporary redeployment of resources the fire department probably already possesses. The precise configuration of temporary mains differed for each damage scenario, and the configuration would probably be determined *ad hoc* by the fire department and water utility in the event of a real emergency. An example of the hydraulic model which includes temporary mains is shown in Figure 6.6.

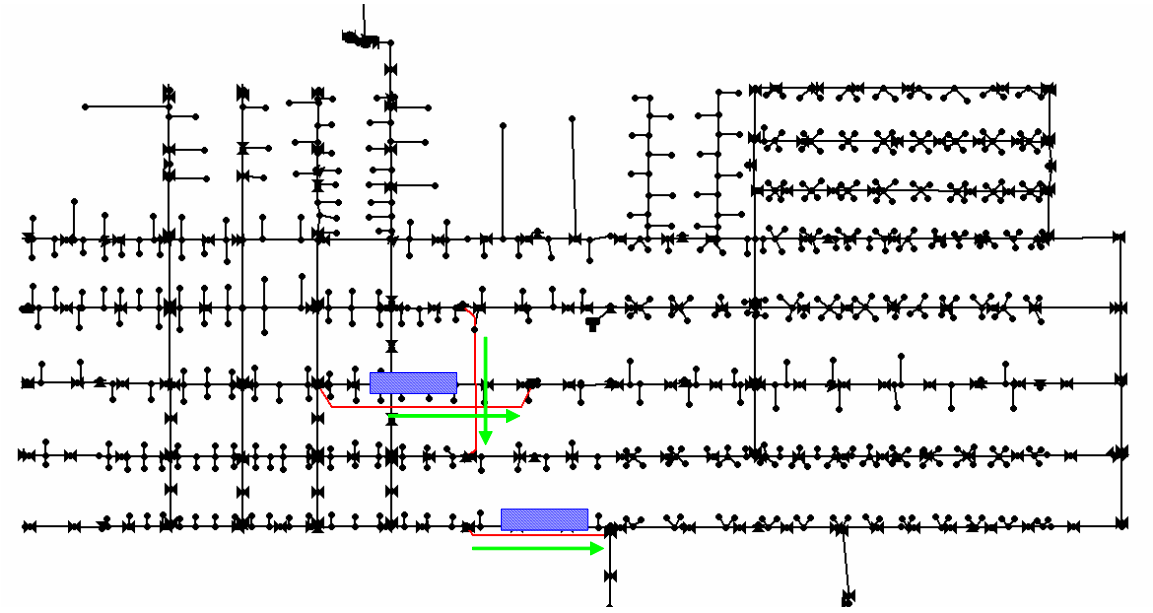

Fig. 6.6. Micropolis water system under damage scenario E04 mitigated by measure M07. Sections blocked by water main breaches are shown in the blue-hatched areas. Temporary water mains are shown by red lines. Dominant directions of water flow through temporary mains are shown by green arrows.

6.3 Simulation of Multi-Mode Attacks and Failures with Mitigation Measures in Place

Modeling every infrastructure damage scenario, or even every high-consequence damage scenario, with every mitigation measure would require an extraordinary commitment of computational resources. However, as with the unmitigated infrastructure damage scenarios, simulating a subset of the mitigated damage scenarios can still provide insight into the effectiveness of the various mitigation measures.

The analysis of most serious target profile/wind direction combinations in Section 5.2 identified ten combinations with consequences falling consistently above 3,300 displaced people. These ten combinations of target profile and wind direction were combined with selected infrastructure damage scenarios to test the effectiveness of the mitigation methods described in the previous section. The infrastructure damage/target profile/wind direction "triplets" tested against the mitigation scenarios are shown in Table 6.1. Each of the most serious target/wind direction combinations are shown in the left column, with the infrastructure damage scenarios modeled in conjunction with these combinations listed in the right column. Thus, urban fire MMAF scenarios involving the ECO ignition point group and a wind direction of 45 degrees (top row) were modeled with all combinations of the mitigation methods and infrastructure damage scenarios D01 and G01. The combinations of target profile, wind direction, and infrastructure damage scenarios were chosen to give a representative sample of of the most serious MMAF damage triplets against which the mitigation measures could be tested. Ideally, every mitigation method would be tested against

every MMAF damage scenario, but the resulting simulations would be prohibitively computationally expensive. (Each mitigation simulation took approximately one and a half hours to run on a personal desktop computer.)

Table 6.1. Damage Scenarios Used in Analysis of Mitigation Method Effectiveness

Target Profile and Wind Direction	**Mitigation Methods Tested against these Infrastructure Damage Scenarios:**
ECO 45	D01, G01
ECO 135	A01, F02
ECO 225	B01, F03
ECO 315	A01, BH2
GOV 45	BH1, F04
GOV 225	A03, H01
GOV 270	B02, E02
GOV 315	E01, E03
POP 225	AD1, D02
POP 315	D01, F05

Each mitigation measure was modeled separately by incorporating the mitigation technique into the model of the damaged water system. The resulting damaged and mitigated infrastructure models were used as inputs to multi-mode attack and failure simulations using the Model of Urban Fire Spread.

Mitigation measures M01 through M06 were tested for all scenarios in Table 6.1; mitigation measure M07 was also tested against scenarios with water system damage in damage profiles E and F. Thus, a total of 126 simulations were conducted in the mitigation analysis. The consequences of each mitigated damage simulation were compared to the consequences of the original unmitigated damage simulation to

determine whether the mitigation measures were successful at reducing the consequences of the damage scenarios. The performance of the various mitigation measures are presented and discussed in Section 7 of this dissertation.

7. RESULTS AND DISCUSSION: MITIGATION MEASURES AND MULTI-MODE ATTACK AND FAILURE SIMULATIONS

7.1. Introduction

The previous section introduced seven potential mitigation measures to decrease the effects on communities of multi-mode attacks and failures (MMAFs) involving urban fires with damage to at least one support infrastructure for fire response. A methodology for testing the effectiveness of the mitigation measures was presented, and the results of the tests are presented here. For convenience, Table 7.1 presents a descriptive summary table of the mitigation measures described in Section 6.2. The following sections present a methodology for analyzing each mitigation method's effectiveness and examples of each mitigation method's performance against the MMAF scenarios presented in Sections 4 and 5.

Table 7.1. Summary of Mitigation Methods

Mitigation Method	Description
M01	Replace all water mains with 12 inch ductile iron pipes
M02	Replace 2 inch diameter water mains with 12 inch ductile iron pipes
M03	Voluntary water conservation: reduce all water demands by half
M04	Auxiliary elevated water storage tank
M05	Additional fire trucks available through mutual aid contracts
M06	Auxiliary water supply line and high-service pump
M07	Bridge isolated pipe sections using temporary portable above-ground water mains

7.2. Analysis of Mitigated MMAF Behavior

The original proposal for this dissertation recommended calculating the consequences of an urban fire by totaling the population of the buildings completely or partially within the fire's final burned area. During the analysis of the mitigation results, however, it became apparent that examining the time distribution of the fire's consequences could yield additional insight into the effectiveness of the mitigation measures.

A mitigation measure might provide three possible benefits to emergency response. The most obvious benefit is decreasing the overall consequences of the urban fire. This effect is here named "Peak Consequence Reduction" (PCR) and is calculated as:

$$PCR = C_{pu} - C_{pm} \tag{7.1}$$

where C_{pu} refers to the peak (final) consequences of the unmitigated MMAF simulation and C_{pm} is the peak consequences of the mitigated MMAF simulation. Both of these parameters are measured in units of displaced people. PCR is shown graphically in Figure 7.1 on a graph of fire consequences vs. time for a mitigated and unmitigated urban fire simulation.

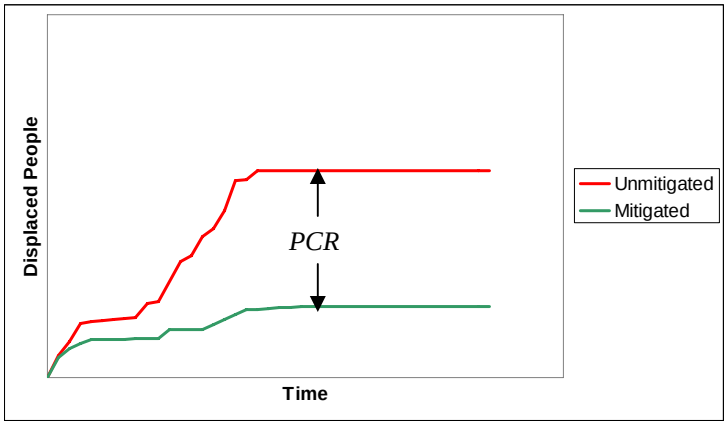

Fig. 7.1. Graphical determination of Peak Consequences Reduction (PCR).

Peak Consequence Reduction is important because it measures the population of buildings which are saved outright by the mitigation measure: in other words, a mitigation measure's PCR is the number of people who do not lose their homes or businesses because of the urban fire, when they would have done so without the mitigation measure in place. This parameter is the single most important measure of a mitigation method's effectiveness, but it is not the only measure.

The second parameter of interest in measuring mitigation effectiveness is "Average Consequence Delay" (ACD). This parameter measures the average amount of time a mitigation measure delays fire event consequences. This delay is averaged across all consequence levels reached by both unmitigated and mitigated fires. (Thus, the average is taken up to the ultimate consequence level of the mitigated fire.) This parameter is important because it represents additional evacuation time afforded by the mitigation measure. For example, an unmitigated and mitigated simulation of a particular damage scenario might both reach a particular damage level – perhaps 2,000

displaced people – and burn approximately the same buildings. Examining only their respective peak consequences level would yield the conclusion that the unmitigated and mitigated fires behaved similarly and that the mitigation measure had no effect. However, as can be seen in Figure 7.2a and 7.2b, the mitigated fire reaches various levels of damage at some time later than the unmitigated fire reaches these levels of damage. Thus, the fire department would have extra time to evacuate people from endangered homes and businesses, which would likely decrease the loss of life and property resulting from the fire. The average value of the delay in attaining all damage levels is used in order to account for delays throughout the firefighting process. The average delay is calculated as:

$$ACD = \frac{\int_0^{t_{pm}} \left[C_u(t) - C_m(t) \right] dt}{C_u(t_{pm}) - C_u(0)} \tag{7.2}$$

where *ACD* is the Average Consequence Delay, the average amount of time the graph of mitigated damages lags behind the graph of unmitigated damages, in units of minutes; t is time after the MMAF's urban fire ignition in minutes; t_{pm} is the time (in minutes after ignition) at which the mitigated MMAF simulation reaches its peak damage level; and $C_u(t)$ and $C_m(t)$ are the consequences of the urban fire at time t for the unmitigated and mitigated MMAF scenarios, respectively. Thus, the integral which appears in the numerator of Equation 7.2 is simply the area between the damage vs. time curves for the unmitigated and mitigated case, measured between the MMAFs' ignition time and the

time when the mitigated MMAF reaches its peak damage. Dividing this area by the increase in unmitigated damages over the early-response period yields the average time lag between the graphs, which is the Average Consequence Delay.

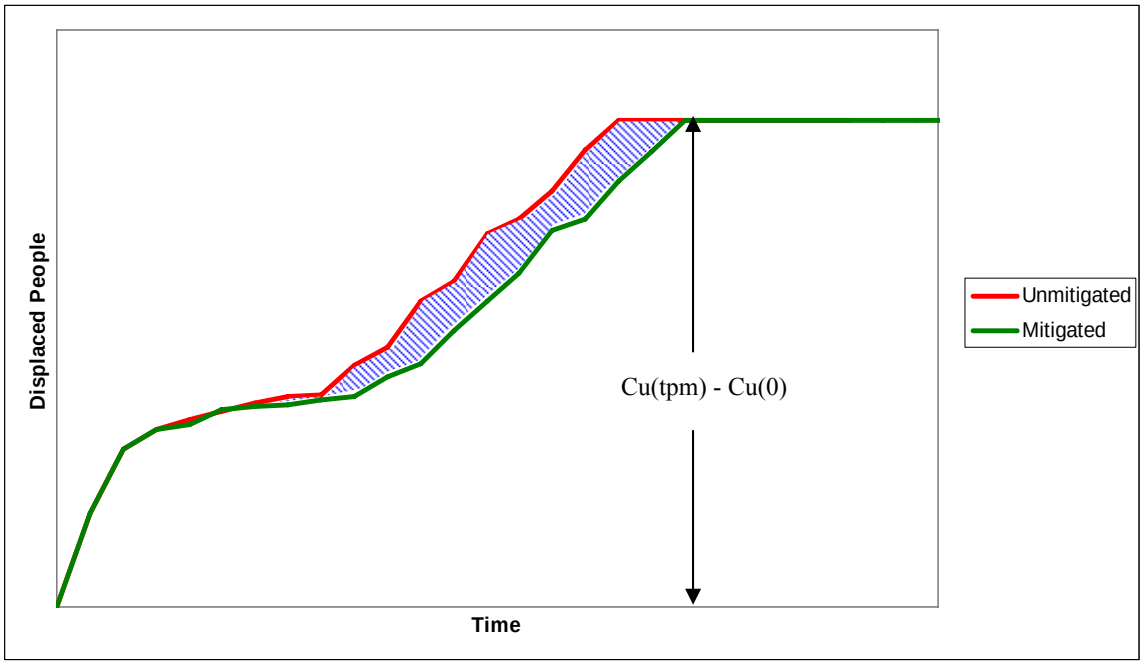

Fig. 7.2a. Key parameters in determining ACD in cases where peak consequences of unmitigated and mitigated damage simulations are the same. The blue-shaded area between the curves is the area represented by the integral in the numerator of equation 7.2. The difference in consequences at time = 0 and the time at which the mitigated simulation reaches its peak is the denominator of Equation 7.2. The area shaded in blue divided by the difference in starting and peak mitigated consquences is the Average Consequence Delay.

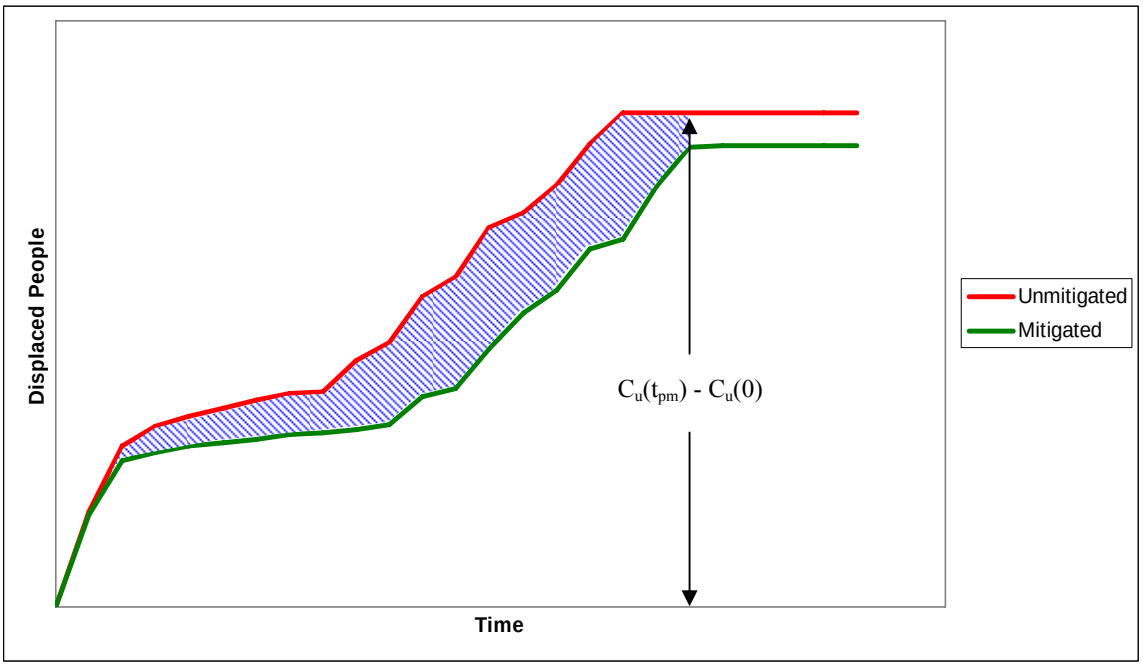

Fig. 7.2b. Key parameters in determining ACD in cases where peak consequences of the mitigated damage simulations are lower than the unmitigated case. Note that the area between the curves is calculated only up to the time when the mitigated damage simulation reaches its peak consequence level.

The third parameter considered in this analysis is the difference in the amount of time it takes the fire department to bring the unmitigated and mitigated scenarios' fires under control – that is, for the fires to reach their peak level of damages. This parameter, named here "Expedited Control Time" (ECT), is calculated as:

$$ECT = t_{pu} - t_{pm} \tag{7.3}$$

where t_{pu} is the time after ignition (in minutes) the unmitigated MMAF simulation reaches its peak consequence level, and t_{pm} is the time in minutes for the mitigated MMAF simulation to reach its peak consequence level. *ECT* has a positive value when

the peak of the mitigated damage simulation occurs earlier than the peak of the unmitigated damage simulation. By contrast, the value is negative when the peak of the mitigated damage simulation comes *after* the peak of the unmitigated damage scenario.

ECT is not sufficient to describe a mitigation measure's effectiveness on its own, because additional information about the temporal distribution of fire consequences is needed to interpret the significance of the ECT value. However, it does provide insight into the mitigation measure's effect on the urban fire's behavior. If the ultimate consequences of the mitigated fire scenario are lower than the unmitigated consequences, a positive ECT value means that the fire department was able to achieve totally effective suppression in the mitigated scenario faster than in the unmitigated scenario. Halting the fire's progress earlier is a benefit to the community for two reasons: first, the spatial extent of the fire (and its resulting consequences) are lower than they would otherwise have been; and, second, the firefighters are freed from active suppression earlier, so they can turn their attention to search and rescue and emergency medical activities. Although MUFS does not directly predict the casualty level from the urban fire, bringing the fire under control sooner and reassigning firefighters to other activities is likely to decrease the injuries and/or mortalities resulting from the fire.

Negative values for ECT (i.e., the peak of the mitigated scenario's damage distribution occurs later than the unmitigated scenario's peak) combined with a significant reduction of consequences from the unmitigated to the mitigated scenario are not necessarily a recommendation against the mitigation method under consideration. As was stated above, the reduction in peak consequences is the most important indicator

of a mitigation method's suitability. In this case, the negative value of ECT simply indicates a long period of partially-effective suppression that eventually ends in totally effective suppression; as a result, the firefighters will be engaged longer with the actual fire fighting than they would have been in the unmitigated case, but the fire suppression will be more successful than for the unmitigated case. The value of ECT can be useful in making the choice between two mitigation alternatives which provide similar reduction in consequences, because the mitigation measure which brings the fire under control sooner is likely to have fewer casualties.

If the consequences of the mitigated urban fire are nearly or exactly the same as the unmitigated fire, however, a positive value of ECT means that the same damage happens for both fire scenarios but the burning is accelerated for the mitigated case. Clearly, this is not a desirable outcome for the mitigation measure. In this case, a positive ECT value should be interpreted as a recommendation *against* the mitigation measure under consideration.

7.3. Mitigated MMAF Simulation Results

All of the mitigation measures were tested for twenty MMAF scenarios as described in Section 6.3, and the aggregate results of the mitigation testing are presented and discussed here. A complete presentation of the mitigation results' performance is included in Appendix A2.

7.3.1. Mitigation Method M01: Performance and Discussion

In general, mitigation method M01 was the most effective of all the mitigation measures tested. A representative example of the method's performance for MMAF damage scenario F02 is shown in Figure 7.2, with the results of the mitigated damage simulation compared to scenario F02's unmitigated results. For both the unmitigated and mitigated simulations, the wind is blowing to the northwest at 10 mph and the urban fire starts at the ignition points specified by the ECO target profile. It is clear from the graph that mitigation method M01 is highly successful by all three effectiveness metrics; this case is generally representative of the mitigation measure's performance with other MMAF damage scenarios. In the case shown in Figure 7.3, the mitigation measure reduces the consequences of the original MMAF scenario by 4,382 displaced people (a reduction of 87% from the original damage level). The ACD for the mitigation measure is about 160 minutes, and the ECT for mitigated damage scenario F02M01 is 240 minutes. (The six-character notation used to describe the mitigated infrastructure damage simulations combines the three-character infrastructure damage scenario notation – in this case, infrastructure damage scenario F02 – with the three-character notation for the mitigation measure – for this example, M01.)

The choice to upgrade all the water mains in the water distribution system has a large benefit for this damage scenario: it saves the homes and businesses of 4,382 people, gives the fire fighters an extra 160 minutes to evacuate the homes and businesses which are still destroyed by the fire, and allows the fire department to stop fighting fires

and focus on search and rescue and emergency medical help four hours sooner than in the unmitigated damage scenario.

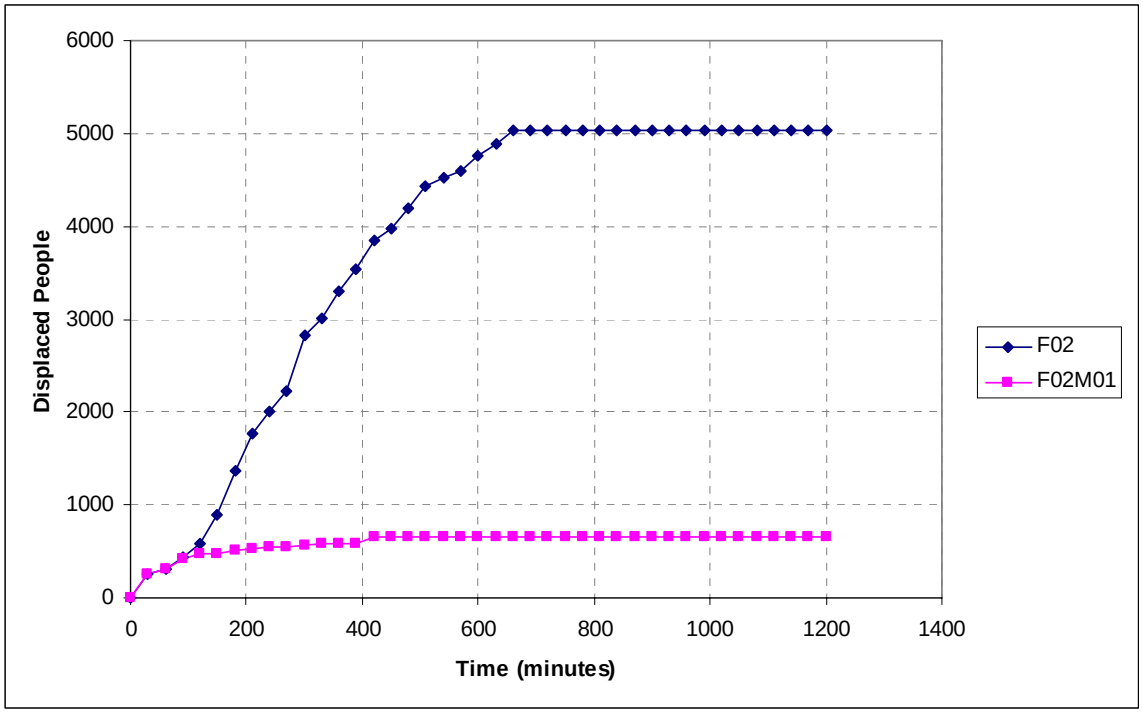

Fig. 7.3. Example of performance of mitigation method M01. The unmitigated damage simulation (blue graph) used water damage scenario F02, with wind blowing to the northwest at 10 mph and the ecoterrorism target profile (ECO).

As seen in Table 7.2 and Figure 7.3, this mitigation measure is highly effective at reducing the consequences of a variety of MMAF scenarios. The major disadvantage to this mitigation measure is its cost of implementation. As discussed in Section 6.2.1, this mitigation measure involves replacing about 38,000 feet of pipe at a cost of $1.8 million. The effort and expense involved may not be feasible for all community water systems. This potential cost hurdle is the reason mitigation method M02 was examined as a special case, in order to investigate the effectiveness of replacing only a subset of the

system's mains (at a fraction of the cost of method M01). The performance of this strategy is discussed in section 7.3.2.

7.3.2. Mitigation Method M02: Performance and Discussion

Mitigation method M02, which involves the replacement of all 2-inch diameter mains with 12-inch ductile iron pipes, performed nearly as well as mitigation method M01 in many cases. A representative example of the measure's effect on MMAF damage scenario A03 is shown in Figure 7.4. For the example shown, the wind is blowing into the southwest at 10 mph and the urban fire starts at the GOV target profile. In this example, the mitigation method's PCR is 2,243 displaced people. The average additional evacuation time, as measured by the mitigation method's ACD, is about 245 minutes. The peak of the mitigated damage vs. time graph occurs later than the peak of the unmitigated graph, so the ECT value is -120 minutes (i.e. the firefighters are engaged in fighting the fire for two hours longer in the mitigated case than the unmitigated case). As discussed in Section 7.2, however, a negative ECT value is not a recommendation against a mitigation strategy in cases like this one where the final consequences of the mitigated MMAF simulation are significantly lower than the consequences of the unmitigated simulation.

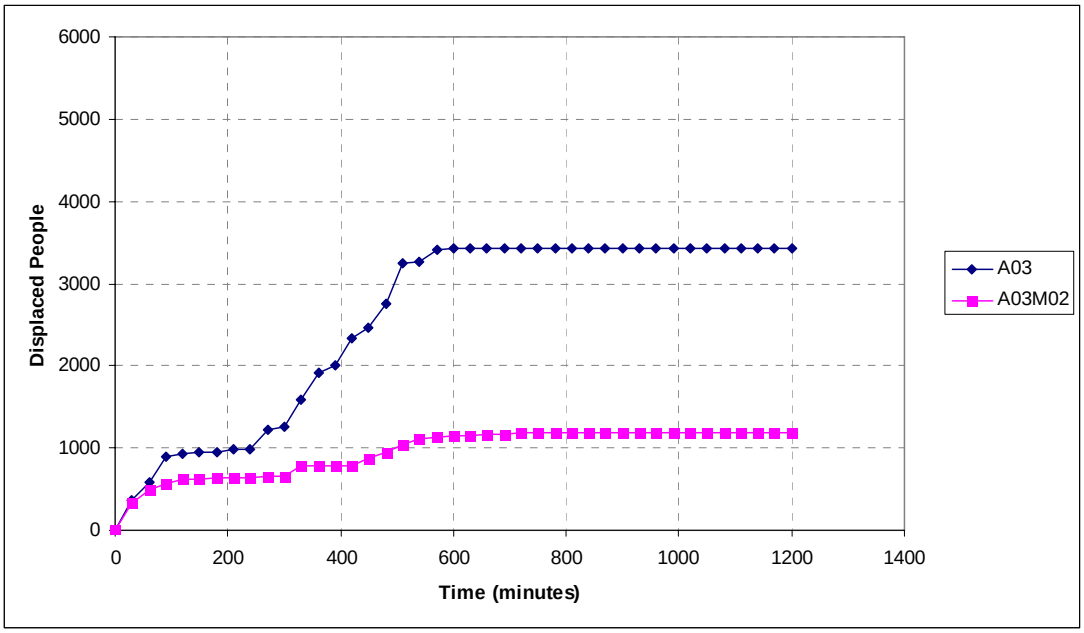

Fig. 7.4. Example of performance of mitigation method M02. Unmitigated damage simulation (blue line) used water damage scenario A03, with wind blowing southwest at 10 mph and the government buildings target profile.

7.3.3. Mitigation Method M03: Performance and Discussion

As discussed in section 6.2.3, mitigation method M03 tests the effect of limiting base-level water demands using voluntary water conservation during fire fighting operations. This mitigation method's performance was inconsistent; it was very effective in some cases and had very little impact in others. Figure 7,5 shows the unmitigated and mitigated consequences over time for the MMAF scenario involving infrastructure damage scenario F04 with an urban fire starting at the GOV ignition point profile and prevailing wind blowing to the northeast at 10 mph: a scenario for which the mitigation method performed well.

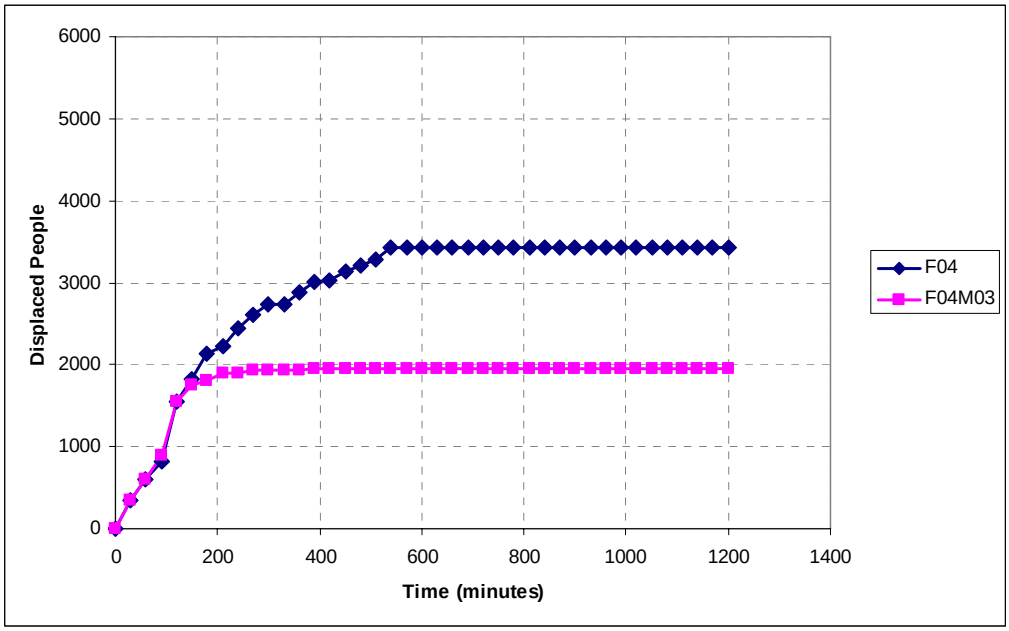

Fig. 7.5. Example of performance of mitigation method M03. Unmitigated damage simulation (blue line) used water damage scenario BH2, with wind blowing northeast at 10 mph and the government buildings target profile.

In the damage and mitigation results shown above, the PCR produced by mitigation measure M03 is 1,472 displaced people. Additional evacuation time yielded by the mitigation measure, as represented by the mitigation measure's ACD, is about 60 minutes. With the reduced demands in place, the fire department was able to bring the fire under control two hours sooner than in the unmitigated case (ECT value of 120 minutes).

The mitigation measure did not provide consistent benefits for all the damage scenarios against which it was evaluated. It is notable, however, that this mitigation method, which has no direct costs of implementation, produced significant benefits in some cases. Although this mitigation measure is not recommended as the only action in

an MMAF mitigation strategy, it is worth considering in conjunction with other mitigation measures.

7.3.4. Mitigation Method M04: Performance and Discussion

The effect of adding an auxiliary elevated storage tank is examined in the mitigated damage simulations using mitigation method M04. Figure 7.6 shows an example of the consequences over time for this mitigation measure, compared to the corresponding unmitigated damage simulation. Both unmitigated and mitigated scenarios involved an MMAF scenario with infrastructure damage scenario BH2 and the ECO urban fire ignition point profile, with prevailing winds blowing 10 mph into the southeast. In the figure below, the peak consequence reduction produced by the mitigation method was 4,200 displaced people. The mitigation technique provided about 150 minutes of additional evacuation time, as shown by the technique's ACD value. The mitigated fire came under total control about 30 minutes later than the unmitigated fire, but as stated earlier this is not a recommendation against the mitigation method because of the considerable reduction in overall consequences for the fire.

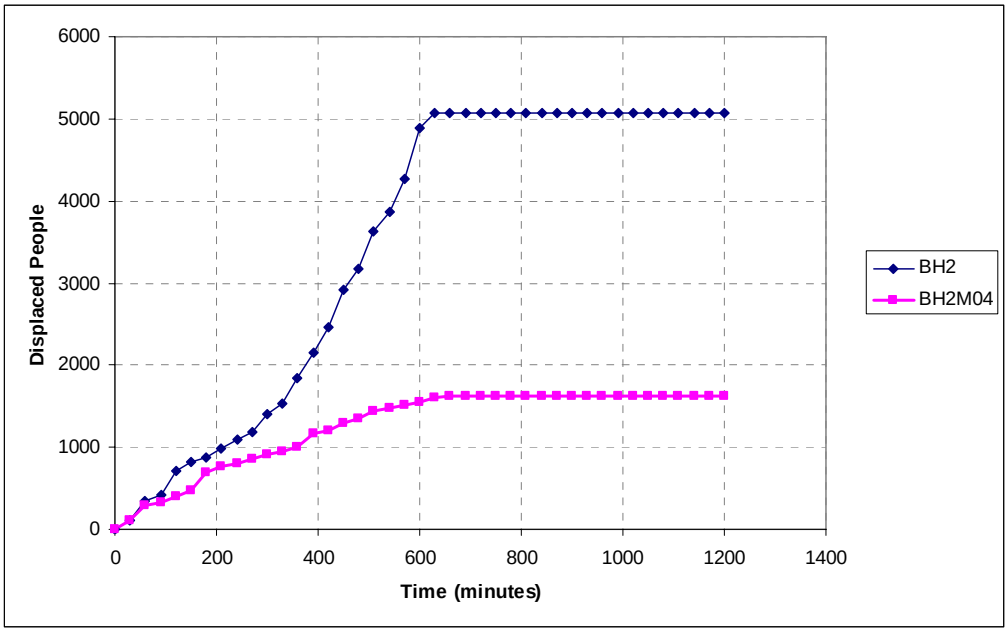

Fig. 7.6. Example of performance of mitigation method M04. Unmitigated damage simulation (blue line) used water damage scenario BH2, with wind blowing southeast at 10 mph and the ecoterrorism buildings target profile.

Mitigation strategy M04 was highly effective when employed against an urban fire starting from the ecoterrorism (ECO) target profile, and the benefits to fire suppression for this target profile were noted across a wide range of infrastructure damage scenarios and wind directions. This effect is probably due mainly to the location of the auxiliary water storage tank on the east side of town, close to the ignition points in the ecoterrorism target group. The mitigation measure was also very effective in scenarios which directly threatened buildings on the eastern side of town: for example, scenarios originating from targets in the Central Business District with wind directions 45 or 315. The mitigation measure was markedly less effective in improving fire suppression for scenarios which did not originate in or directly threaten the eastern side

of town, which suggests that the effects of the effect of the auxiliary stoage tank were highly localized. Modifying this mitigation method to provide the benefit to the entire urban area might require the construction of several auxiliary storage tanks, which would greatly increase the cost of implementing the mitigation measure.

The observation that, in many of the ecoterrorism damage scenarios, installing the auxiliary water storage tank is approximately as effective as mitigation measure M01 suggests that the limiting factor in effective fire response to this target profile may be the difficulty in getting water at sufficient pressure for firefighting in the area surrounding the ignition points. As discussed in Section 6.2.4, the pressure loss is caused by the fact that this area of town is hydraulically distant from the high-service pumps, and the water must pass through small-diameter pipes to reach the area. Mitigation measures which reduce energy loss caused by friction (such as M01 and M02) or provide an alternate water supply for the area (such as M04 and M06) were generally highly successful.

7.3.5. Mitigation Method M05: Performance and Discussion

Mitigation method M05 takes a different approach from the techniques examined in previous sections. While many of the mitigation techniques evaluated in this project mitigate MMAF damage by making more water available for firefighting, this technique augments firefighting ability by making more fire trucks available through mutual aid contracts. This technique was added to the group of possible mitigation strategies in order to determine the extent to which lack of available fire trucks is the limiting factor in effective MMAF fire suppression.

In most cases, mitigation technique M05 had little or no effect on the MMAF scenario's final consequences, but the availability of additional trucks and fire fighters did provide a small amount of extra time (usually about 30 minutes) for evacuation of the affected buildings. An example of this type of effect is shown in Figure 7.7. For both simulations in the figure, the infrastructure damage scenario is D01, the urban fire starts at the POP ignition point profile, and the wind is blowing 10 mph into the southeast.

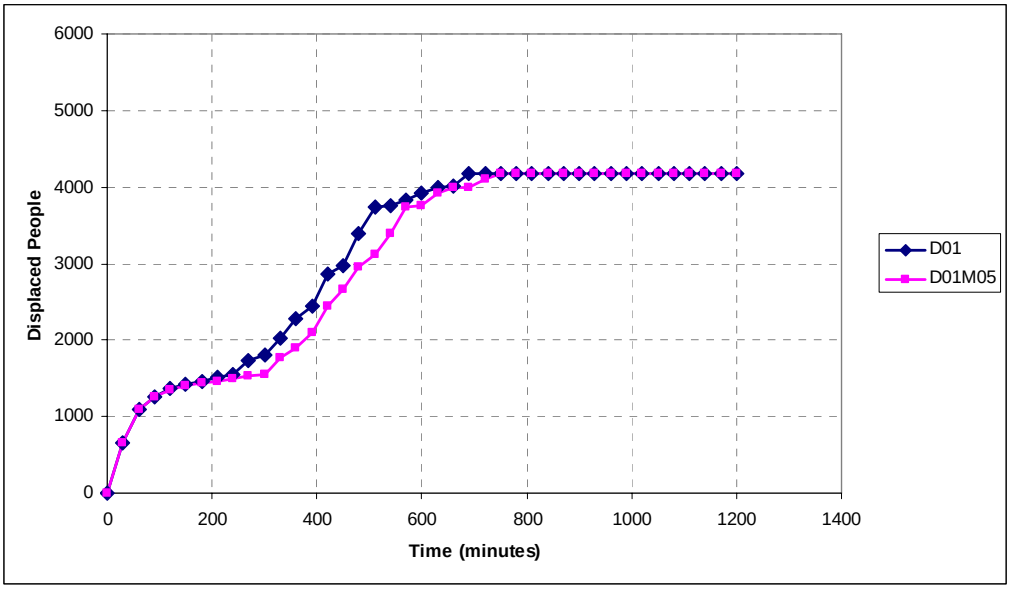

Fig. 7.7. Example of performance of mitigation method M05 with low effectiveness. Unmitigated damage simulation (blue line) used water damage scenario D01, with wind blowing southeast at 10 mph and the high-population buildings target profile.

In the example shown above, the reduction in ultimate consequences is 0 displaced people. The only benefit afforded by the additional firefighters was an ACD of 31.3 minutes. The firefighters were actively engaged in fighting the fire for 60 minutes longer in the mitigated case than in the unmitigated case. Although some

benefit is derived from the half hour of additional evacuation time, the above scenario (and the other scenarios with similar results for this mitigation measure) did not receive a significant benefit from the additional firefighting resources. For these scenarios, it is clear that the number of fire trucks available was not the limiting factor in successful fire suppression, so making more fire trucks available produced no substantial effect.

In other cases, however, the addition of extra fire trucks had a significant effect on MMAF consequences. This effect was observed most frequently in MMAF scenarios originating at the government building target profile. An example of this type of effect is shown in Figure 7.8 (infrastructure damage scenario E02, wind 10 mph to the south).

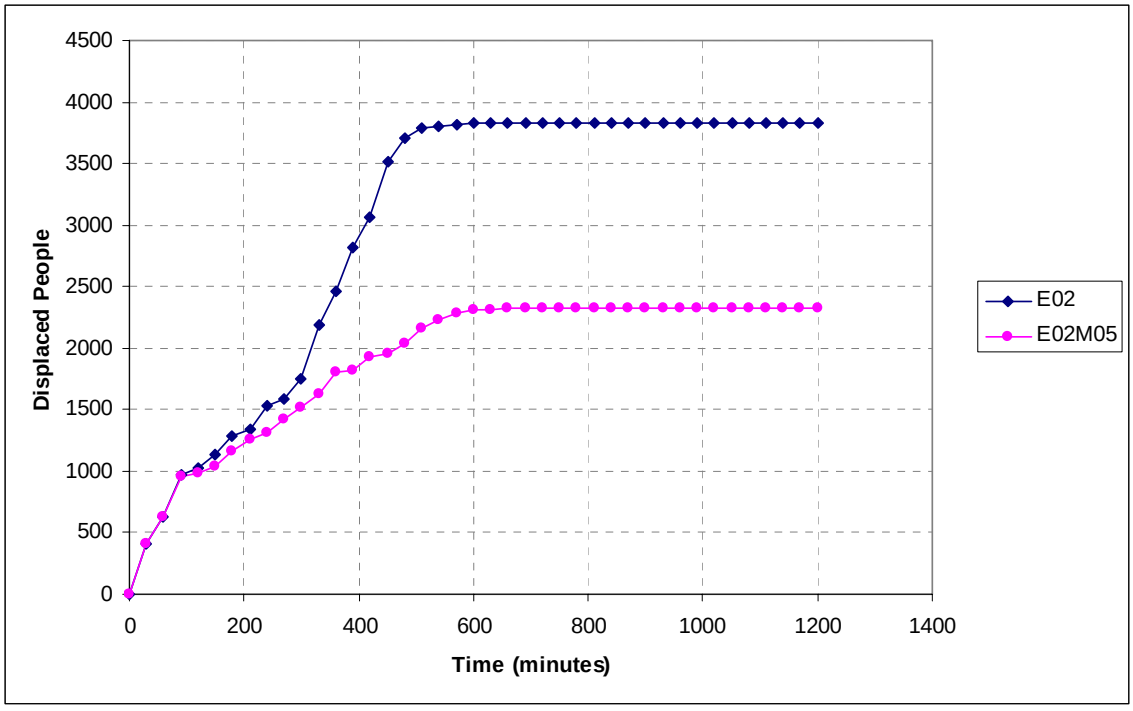

Fig. 7.8. Example of performance of mitigation method M05 with high effectiveness. Both damage damage simulations (used water damage scenario E02, with wind blowing southward at 10 mph and the government buildings target profile.

In the MMAF scenario shown above, assigning additional fire trucks to the fire response effort decreases the ultimate consequences of the urban fire by 1,496 displaced people. In addition, the mitigation effort provides substantial extra evacuation time, with an ACD value of about 125 minutes. The ECT value of the mitigated damage vs. time graph is -60 minutes.

The success of this method in scenarios involving the government target profiles implies that, for these scenarios, the limiting factor in effective fire response was the number of fire trucks available, not the amount of water for firefighting. The government buildings used as ignition points in these scenarios are comparatively tightly clustered in the central business district; other target profiles are spread more widely throughout the urban area. The tight clustering would permit the fire department to form a perimeter around the burned area more effectively than the widespread targets, so additional fire trucks would be more likely to have a measurable effect on reinforcing the perimeter.

As with mitigation measure M03, this mitigation measure has no direct cost of implementation (although it may ultimately have some associated costs, as the fire department will be called out more frequently to assist with fires in other communities due to the more extensive mutual aid contracts). Although it is not effective in all situations and probably should not be the only technique in this community's mitigation strategy, it produced significant benefits in some of the MMAF scenarios and is worth considering as a backup mitigation measure.

7.3.6. Mitigation Method M06: Performance and Discussion

The technique of augmenting the water supply for firefighting by installing an auxiliary water supply line to the east side of the urban area was effective for many of the MMAF scenarios. This method produced the most consistent benefits for fire scenarios beginning at the ecoterrorism targets, which is not surprising since the buildings most directly threatened by these targets are close to the auxiliary supply pipeline's outflow to the water distribution system. This mitigation method also performed well across a variety of urban fire ignition point profiles for infrastructure damage scenarios like A01 and D01 which severely limited the supply of water for firefighting, and for infrastructure damage scenario F01, which introduced a blockage in a high-conveyance section of the water distribution system. (In this scenario, the auxiliary supply line functioned as a low-friction alternate path for water bound to the eastern side of the urban area.) An example of the consequences over time for a successful application of this mitigation method is shown in Figure 7.9. For the unmitigated and mitigated damage simulations shown, the model used infrastructure damage scenario A01 with an urban fire starting at the ECO target profile and the prevailing wind blowing 10 mph towards the southeast. In this case, the auxiliary water supply line reduced the overall consequences of the urban fire by 4,118 people. This mitigation method allowed an average consequence delay of about 70 minutes and brought the urban fire under control 210 minutes faster than the unmitigated MMAF scenario.

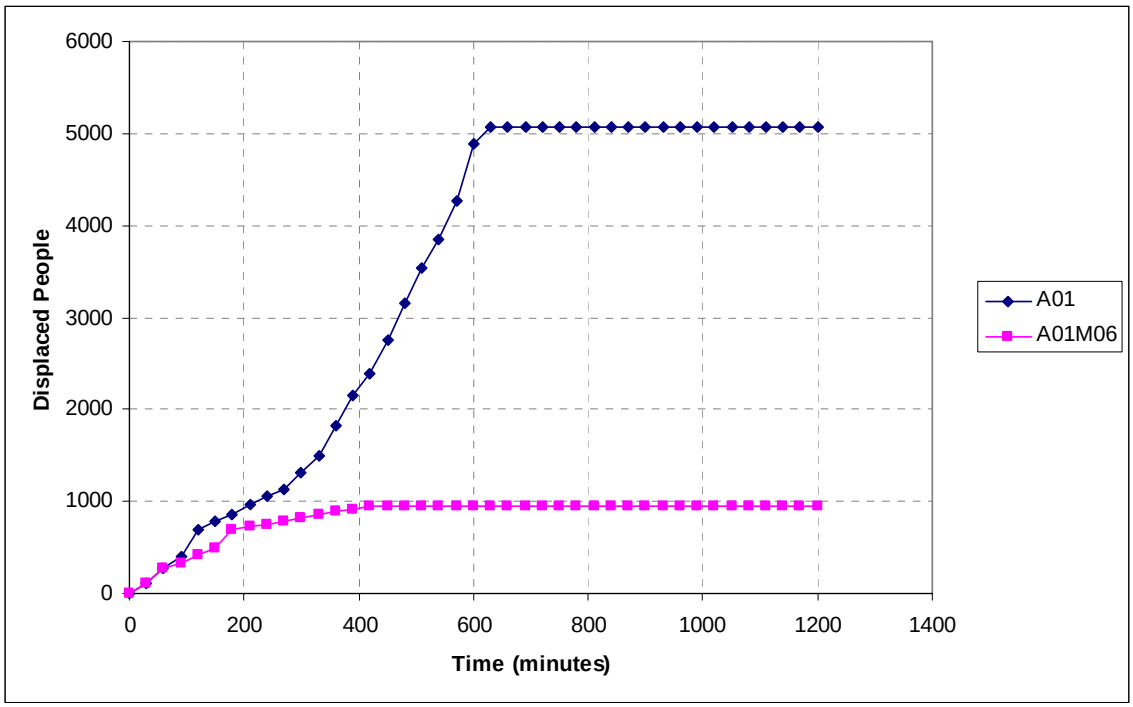

Fig. 7.9. Example of performance of mitigation method M06. Unmitigated damage simulation (blue line) used water damage scenario A01, with wind blowing southeast at 10 mph and the ecoterrorism target profile.

In a few MMAF scenarios, however, the auxiliary supply line did not have a significant effect on the urban fire's consequence. One vulnerability of the auxiliary water supply pump and pipeline is that its water source is the same water treatment plant as the primary high service pumps. Flow into the water treatment plant is driven by a grouping of smaller pumps from the local reservoir and wellfield. These pumps are on the same electrical power circuit as the primary high-service pumps, so the infrastructure damage scenarios B01, B02, and B03, which cut power to all of these pumps, cut off the supply of water to the auxiliary pipeline. Thus, this mitigation method was not successful in reducing the impact of any of the power-outage infrastructure damage scenarios, although it probably would have been successful in these cases if the auxiliary

supply line were coupled with backup power supplies for the pumps which supply raw water to the water treatment plant. This mitigation measure was also mostly ineffective when employed against MMAF scenario G01, which involves a 30-minute delay before the water system is accessed for firefighting. (Few water-infrastructure mitigation methods were effective against this damage scenario.)

7.3.7. Mitigation Method M07: Performance and Discussion

The damage simulations involving mitigation method M07 tested the effectiveness of bridging blocked areas of the water distribution system with temporary, portable, above-ground water mains. The damage simulations were designed to use pipes with the properties of sections of 10-inch fire hose connected between fire hydrants, since these are easy access points to the water system and readily available improvised pipelines. This mitigation measure was tested for damage categories E and F, which dealt with water main breaches and self-imposed isolations of sections of the water distribution system to contain localized drinking water contaminations.

This mitigation measure generally was not successful; in most of the damage scenarios for which it was tested, it had no effect at all on the distribution of urban fire consequences over time. Figure 7.10 shows an example of a damage scenario in which this mitigation method did have a small beneficial effect on the mitigated damage simulation. In this case, the mitigation method did not reduce the overall consequences of the MMAF, it did lag the damage-vs.-time curve behind the unmitigated simulation results by about half an hour. The ACD for this case was just under 35 minutes; the

ECT was -30 minutes. The simulations shown use the infrastructure damage profile F02 and ECO urban fire target profile, with the prevailing wind blowing 10 mph into the northwest.

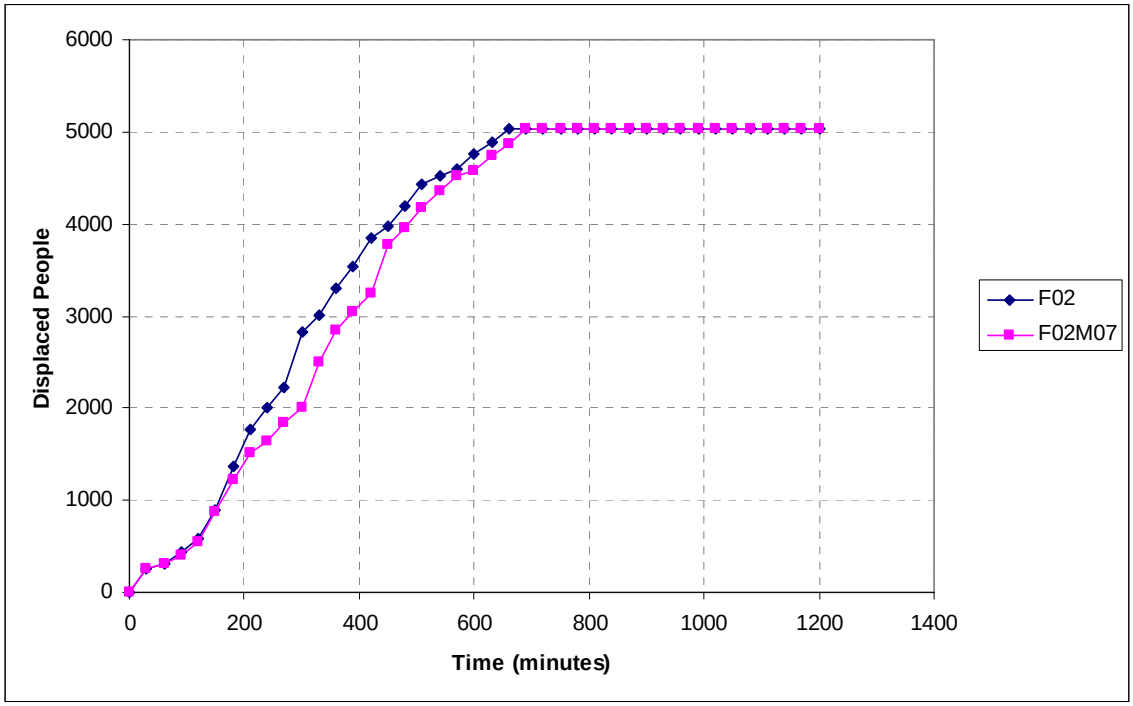

Fig. 7.10. Example of performance of mitigation method M07. Unmitigated and mitigated damage simulations use water damage scenario F02, with wind blowing northwest at 10 mph and the ecoterrorism target profile.

The main reason for this mitigation method's failure is probably the severe energy loss induced by the mechanical linkages required to connect the temporary mains. This type of energy loss, known in fluid mechanics as *minor loss*, occurs when the water in the pipes makes sudden changes in direction and when the pipes used to convey the water have abrupt changes in diameter. The path taken by water flowing through the temporary mains requires at least six 90-degree bends and four abrupt

changes of pipe diameter (from water main to hydrant connection pipe to temporary pipeline, and then the same transitions occur again in reverse). Furthermore, the magnitude of the energy loss is proportional to the square of the velocity in the pipes; flow velocities are especially high under fire fighting conditions because of the large required flows. The proportionality constant used for each pipe in the minor loss calculations was 2.0, which is consistent with the mechanical fittings present but creates a large loss of energy due to friction with the fittings. The energy loss causes a decrease in pressure for the water flowing through the pipes, which decreases the amount of water available at firefighting pressures when the water reaches its destination.

Although this particular test of temporary portable water mains was not successful, further investigation of this technique as a potential mitigation measure is warranted. The failure of this technique can inform the design of future temporary main configurations. In order to minimize the energy loss due to friction, the pipes used should have very smooth interior walls. It would be difficult to eliminate the minor losses caused by hydrant fittings, but one way to overcome the energy loss would be to introduce a small booster pump into the temporary water main system in order to add the lost energy back into the system. It may be very difficult for fire departments engaged in fighting large-scale urban fires to spare a pumper truck for every temporary water main, but this variety of fire truck could be a solution to the problem of the excessive energy loss. These trucks are highly portable, have connections for fire hose-sized pipes already in place, and have appropriately-sized pump equipment on board. Communities which do not find fire hoses sufficient on their own as portable water mains may evaluate the

effect of using pumper trucks or other portable pumping equipment to improve the water flow through the temporary pipeline system.

7.4. Mitigation Methods and Worst-Case Damage Scenario

The final test of the mitigation methods was against the worst-case damage MMAF scenario determined by the total enumeration optimization in Section 5.5. Figure 7.11 shows the performance of the various mitigation methods against this ignition point arrangement. For these simulations, the prevailing wind is blowing eastward at 10 mph.

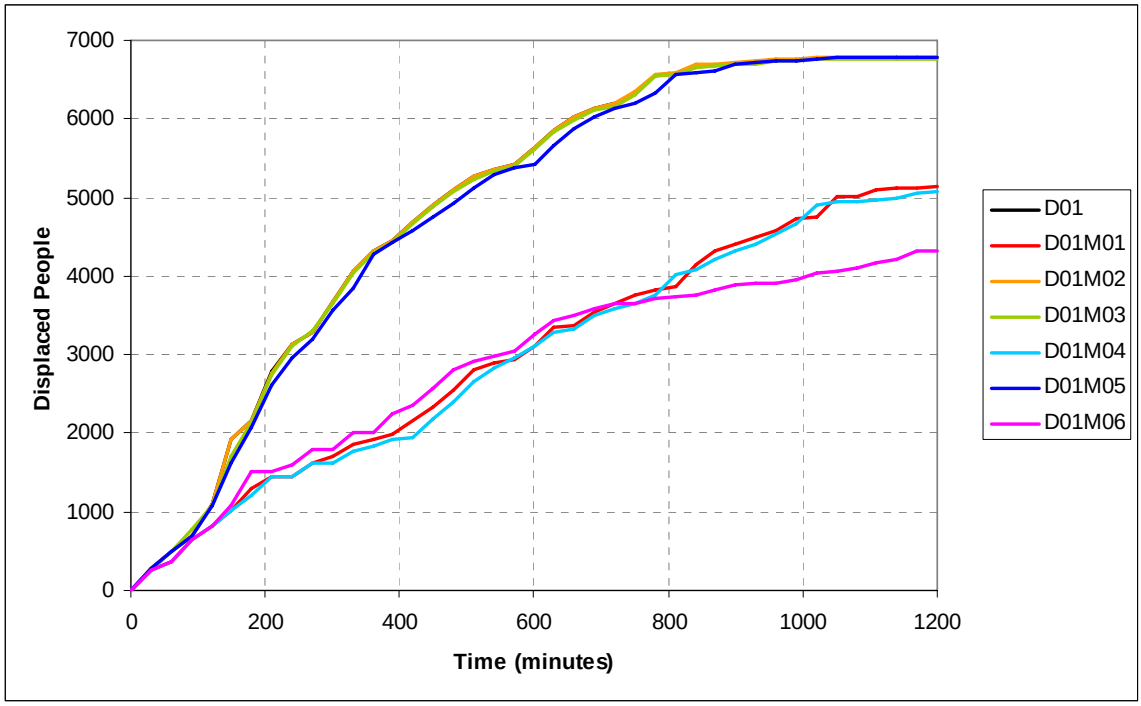

Fig. 7.11. Performance of mitigation measures against optimized worst-case arrangement of urban fire ignition points. The unmitigated damage distribution (black line) is not readily visible because it is nearly identical to (and plotted underneath) the orange line for the consequence distribution of mitigation measure M02. The MMAF simulations reported here used infrastructure damage profile D01, and the prevailing wind was eastward at 10 mph.

As stated in Section 5.5, this ignition point arrangement was paired with infrastructure damage scenario D01. The predetermined infrastructure damage scenario had an impact on the mitigation methods which were most effective against the urban fire. Because this infrastructure damage scenario removes access to the city's elevated storage tank, it is perhaps not surprising that mitigation method M06, which replaces half of the lost storage capacity, yields the greatest reduction in consequences. Mitigation methods M01 and M04 were also successful at reducing and delaying the consequences, which affords substantial extra evacuation time for the homes and businesses destroyed by the fire. Mitigation methods M02, M03, and M05 had very little effect on the urban fire's progress.

7.5 Overall Mitigation Results

Although the mitigation measures performed differently in various MMAF scenarios, it is useful to examine the techniques' average results in order to gain insight into their overall effectiveness. Table 7.2 lists the mitigation measures' average (over all mitigated damage simulations which involved the mitigation measure) PCR, ACD, and ECT values, along with their cost of implementation.

Table 7.2. Average Effectiveness and Implementation Costs of Mitigation Measures

Mitigation Method	PCR (Displaced People)	ACD (min)	ECT (min)	Estimated Cost	PCR Unit Cost
M01	1751	96	51	$1,800,000	$1,027.81
M02	1436	110	-12	$200,000	$139.24
M03	550	45	-6	$50,000	$90.91
M04	1439	99	-2	$475,000	$330.15
M05	184	34	-51	$0	$0.00
M06	1049	76	38	$240,000	$228.87
M07	0	5	-5	$0	N/A

Mitigation method M01 is the most effective, but it is also the most expensive by a substantial margin. Even when the total cost of the mitigation measure is divided by the measure's PCR to give the unit cost of saving each person's home or business, method M01 is more than three times as expensive as the next most costly alternative. Method M02 provides the best combination of low cost and high effectiveness; methods M04 and M06 also provide good results at moderate cost. Methods M03, M05, and M07 have no (or very low) implementation cost but lower average benefits; this suggests that they may be helpful in defending the community against MMAFs but probably should not be the community's only mitigation strategy.

Expressing the mitigation methods' implementation cost in terms of unit cost per consequence reduction is not the only possible way to evaluate the tradeoff between cost and effectiveness; it is simply the most straightforward method. The extra evacuation time and earlier fire control times afforded by the mitigation methods allow the fire fighters to be more effective in their rescue and evacuation duties. This added effectiveness could also be accomplished by having additional rescue workers at the scene; in other words, a team can accomplish more either by having more time to work

(because of the mitigation methods' consequence delay and expedited control times) or more people to work (by hiring extra rescue workers). Future research may develop an equivalency scale between the extra time that the mitigation methods afford and the equivalent number of rescue workers this saves. This would allow decision-makers to assign a monetary benefit – the cost of hiring the equivalent number of additional rescue workers for the unmitigated MMAF – to counter the cost of the mitigation method. Further investigation of this relationship is necessary to make this approach a reliable input to decision-making, but it would yield a better understanding of the mitigation methods' benefits.

8. CONCLUSION

8.1. Summary of Work Presented

This dissertation has discussed the importance of considering communities' vulnerability to multi-mode attacks and failures (MMAFs). An important primary step in creating security strategies which take interdependent infrastructures into account is developing the capability to model the interaction of interdependent infrastructures in MMAF scenarios. The Model of Urban Fire Spread (MUFS) is presented as a tool to simulate complex infrastructure interactions during a joint water infrastructure failure/urban fire event.

Using the MUFS simulation tool, an extensive vulnerability analysis of "Micropolis," an example community, was performed using a wide range of infrastructure damage scenarios and urban fire ignition profiles to provide insight into the range of damages this type of MMAF could produce. In addition, the worst-case arrangement of urban fire ignition points was determined using an enumeration optimization algorithm. Two other optimization algorithms were evaluated for this application but were determined to be inappropriate.

Analysis of the results of the simulations identified the most serious MMAF scenarios, including the highest-consequence modes of infrastructure failure. Seven potential mitigation strategies were designed to counter these modes of failure and reduce the consequences of the MMAF scenarios by improving the water systems' ability to provide water for fire fighting even under heavy damage. These mitigation

measures were tested against the highest-consequence MMAF scenarios using the MUFS simulation tool. The results of these mitigated MMAF simulations identified the most effective mitigation strategy for each infrastructure damage scenario and overall. Effectiveness of a mitigation strategy was evaluated using three criteria: overall reduction of the number of people displaced by the urban fire; additional evacuation time afforded by the mitigation measure's delay of fire consequences; and expedited control of the urban fire. The effectiveness of each mitigation method was compared to its cost of implementation to determine the best overall strategy. Mitigation method M01, which involved the replacement of most of the city's water mains with larger, more modern pipes, was found to be the most effective strategy, but its cost of implementation was very high. Mitigation method M02, which called for the replacement of a small subset of the city's water mains, was found to be the best balance between implementation cost and effectiveness of the mitigation measures tested.

8.2. Future Work: Model of Urban Fire Spread

Following the Hamada equations and the approach of the Fire Following Earthquake model in HAZUS-MH, MUFS approximates urban fire growth by calculating the fire's progress along four directions. During the course of developing MUFS, however, it was hypothesized that, during an actual urban fire, each fire front point would behave as a new ignition point, itself engendering fire spread in each of the three open fire spread directions (the fourth direction, from which the new ignition point came, is not available for fire spread because it has already been burned). This fractal-

like approach is illustrated in Figure 8.1. Although the number of front points needed to define the burned area polygon would grow exponentially at each time step and quickly become unmanageable, an approximation of the fractal fire growth process could probably be developed which would preserve the realism of the fractal fire growth pattern while limiting the number of burned area perimeter points to a computationally feasible value.

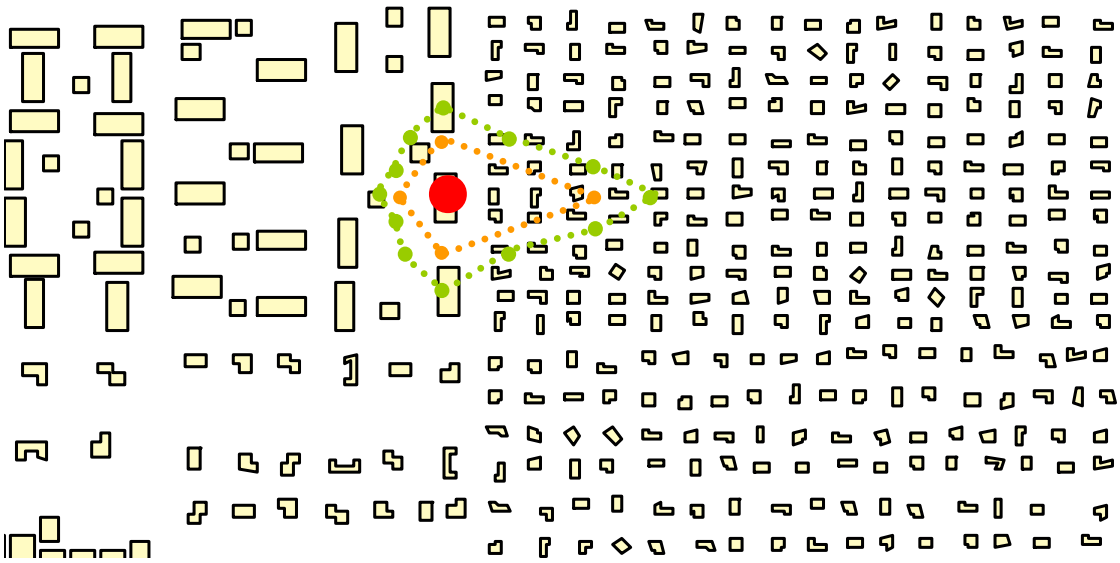

Fig. 8.1. Schematic diagram of process for calculating fire spread under the fractal fire spread model. The large red circle denotes the fire's ignition point. Orange points are the burn perimeter points at the end of the first time step, and the orange dotted line shows the burned area perimeter at this time step. For the next time step, each of the orange points is treated as a new ignition point, so fire spread is calculated in each feasible direction (neglecting directions which have already been burned). The green points show the burn perimeter points at the end of the second time step; note that there are twelve burn perimeter points in the second time step instead of just four.

One important benefit of this new approach to calculating the extent of the burned area is that it would minimize the occurrence of geometrical inaccuracies in fire extent, particularly in small or sparsely-developed urban areas. Currently, MUFS

determines the extent of the urban area by searching for intersections between the fire spread vectors and the buildings in the urban area. In any particular direction, the end of the urban area is defined as the fire spread vector's exit point from the building furthest from the ignition point. This building may not actually be at the edge of the urban area, but if no other buildings lie directly in the fire's path then the fire's spread will stop at that building, even if totally effective suppression is not achieved. This can lead MUFS to underestimate the extent of fires in small or low-density urban areas, where the odds of a fire spread vector ending prematurely are increased (because there are fewer buildings for the vector to intersect).

With the fractal fire spread growth pattern, the importance of premature terminations of fire spread in any one direction would decrease, because even if one fire spread front ended prematurely, the other nearby front points would compensate by spreading through the area that was inaccurately removed from burning.

A disadvantage to this approach is that it would complicate the process of determining fire spread extent, particularly the suppressed fire spread calculations (which are currently responsible for the majority of the computational requirements of the simulation). Future efforts to refine the simulation algorithms may make them more efficient, which would lessen the impact of the added complexity imposed by the fractal fire spread approach.

Another proposed change to the Model of Urban Fire Spread would improve the realism of how it calculates fire suppression in the early stages of the urban fire. MUFS treats fire spread separately in each of the four fire spread directions, so if a large fire is

totally suppressed in one direction it can continue to spread in other directions until the fire is brought under totally effective suppression in all four fire spread directions. The effectiveness of the fire suppression is calculated by assigning each building to its closest fire spread direction. Each building can only be assigned to *one* fire spread direction. This approach is realistic for urban fires which are large compared to the buildings they burn, because the buildings can be approximated as points which are definitely closest to one single fire spread direction. During the analysis of the urban fires' burn profiles, however, it was noticed that this approach may not be appropriate for urban fires which are not large compared to the surrounding buildings – that is, fires early in their development. Buildings being burned by small fires are still only assigned to a single fire spread direction, even though the fire may be burning those buildings on multiple fronts. Likewise, the benefits of the resources designated for fighting the fire in that building are assigned only to one fire spread direction, which may under-represent the effectiveness of fire suppression in the fire's earliest stages. The planned solution for this issue is to define some threshold time or stage of development before which the fire's burning buildings, and their accompanying fire suppression activities, may be assigned to as many fire spread directions as are appropriate. After this threshold time or development stage, fire suppression will follow the current approach of determining only *one* nearest fire spread direction.

This approach raises the question of when this threshold time or development stage should occur. The simplest answer is that a fire which has entered more than one building should transition from a "small" to a "large" fire; however, because the fire

front moves at different speeds in each direction, one direction's fire front could enter a new building a few time steps before the others leave the building of origin. Adopting this simple threshold may reintroduce the inaccuracy the approach was designed to avoid. The effects of several different approaches to defining the transition from small fire to large fire will be examined, and the most realistic option will be adopted.

Evaluating the overall realism of the urban fire spread simulations in MUFS is the subject of a third topic for future investigation. Although the fire spread equations adopted by MUFS were based on decades of empirical data on historical urban fires, it is desirable to compare the model's simulation results with the burned area of historical fires in which firefighting was compromised – for example, the second great London Fire (Johnson 1980) or the San Francisco fire of 1906 (Nolte 2006) -- to further validate the model of complex infrastructure interactions. The main challenge of this task is the difficulty of finding sufficiently detailed information about the historical MMAF events, particularly burned area profiles over time. The search for information on historical MMAF events will continue in the future and will inform future efforts to validate the model's performance.

MUFS's current focus is on the interaction between water distribution systems and fire response, although the simulation tool can indirectly model the effects of failures of the electrical grid, communications systems, and transportation networks. Future work will seek to incorporate more sophisticated models of other interdependent infrastructures: for example, MUFS might benefit from an analysis of transportation delays derived from a dynamic transportation network model, instead of using a static,

user-specified delay to represent traffic delays. In addition, more information on fire response's relationship with the public health system (another critical infrastructure) may provide better insight into the injuries and mortalities resulting from MMAF scenarios. In its current form MUFS cannot predict the casualties resulting from an MMAF scenario, but this is nevertheless an important consideration in planning emergency mitigation and response strategies. Integrating additional infrastructure models will make MUFS a more complete MMAF model and a better decision support tool.

MUFS will be made freely available to other researchers and to water utilities and to emergency planners who wish to use the MMAF simulation tool to conduct their own vulnerability analyses.

8.3. Future Work: MMAF Vulnerability and Mitigation Analysis

This project tested the viability of using dynamic programming to determine the highest-consequence arrangement of urban fire ignition points. Although dynamic programming was not appropriate for this application for the reasons discussed in Section 5.4, determining the worst-case MMAF scenario is still an important component of the vulnerability assessment and mitigation design process. The enumeration-based optimization method provided the worst-case configuration of ignition points, but this technique is extremely computationally expensive, and a more efficient technique would be a great benefit to future vulnerability analyses.

To this end, future research efforts will investigate the possibility of using other optimization methods to determine worst-case MMAF scenarios. Genetic algorithms seem particularly well-suited to this task, and the investigation will most likely begin with this technique.

Understanding of the risks facing water utilities and the available mitigation strategies is constantly evolving, and the methodology for assessing these risks and choosing the best mitigation strategies will continue to evolve as well. The methodology presented in this dissertation is intended to be flexible, able to adapt to the needs of individual water systems and to new threat information as it arises, and it is hoped that it will continue to provide benefit to water distribution systems' security in the future.

REFERENCES

Abelin, S.M.,Pritchard, M.T., and R.L. Sanks. (2006). "Costs." In *Pumping Station Design, 3rd ed.*, Chapter 29, G.M. Jones, ed. Elsevier, Inc., Boston.

American Water Works Association (AWWA). (2004). *Interim voluntary security guidance for water utilities*, Denver, CO.

Bertinshaw, D., and H.W. Guesgen. (2004). "Physical approximations for urban fire spread simulations." *Proceedings of the Seventeenth International Florida Aritificial Intelligence Research Society Conference.* FLAIRS, Menlo Park, CA.

British Broadcasting Corporation (BBC). (2004). "As it happened: Russian school siege." (http://news.bbc.co.uk/2/hi/europe/3624136.stm.) [Accessed 5 Sept. 2006].

Brown, T., Beyeler, W., and D. Barton. "Assessing infrastructure interdependencies: the challenge of risk analysis for complex adaptive systems." *International Journal of Critical Infrastructures,* 1(1), 108-117.

Brumbelow, K., Bristow, E.C., Torres, J., and D. Harris. (2006). "Micropolis: A virtual city model for detailed water distribution system simulations." (in preparation)

Caldwell, A. (2006). "4 indicted in Vail resort fires." The Denver Post, (http://www.denverpost.com/search/ci_3844773,) (May 20, 2006).

Canham, M. (2004). "Eco-terror group claims it caused lumberyard fire; Earth Liberation Front: The assertion is posted on the official Web site, and it threatens more Utah targets." Salt Lake Tribune, June 18, C3.

Clark, R.M., Grayman, W.M., Buchberger, S.G., Lee, Y., and D.J. Hartman. (2004). "Drinking water systems: An overview," in *Water Supply Systems Security*, Chapter 4, Larry W. Mays, Ed. McGraw-Hill Professional Engineering, New York.

Clinton, W. J. (1998). "Presidential Decision Directive/NSC-63: Critical Infrastructure Protection." (http://www.fas.org/irp/offdocs/pdd/pdd-63.htm). [Accessed October 10, 2005].

Copeland, C., and B. Cody (2003). "Terrorism and Security Issues Facing the Water Infrastructure Sector." Report for Congress, Congressional Research Service, Order Code RS21026, Washington, DC.

Department of Homeland Security (DHS) and Texas Engineering Extension Service (TEEX). (2004). *Public Works: WMD/Terrorism Preparedness and Response for Water and Wastewater Utility Operations*. TEEX, College Station, TX.

Eckman, W.F. (1994). *The Fire Department Water Supply Handbook.* Fire Engineering Books & Videos, Saddle Brook, NJ.

Environmental Protection Agency (EPA). 2002. "Guidance for water utility response, recovery, & remediation actions for man-made and/or technological emergencies." Office of Water, Washington, D.C.

Environmental Protection Agency (EPA). 2004. *Response Protocol Toolbox: Planning for and Responding to Drinking Water Contamination Threats and Incidents: Response Guidelines, Interim Final*. EPA: Washington, D.C.

Federal Emergency Management Agency (FEMA). (2003a). *HAZUS-MH Technical Manual.* FEMA, Washington, D.C.

Federal Emergency Management Agency (FEMA). (2003b). *HAZUS-MH User's Manual.* FEMA, Washington, D.C.

Friedman, R. (1992). "An international survey of computer models for fire and smoke." *Journal of Fire Protection Engineering*, 4(3), 81-92.

Fujita, T. (1975). "Simulation of spreading fires caused by a strong earthquake and of behavior of people taking refuge from them." *Proc. 1975 Joint JSME-ASME Applied Mechanics Western Conference*, Japan Society of Mechanical Engineers, Honolulu, HI.

Haimes, Y.Y. (2004). *Risk Modeling, Assessment, and Management.* Wiley Interscience, New York, NY.

Haimes, Y.Y., and P. Jiang. (2001). "Leontief-based model of risk in complex interconnected infrastructures." *Journal of Infrastructure Systems*, 7(1), 1-12.

Himoto, K., and T. Tanaka. (2000). A preliminary model for urban fire spread. *Proc. Fifteenth Meeting of the UJNR Panel on Fire Research and Safety, March 1-7, 2000.* S.L. Bryner, ed. National Institute of Standards and Technology, 309-319.

Johnson, David. (1980). *The City Ablaze: The Second Great Fire of London, 29th December 1940.* William Kimber, London.

Johnston, David. (1995). "Terror in Oklahoma City: The investigation; At least 31 are dead, scores are missing after car bomb attack in Oklahoma City wrecks 9-story federal office building." The New York Times, April 20, A1.

Karlsson, B. and J.G. Quintiere. (2000). *Enclosure Fire Dynamics*. CRC Press, Boca Raton, FL.

Knickmeyer, E. and K.I. Ibrahim. (2006). "Bombing shatters mosque in Iraq." *Washington Post Foreign Service*, (http://www.washingtonpost.com/wp-dyn/content/article/2006/02/22/AR2006022200454.html) (February 23, 2006).

Mahoney, E.F. (1980). *Fire Department Hydraulics*. Allyn and Bacon, Inc., Boston, MA.

Mays, L.W. (2004). "Water supply security: An introduction," in *Water Supply Systems Security*, Chapter 1, Larry W. Mays, Ed. McGraw-Hill Professional Engineering, New York.

Memorial Institute for the Prevention of Terrorism (MIPT). (2006). "Terrorism Knowledge Base." (http://www.tkb.org). (October 13, 2006).

Mitler, H.E. and H.W. Emmons. (1981). *Documentation for CFC V, the fifth Harvard computer fire code.* NBS publication NBS-GCR-81-344. Center for Fire Research, National Bureau of Standards, Washington, D.C.

National Commission on Terrorist Attacks upon the United States (NCTAUS). (2004). *The 9/11 Commission Report*. W.W. Norton & Co., New York.

National Fire Protection Association (NFPA). (2006). *NFPA1: Uniform Fire Code, 2006 Edition.* NFPA: Quincy, MA.

Nolte, C. (2006). "The Great Quake: 1906-2006 -- The Great Fire." The San Francisco Chronicle. April 12. A11.

Office of Homeland Security (OHS). *National Strategy for Homeland Security*. The White House, Washington, D.C. (http://www.whitehouse.gov/homeland/book.) [Accessed September 15, 2006].

President's Critical Infrastructure Protection Board (PCIPB). (2003). *National Strategy for the Physical Protection of Critical Infrastructures and Key Assets*. The White House, Washington D.C., (www.whitehouse.gov/pcipb/physical.html.) [Accessed June 20, 2005].

Peacock, R.D., Forney, G.P., Reneke, P.A., Portier, R.M., and W.W. Jones. (2000). *CFAST, the Consolidated Model of Fire Growth and Smoke Transport.* NIST Technical Note 1299. National Institute of Standards and Technology, Building and Fire Research Laboratory, Gaithersburg, Maryland.

Perrow, C. (1984). *Normal Accidents.* Basic Books, Inc., New York, NY.

Platt, D.G. (1994). "A probabilistic model of fire spread with time effects." *Fire Safety Journal*, 22, 367-398.

Public Health, Security and Bioterrorism Preparedness and Response Act ("Bioterrorism Act,") (PL 107-88), June 2002.

"Taking Due Account of Terrorism." (2004). *Engineers Australia*, 76(1), 42.

Uniting and Strengthening America by Providing Appropriate Tools Required to Intercept and Obstruct Terrorism ("USA PATRIOT Act"), (PL 107-56), October 2001.

Rinaldi, S.M., Peerenboom, J.P., and T.K. Kelly (2001). "Identifying, understanding, and analyzing critical infrastructure interdependencies." *IEEE Control Systems Magazine*, 21, 11-25.

Rossman, L.A. (2000). *EPANET 2: Users Manual. EPA/600/R-00/057*. National Risk Management Research Laboratory, U.S. Environmental Protection Agency, Cincinnati, OH.

R.S. Means Company. (1996). *Mechanical Cost Data 1997*. Melville J. Mossman, ed. R.S. Means Company, Inc., Kingston, MA.

Seger, K.A. (2003). *Utility Security: The New Paradigm*. PennWell Corporation, Tulsa, OK.

Tidwell, V.C., Cooper, J.A., and C.J. Silva. (2005). "Threat assessment of water supply system using Markov latent effects modeling." *Journal of Water Resources Planning and Management*, 131(3), 218-227.

Tierney, K.J., Lindell, M.K., and R.W. Perry. (2001). *Facing the Unexpected: Disaster Preparedness and Response in the United States*. Joseph Henry Press, Washington, D.C.

Zimmerman, R. (2001). "Social Implicatons of Infrastructure Network Interactions." *Journal of Urban Technology*, 8(3), 97-119.

APPENDIX 1

Derivation of Fire Hydrant Emitter Coefficient

Section 3.5.2 of this dissertation presents a methodology for determining available fire flow at a pressure of 20 psi, the minimum water pressure required for effective fire suppression. If the Model of Urban Fire Spread (MUFS) is unable to obtain the full fire flow of 1000 gpm from a fire hydrant, it determines the available flow at the minimum pressure by converting the hydrant node to an "emitter," which models uncontrolled flow to the environment through an open orifice, with an emitter coefficient of 1850 gpm/psi$^{1/2}$. The derivation of this value is presented here.

The discharge through an orifice flow depends on the size of the orifice (which is here assumed to be the 10-inch diameter outflow of a fire hydrant) and the pressure immediately upstream of the orifice. This relationship is expressed:

$$Q = C_d \cdot A \cdot H^{1/2} \sqrt{2g} \tag{A1.1}$$

where Q is the flow through the orifice in cubic feet per second (cfs), A is the cross-sectional area of the orifice in square feet, H is the head equivalent (in feet) of the pressure at the orifice, and g is the gravitational acceleration, 32.2 ft/sec^2. The discharge coefficient C_d has a value of 0.62 (unitless) for a sharp-edged orifice.

The emitter equation used by EPANet is an adaptation of the orifice discharge equation (Rossman 2000):

$$Q = C \cdot p^{1/2} \tag{A1.2}$$

where C is the "emitter coefficient," a required user input to the hydraulic model, and p is the pressure in pounds per square inch (psi), which is physically the same as H head above the orifice. C can be determined by setting the right-hand sides of Equations A1.1 and A1.2 equal to each other and rearranging the terms to give:

$$C = C_d \cdot A \cdot \left(\frac{H}{p} \right)^{1/2} \sqrt{2g} \tag{A1.3}$$

Solving equation A1.3 using values of 0.62 for C_d, 0.55 ft^2 for the area of a 10-inch circular orifice, and the standard value (for water) of 1 ft head per 0.433 psi of pressure yields a value of 4.124 ft^3/sec/psi$^{1/2}$ or 1850 gpm/psi$^{1/2}$, the value used for C in this analysis.

APPENDIX 2

Notes on Appendix 2

This section presents the results of the simulations of multi-mode attack and failure (MMAF) urban fires under various infrastructure damage profiles with mitigation measures in use. Pages 145-147 contain a summary table of the results of 126 separate simulations which tested the seven mitigation measures discussed in Section 6 against 20 different combinations of urban fire ignition point distribution, wind direction, and infrastructure damage scenario.

Each simulation's results are quantified using three novel analysis metrics introduced in section 7.2 of this dissertation. Peak Consequences Reduction (PCR) measures the reduction (from the unmitigated MMAF simulation to the mitigated case) in the number of people who are displaced by the urban fire. Average Consequence Delay (ACD) is the extra evacuation time (in minutes) afforded by the mitigation measure. Expedited Control Time (ECT) is a measure of how much sooner (in minutes) the fire department is able to bring the mitigated urban fire under total control (as compared to the unmitigated damage simulation with the same target/wind direction/infrastructure damage profile).

The graphs presented on pages 148-157 show the development over time of the consequences of MMAF urban fires with various mitigation measures in place. Consequences were calculated at time steps of 5 minutes for the entire duration of the damage simulation. For clarity, individual data point markers are omitted. In some of the figures, the unmitigated damage scenario graphs (black lines) are covered by the graphs of mitigation measures which did not have a significant effect on the simulation results.

Table A2.1. Results of Mitigated MMAF Simulations

Damage Scenario/ Mitigation Measure	Peak Damages (Displaced Persons)	PCR (Displaced Persons)	ACD (min)	ECT (min)
A01M01	2023	3046	148.7	-30
A02M01	1198	3839	471.4	-210
A03M01	1178	2243	247.3	-120
AD1M01	4164	16	6.9	0
B01M01	486	4583	33.9	510
B02M01	3212	618	41.6	90
BH1M01	3500	994	66.4	0
BH2M01	862	4200	113.8	120
D01M01	3145	1033	67.6	120
D01M01	4975	25	42.7	-60
D02M01	4164	2	3.2	-30
E01M01	3537	691	99.4	-30
E02M01	3801	27	-3.0	-30
E03M01	3537	691	99.3	-30
F02M01	653	4384	158.4	240
F03M01	486	4555	34.1	510
F04M01	2967	458	84.4	-60
F05M01	3145	225	77.6	-90
G01M01	1721	3316	100.7	120
H01M01	4364	80	29.1	0
A01M02	2023	3046	145.8	-30
A02M02	1198	3839	416.3	-150
A03M02	1178	2243	247.3	-120
AD1M02	4164	16	6.9	0
B01M02	486	4583	33.9	510
B02M02	3212	618	33.8	120
BH1M02	3434	1060	73.8	0
BH2M02	1628	3434	150.8	-30
D01M02	4178	0	0.7	0
D01M02	5000	0	0.0	0
D02M02	4164	2	1.7	0
E01M02	3534	694	100.7	-30
E02M02	3801	27	-8.0	-30
E03M02	3537	691	99.4	-30
F02M02	1352	3685	380.7	-120
F03M02	1015	4026	311.9	-180
F04M02	2967	458	85.8	-60
F05M02	3145	225	63.1	-60
G01M02	5037	0	31.9	-30
H01M02	4364	80	26.3	0

Table A2.1 (continued). Results of Mitigated MMAF Simulations

Damage Scenario/ Mitigation Measure	Peak Damages (Displaced Persons)	PCR (Displaced Persons)	ACD (min)	ECT (min)
A01M03	5005	64	30.6	-30
A02M03	2465	2572	208.4	0
A03M03	3421	0	0.0	0
AD1M03	4166	14	2.5	0
B01M03	5041	28	25.2	0
B02M03	3830	0	1.0	0
BH1M03	4494	0	0.0	0
BH2M03	5005	57	29.7	-30
D01M03	4178	0	0.1	0
D01M03	5000	0	-0.2	0
D02M03	4166	0	1.6	0
E01M03	4228	0	0.0	0
E02M03	3828	0	1.9	0
E03M03	4222	6	-2.4	0
F02M03	2385	2652	212.7	0
F03M03	1015	4026	311.6	-180
F04M03	1953	1472	59.3	120
F05M03	3270	100	21.3	0
G01M03	5037	0	2.7	0
H01M03	4444	0	0.0	0
A01M04	954	4115	83.9	180
A02M04	1198	3839	444.8	-180
A03M04	3421	0	4.3	0
AD1M04	4163	17	5.3	0
B01M04	892	4177	435.3	-240
B02M04	3806	24	6.8	0
BH1M04	4494	0	3.9	0
BH2M04	1628	3434	149.6	-30
D01M04	3989	189	48.4	-180
D01M04	5000	0	42.2	-60
D02M04	4166	0	3.8	0
E01M04	3544	684	95.2	-30
E02M04	3828	0	11.1	0
E03M04	3544	684	95.6	-30
F02M04	1352	3685	407.4	-150
F03M04	486	4555	34.1	510
F04M04	3435	-10	-1.0	0
F05M04	3265	105	19.8	0
G01M04	1760	3277	74.6	180
H01M04	4444	0	5.0	0

Table A2.1 (continued). Results of Mitigated MMAF Simulations

Damage Scenario/ Mitigation Measure	Peak Damages (Displaced Persons)	PCR (Displaced Persons)	ACD (min)	ECT (min)
A01M05	5069	0	34.3	-60
A02M05	5037	0	12.7	-30
A03M05	3421	0	1.2	-30
AD1M05	4180	0	22.6	-90
B01M05	5069	0	28.4	-30
B02M05	2332	1498	116.2	-30
BH1M05	4494	0	3.3	-30
BH2M05	5069	-7	30.5	-60
D01M05	4178	0	31.3	-60
D01M05	5000	0	17.4	-60
D02M05	4166	0	28.0	-90
E01M05	4222	6	22.1	-30
E02M05	2332	1496	125.7	-60
E03M05	4222	6	23.0	-30
F02M05	5037	0	14.7	-30
F03M05	5041	0	31.7	-60
F04M05	3425	0	-0.4	-30
F05M05	3375	-5	31.8	-90
G01M05	5037	0	21.0	-30
H01M05	3760	684	87.3	-90
A01M06	951	4118	72.2	210
A02M06	1198	3839	468.4	-210
A03M06	3421	0	0.7	0
AD1M06	3390	790	8.4	300
B01M06	5069	0	10.9	-30
B02M06	3830	0	0.1	0
BH1M06	4494	0	0.0	0
BH2M06	5069	-7	2.0	0
D01M06	3994	184	48.1	-150
D01M06	5000	0	13.9	-30
D02M06	3390	776	6.6	300
E01M06	3544	684	106.1	-30
E02M06	3828	0	20.4	0
E03M06	3544	684	94.7	-30
F02M06	1352	3685	558.8	-330
F03M06	486	4555	34.1	510
F04M06	1860	1565	19.6	270
F05M06	3270	100	21.4	0
G01M06	5037	0	34.5	-30
H01M06	4444	0	1.0	0
E01M07	4228	0	0.0	0
E02M07	3828	0	-7.6	0
E03M07	4228	0	0.0	0
F02M07	5037	0	33.3	-30
F04M07	3425	0	4.4	0
F05M07	3370	0	0.0	0

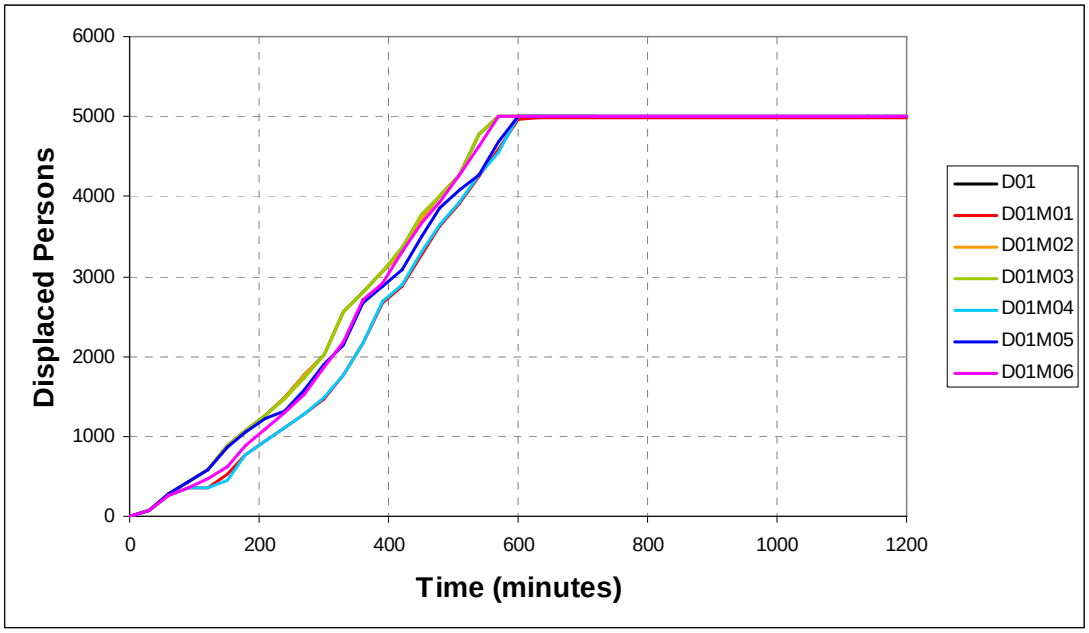

Fig. A2.1. Comparison of mitigated consequence development over time for MMAF urban fire originating at ECO target profile, with wind blowing 10 mph at 45 degrees and infrastructure damage scenario G01 using various mitigation methods. For clarity, individual data point markers are omitted.

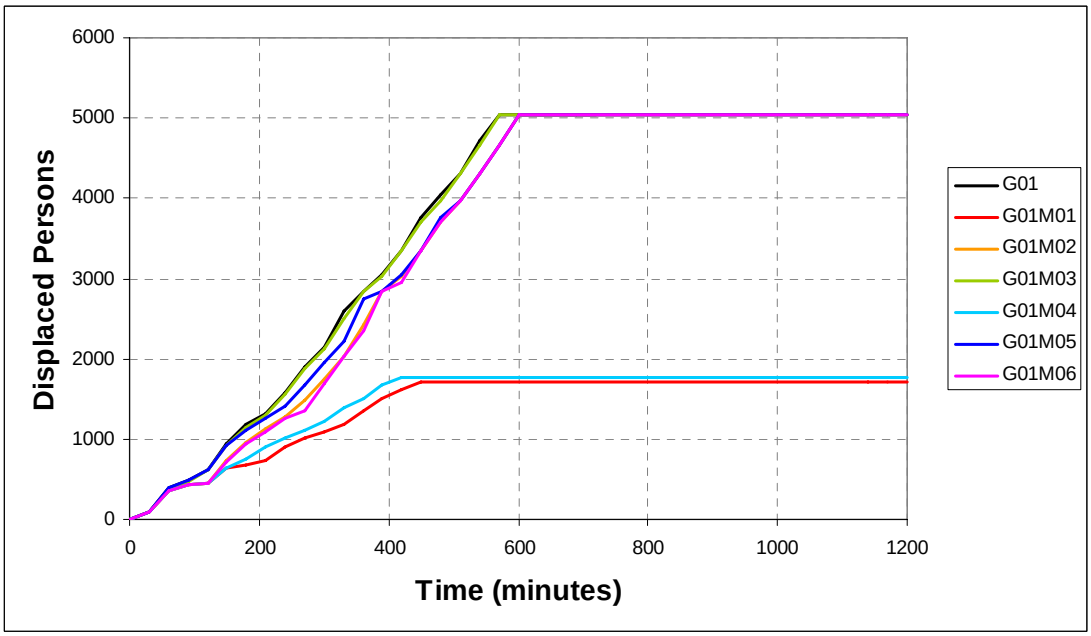

Fig. A2.2. Comparison of mitigated consequence development over time for MMAF urban fire originating at ECO target profile, with wind blowing 10 mph at 45 degrees and infrastructure damage scenario D01 using various mitigation methods.

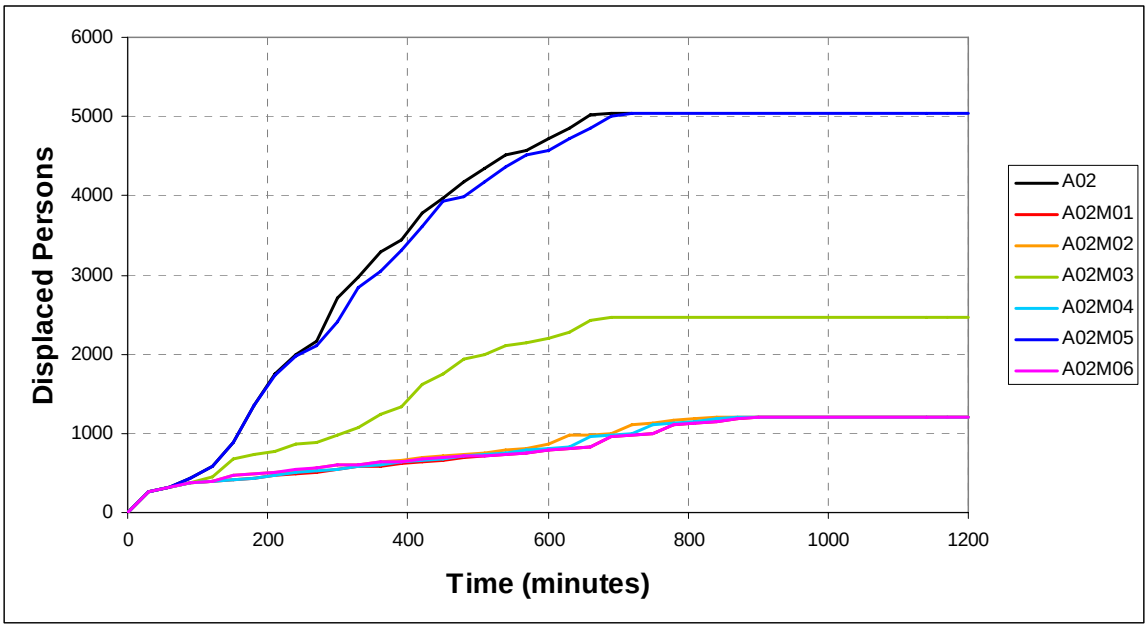

Fig. A2.3. Comparison of mitigated consequence development over time for MMAF urban fire originating at ECO target profile, with wind blowing 10 mph at 135 degrees and infrastructure damage scenario A02 using various mitigation methods.

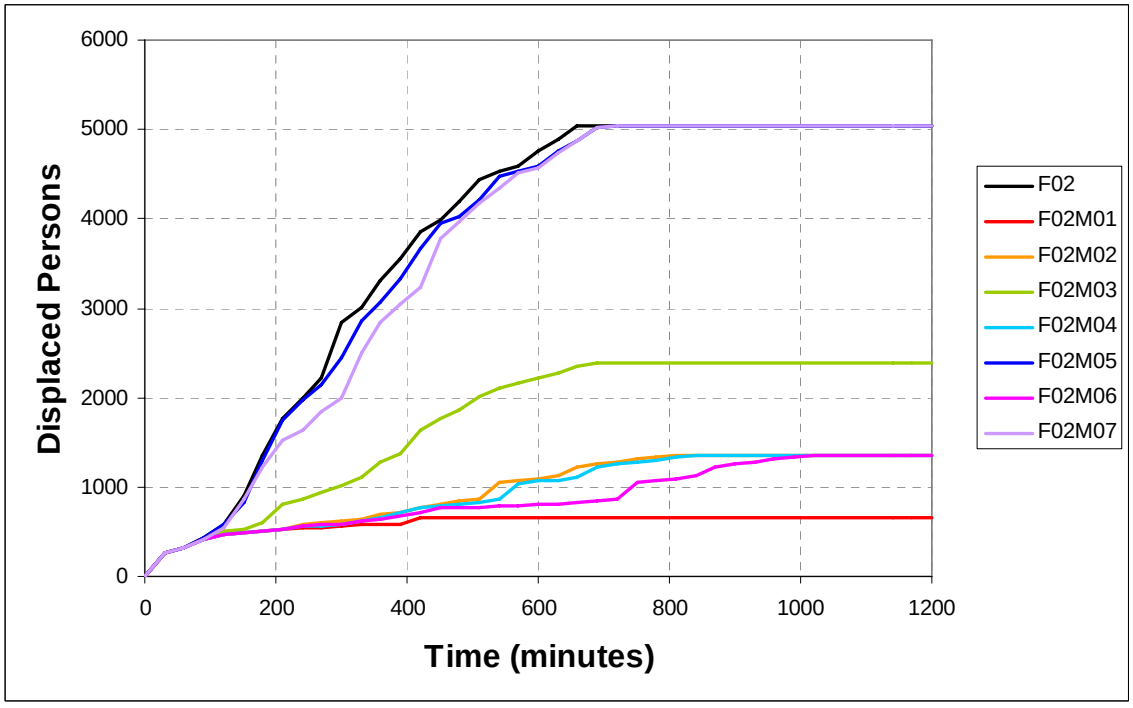

Fig. A2.4. Comparison of mitigated consequence development over time for MMAF urban fire originating at ECO target profile, with wind blowing 10 mph at 135 degrees and infrastructure damage scenario F02 using various mitigation methods.

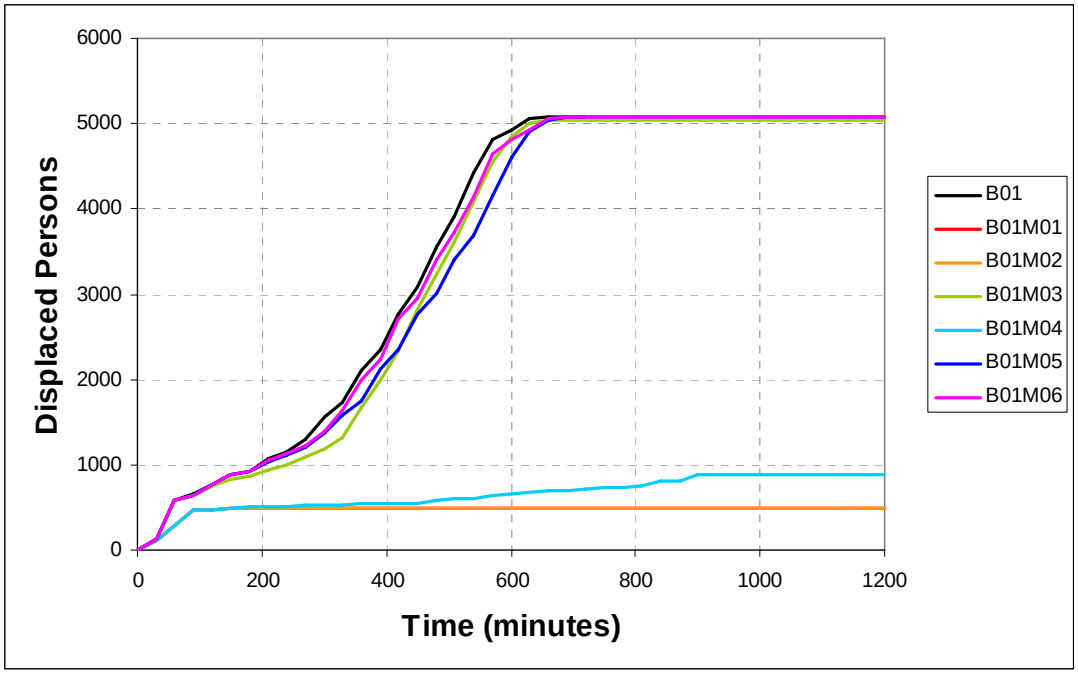

Fig. A2.5. Comparison of mitigated consequence development over time for MMAF urban fire originating at ECO target profile, with wind blowing 10 mph at 225 degrees and infrastructure damage scenario B01 using various mitigation methods.

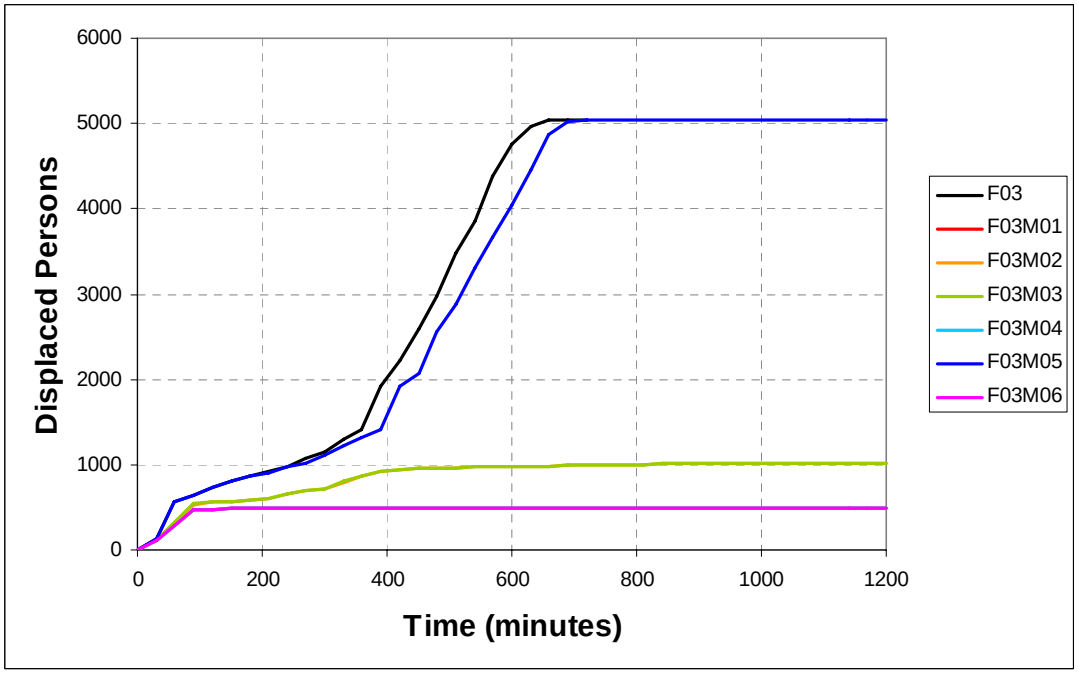

Fig. A2.6. Comparison of mitigated consequence development over time for MMAF urban fire originating at ECO target profile, with wind blowing 10 mph at 225 degrees and infrastructure damage scenario F03 using various mitigation methods.

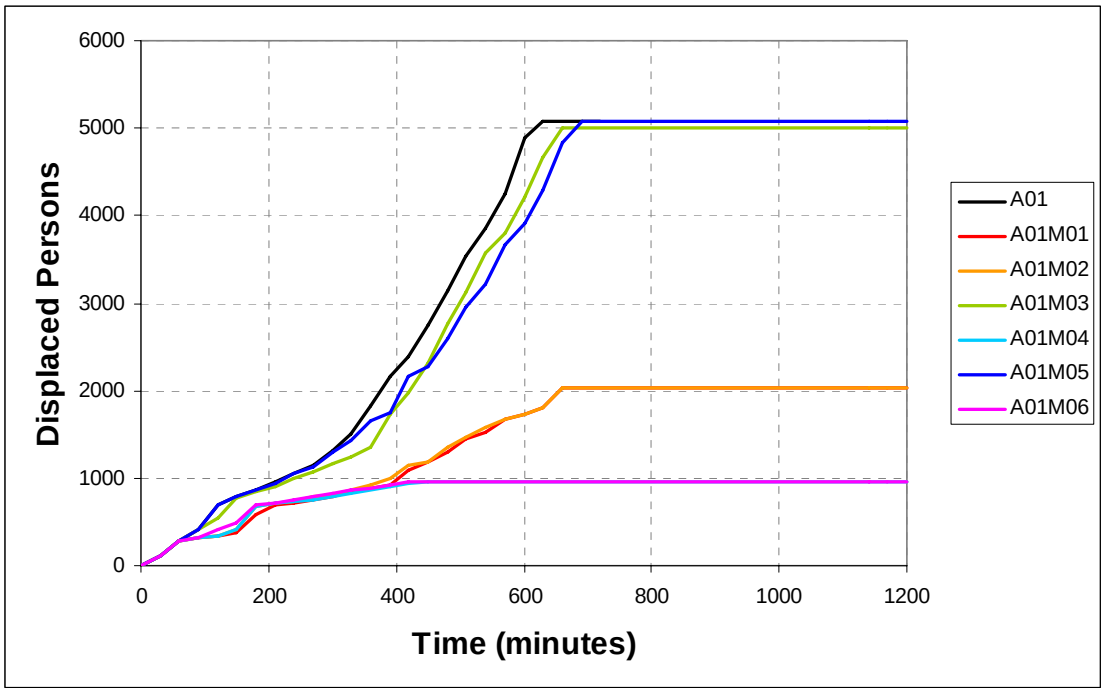

Fig. A2.7. Comparison of mitigated consequence development over time for MMAF urban fire originating at ECO target profile, with wind blowing 10 mph at 315 degrees and infrastructure damage scenario A01 using various mitigation methods.

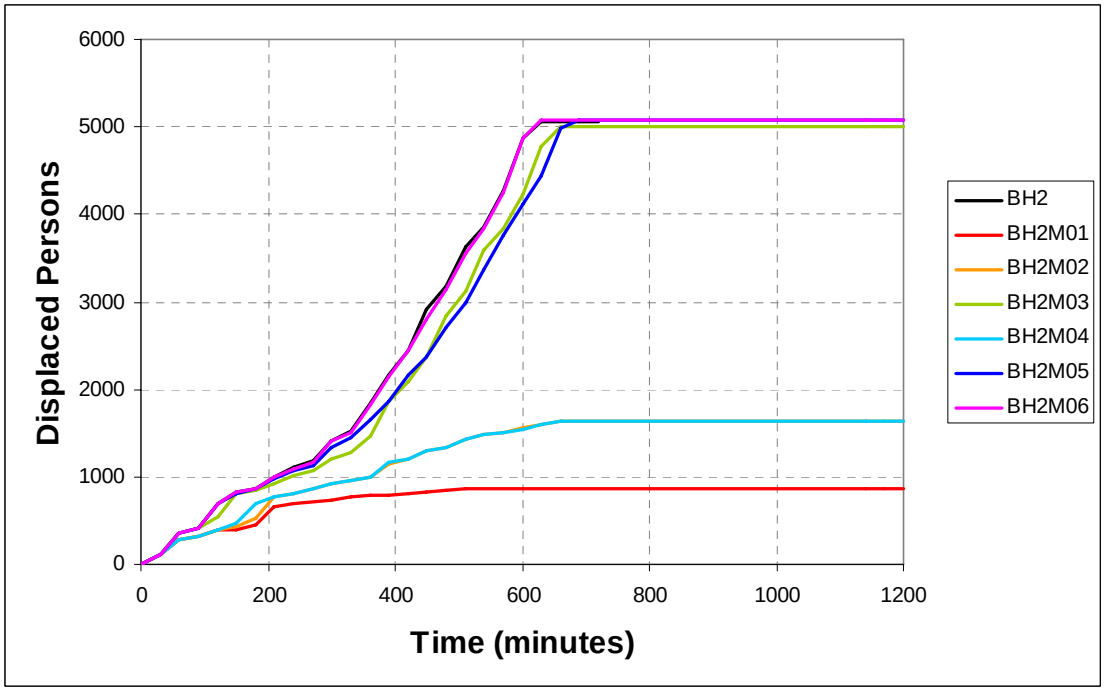

Fig. A2.8. Comparison of mitigated consequence development over time for MMAF urban fire originating at ECO target profile, with wind blowing 10 mph at 315 degrees and infrastructure damage scenario BH2 using various mitigation methods.

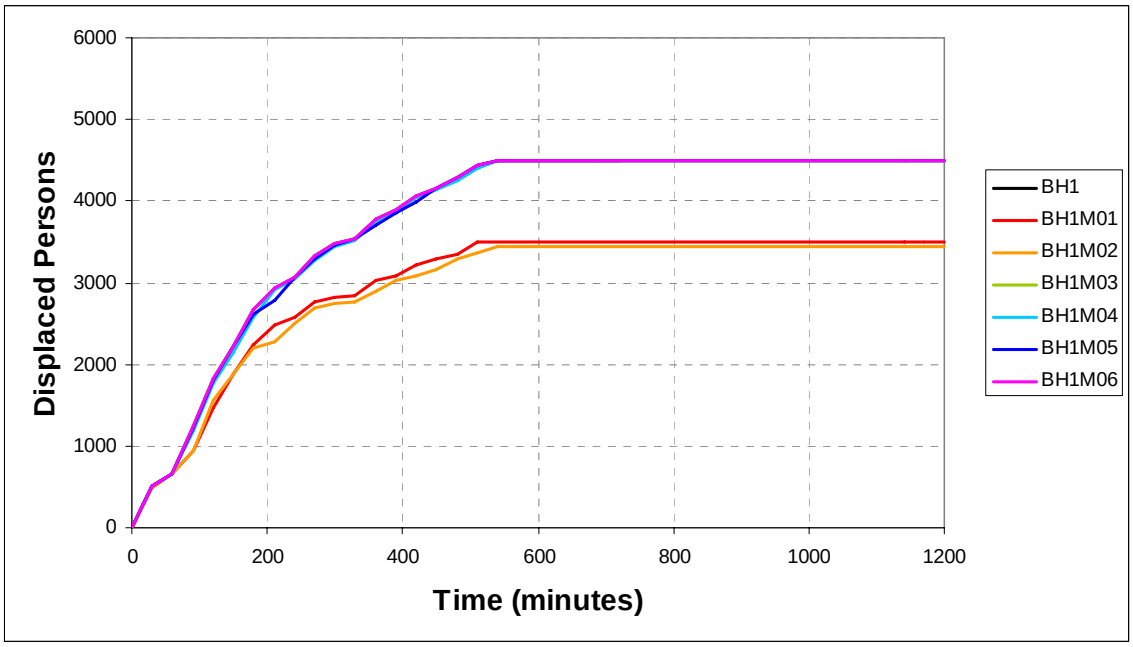

Fig. A2.9. Comparison of mitigated consequence development over time for MMAF urban fire originating at GOV target profile, with wind blowing 10 mph at 45 degrees and infrastructure damage scenario BH1 using various mitigation methods.

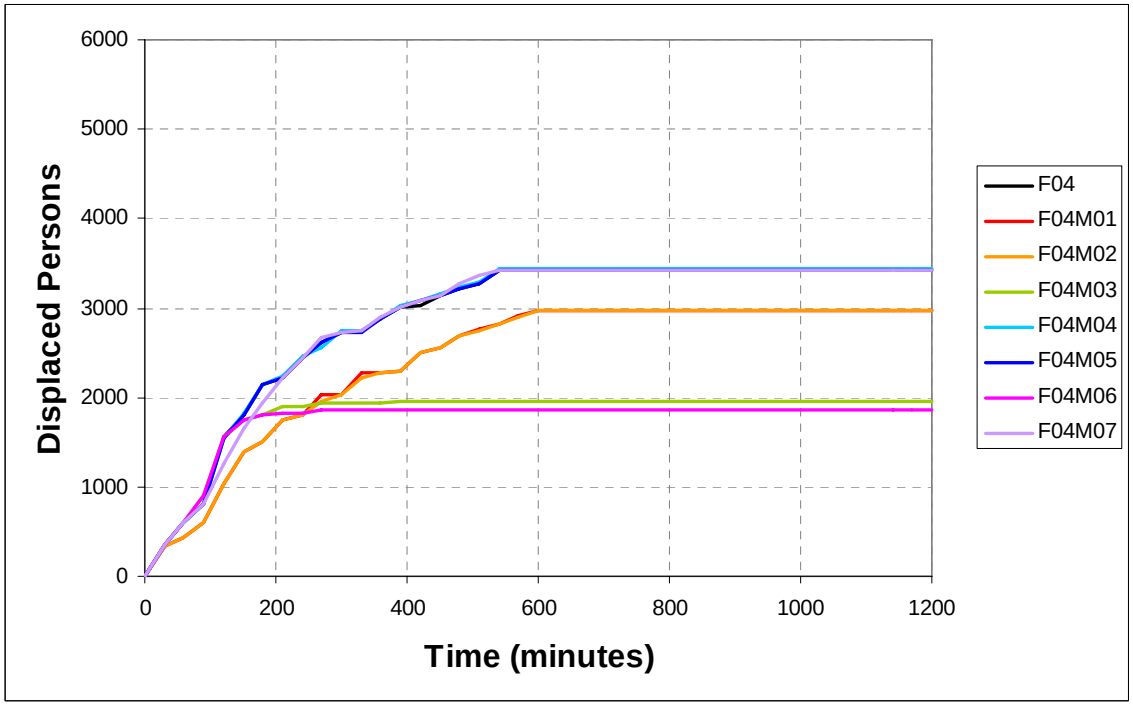

Fig. A2.10. Comparison of mitigated consequence development over time for MMAF urban fire originating at GOV target profile, with wind blowing 10 mph at 45 degrees and infrastructure damage scenario F04 using various mitigation methods.

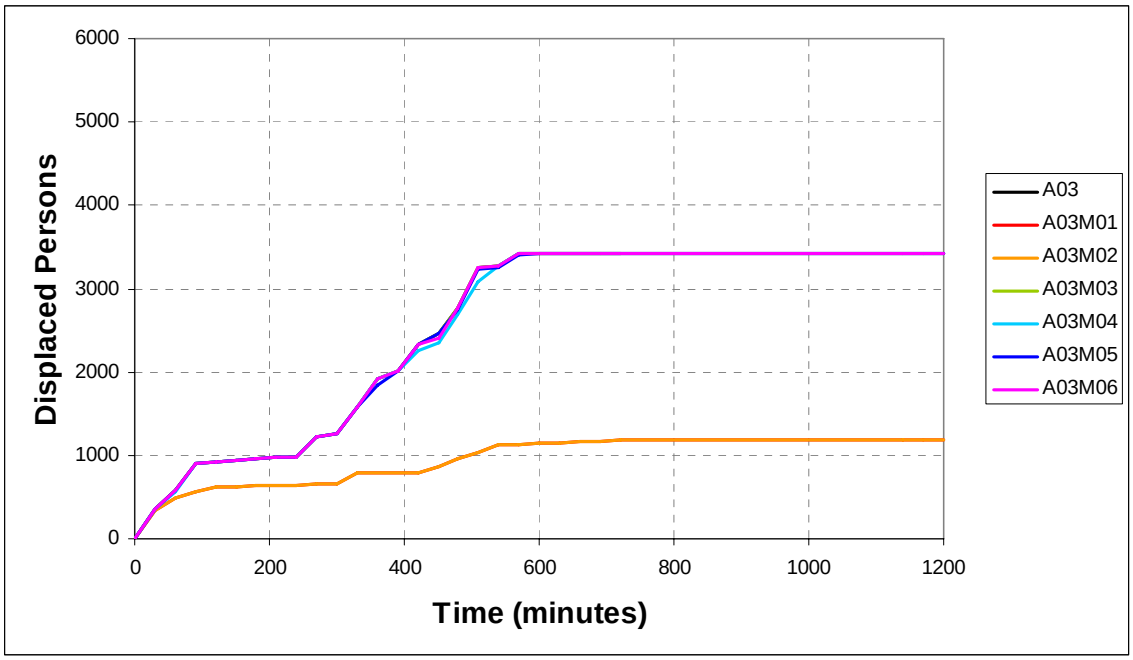

Fig. A2.11. Comparison of mitigated consequence development over time for MMAF urban fire originating at GOV target profile, with wind blowing 10 mph at 225 degrees and infrastructure damage scenario A03 using various mitigation methods.

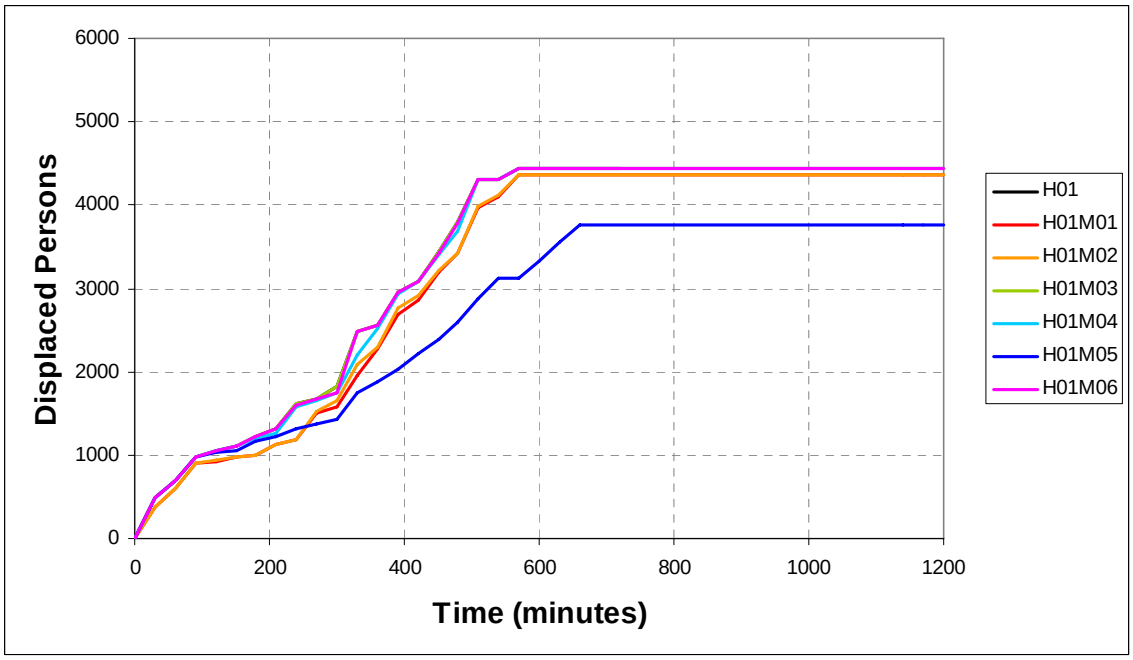

Fig. A2.12. Comparison of mitigated consequence development over time for MMAF urban fire originating at GOV target profile, with wind blowing 10 mph at 225 degrees and infrastructure damage scenario H01 using various mitigation methods.

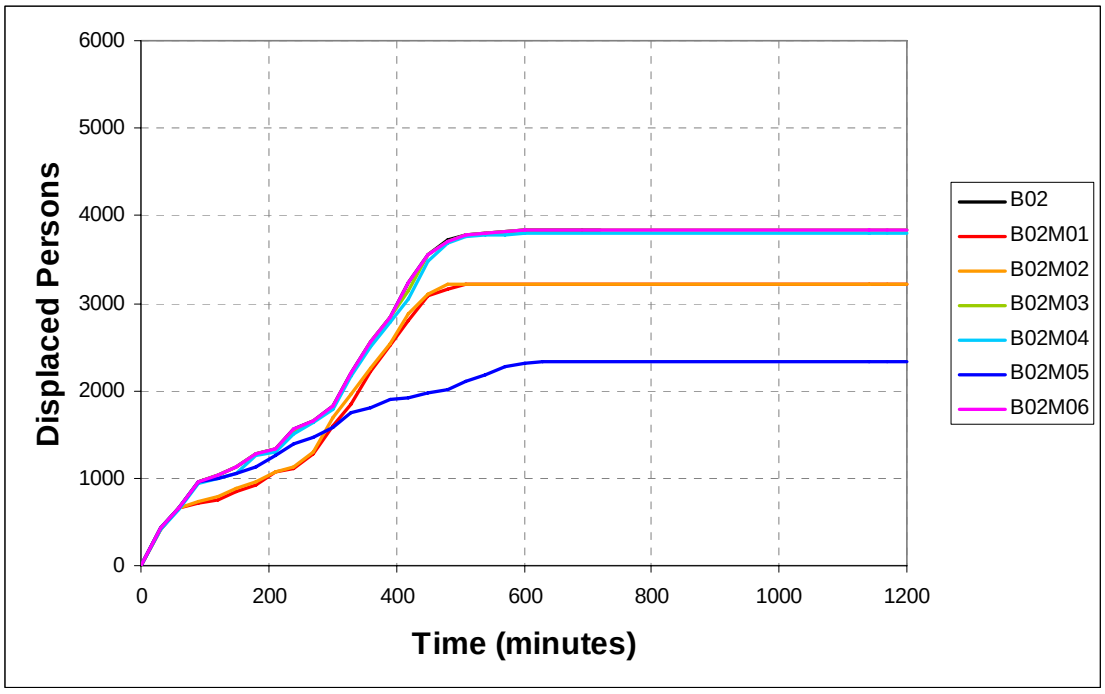

Fig. A2.13. Comparison of mitigated consequence development over time for MMAF urban fire originating at GOV target profile, with wind blowing 10 mph at 270 degrees and infrastructure damage scenario B02 using various mitigation methods.

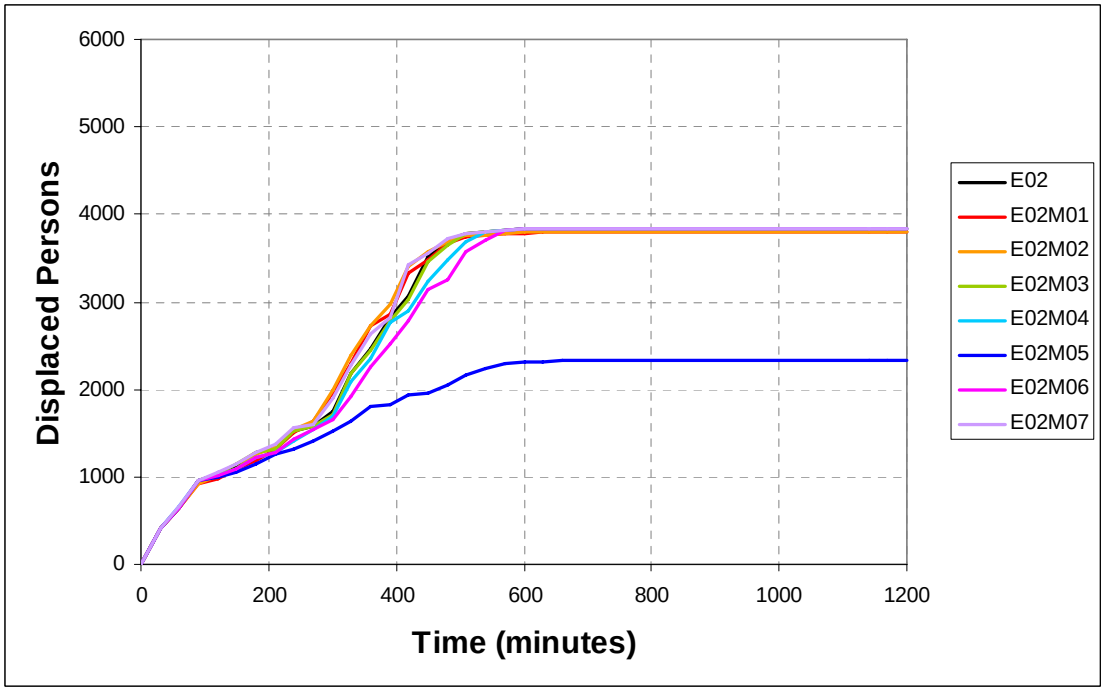

Fig. A2.14. Comparison of mitigated consequence development over time for MMAF urban fire originating at GOV target profile, with wind blowing 10 mph at 270 degrees and infrastructure damage scenario E02 using various mitigation methods.

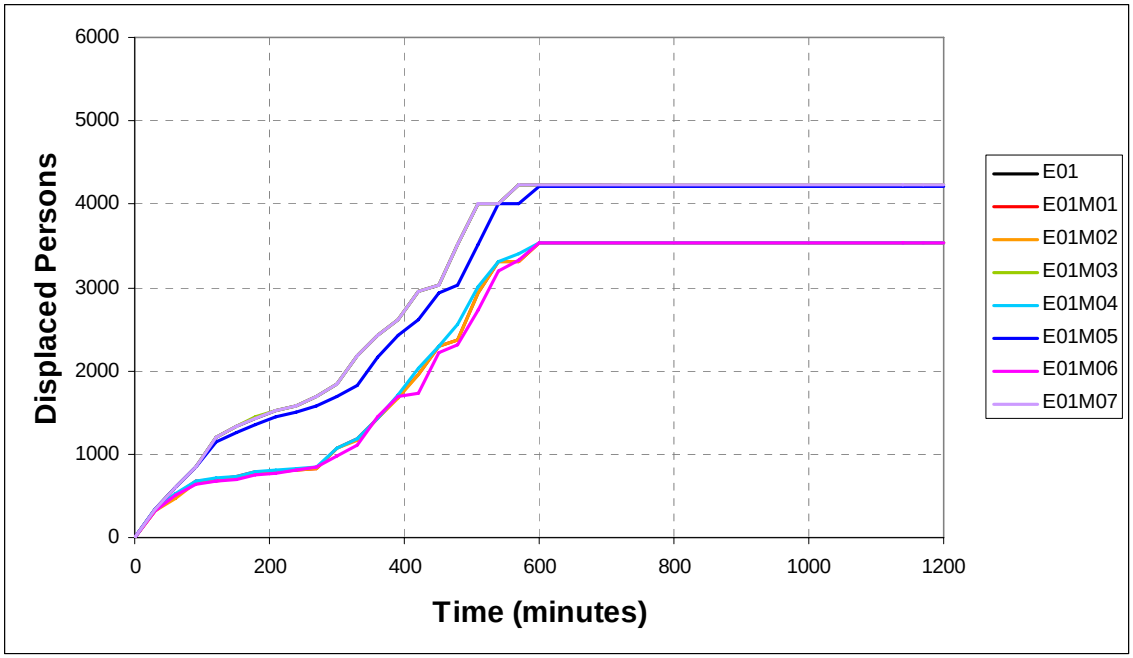

Fig. A2.15. Comparison of mitigated consequence development over time for MMAF urban fire originating at GOV target profile, with wind blowing 10 mph at 315 degrees and infrastructure damage scenario E01 using various mitigation methods.

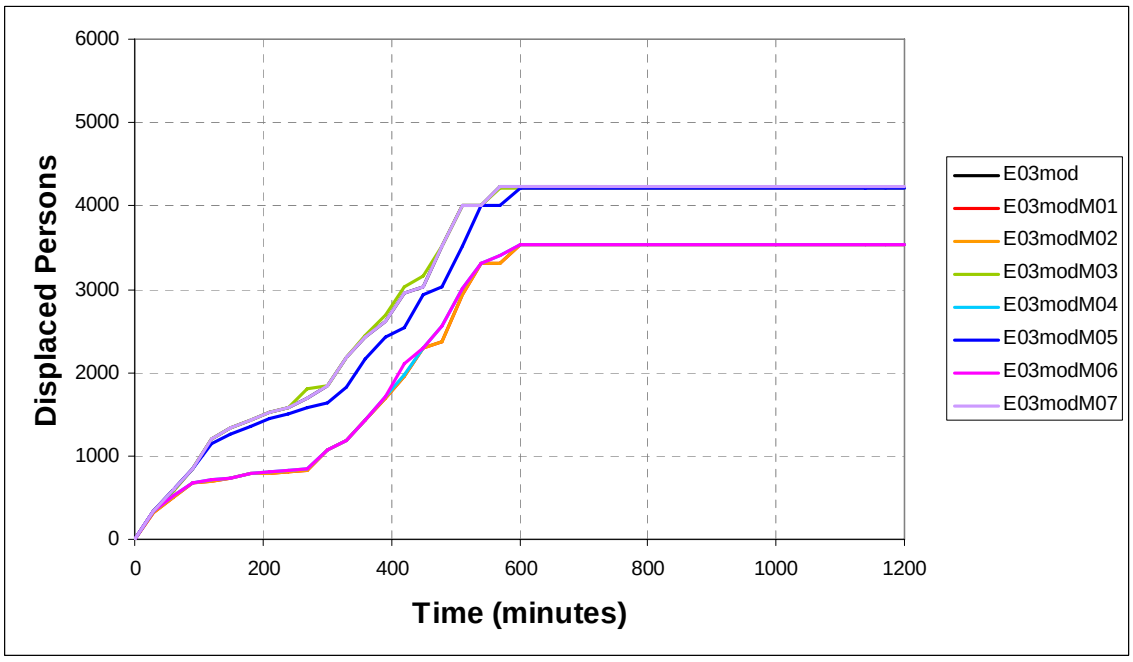

Fig. A2.16. Comparison of mitigated consequence development over time for MMAF urban fire originating at GOV target profile, with wind blowing 10 mph at 315 degrees and infrastructure damage scenario E03 using various mitigation methods.

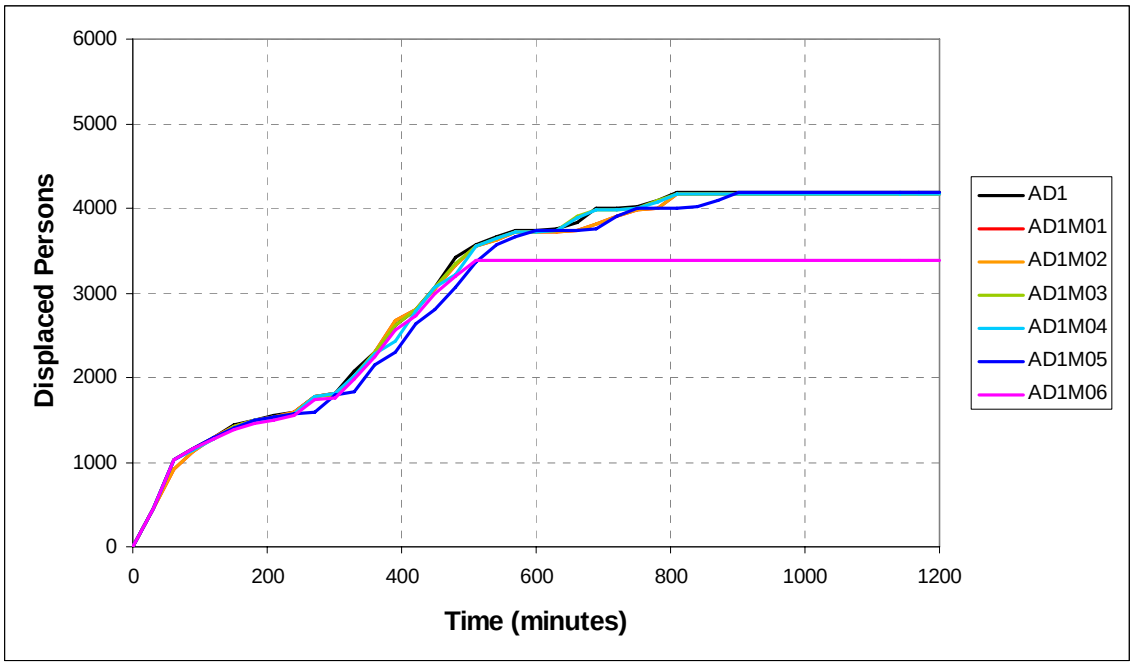

Fig. A2.17. Comparison of mitigated consequence development over time for MMAF urban fire originating at POP target profile, with wind blowing 10 mph at 225 degrees and infrastructure damage scenario AD1 using various mitigation methods.

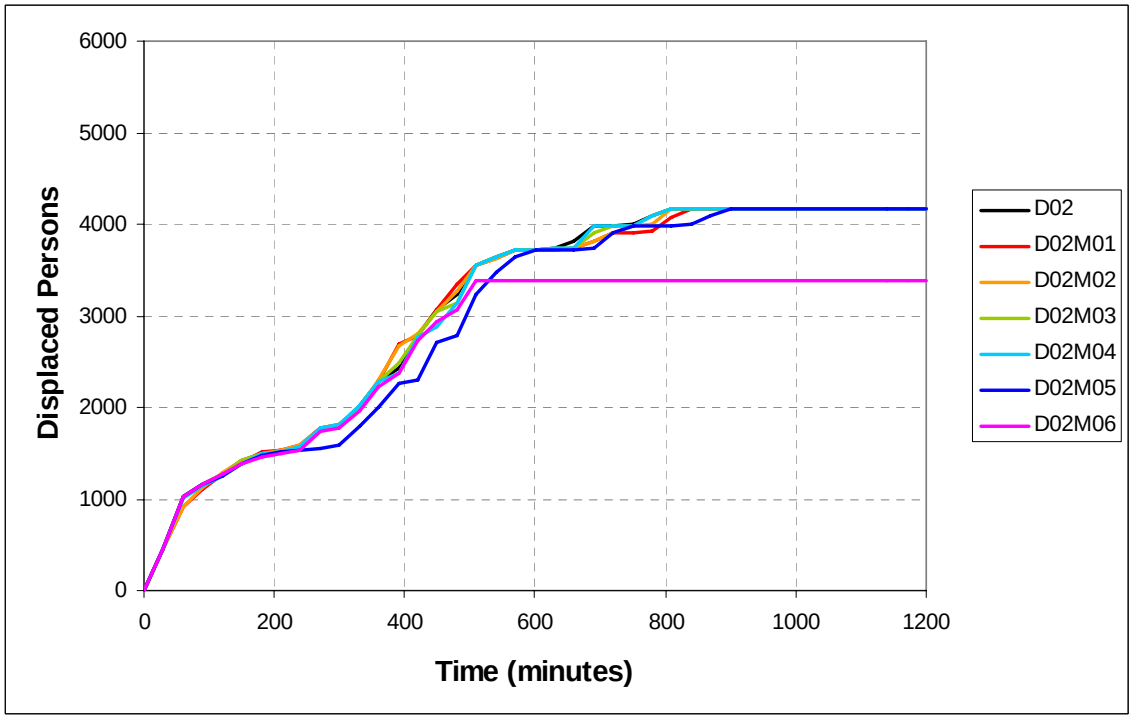

Fig. A2.18. Comparison of mitigated consequence development over time for MMAF urban fire originating at POP target profile, with wind blowing 10 mph at 225 degrees and infrastructure damage scenario D02 using various mitigation methods.

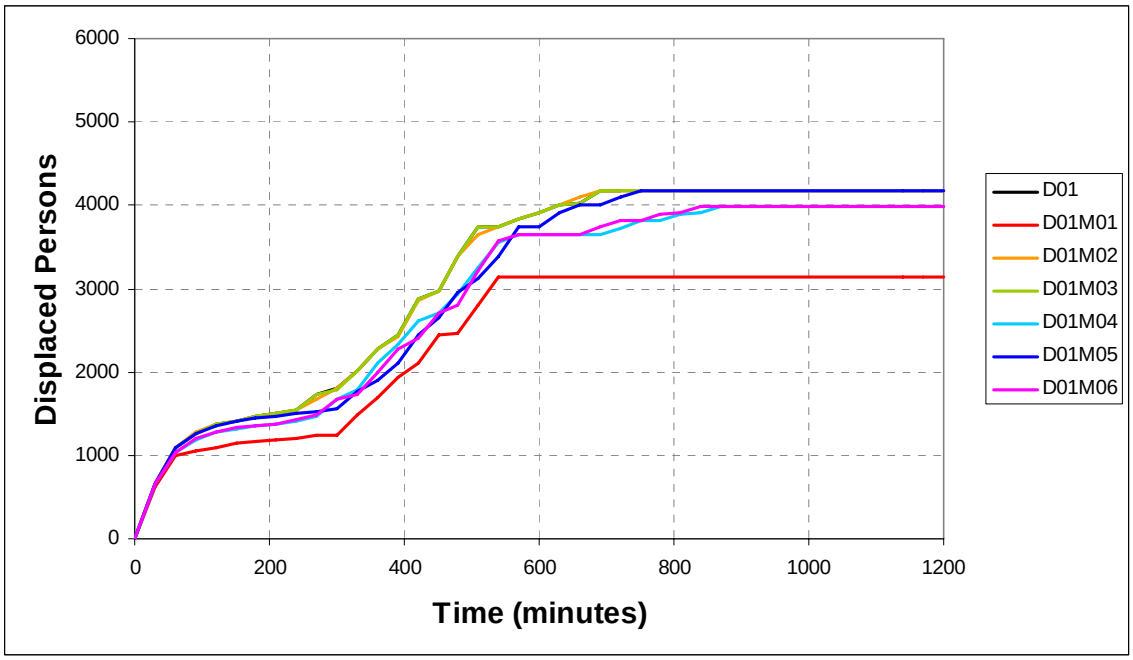

Fig. A2.19. Comparison of mitigated consequence development over time for MMAF urban fire originating at POP target profile, with wind blowing 10 mph at 315 degrees and infrastructure damage scenario D01 using various mitigation methods.

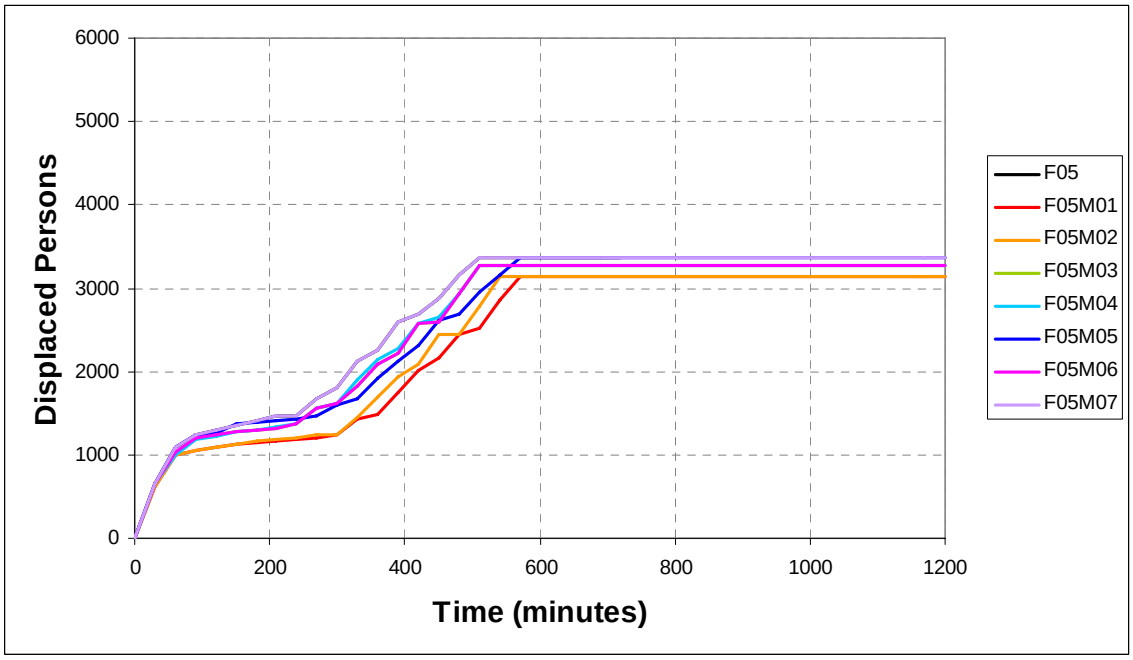

Fig. A2.20. Comparison of mitigated consequence development over time for MMAF urban fire originating at ECO target profile, with wind blowing 10 mph at 315 degrees and infrastructure damage scenario D01 using various mitigation methods.

VITA

Elizabeth Catherine Bristow earned a Bachelor of Science degree in Civil Engineering in 2002 from Texas A&M University. She continued her studies at the graduate level, earning a Master of Engineering in Civil Engineering with a specialty in Water Resources Engineering from Texas A&M University in 2004. From 2004 to 2006, she has worked towards a Doctor of Philosophy degree from Texas A&M University, focusing her studies on the security concerns of urban water distribution systems and the integration of water distribution network modeling with simulation of urban fire spread and suppression. During this time, she also earned the Certificate in Advanced International Affairs with a concentration in homeland security issues from the Bush School of Government and Public Service at Texas A&M University.

Elizabeth's graduate study has been supported by a U.S. Department of Homeland Security Graduate Fellowship, a U.S. Department of Homeland Security Dissertation Fellowship, and the American Association of University Women's Engineering Dissertation Fellowship. She has interned with Dodson & Associates, Inc., a hydrology and water resources engineering consulting firm in Houston, Texas (Summer 2002) and with Pacific Northwest National Laboratory in Portland, Oregon (Summer 2004). Upon conclusion of her doctoral studies, she will begin work as an Assistant Professor in the Department of Civil and Mechanical Engineering at the U.S. Military Academy in West Point, New York.

Elizabeth Bristow can be reached at the following address: Department of Civil and Mechanical Engineering, United States Military Academy, West Point, NY, 10996.